DEFINING THE ROLE OF HSP90 IN THE STABILITY OF FGFR3 AND AS A DRUG TARGET FOR THE TREATMENT OF SKELETAL DISEASES AND CANCER

By

Melanie B. Laederich

A DISSERTATION

Presented to the Department of Cell & Developmental Biology
and the Oregon Health & Science University
School of Medicine
in partial fulfillment of
the requirements for the degree of
Doctor of Philosophy
September 2011

School of Medicine

Oregon Health & Science University

CERTIFICATE OF APPROVAL

This is to certify that the Ph.D. dissertation of
Melanie Brenda Laederich
has been approved

Dissertation Advisor — William A. Horton, M.D.

Committee Chair — Linda Musil, Ph.D.

Committee Member — William Skach, M.D.

Committee Member — Philip Stork, M.D.

Committee Member — Brian Johnstone, Ph.D.

TABLE OF CONTENTS

LIST OF FIGURES……iii

LIST OF ABBREVIATIONS……...…..v

ACKNOWLEDGEMENTS……...……....vii

ABSTRACT……...…...……...viii

CHAPTER 1: INTRODUCTION AND BACKGROUND……..….1

1.1 OVERVIEW……....……1

1.2 FGFR3 AND DISEASE……..2

1.3 THE HSP90 CHAPERONE SYSTEM……..……18

CHAPTER 2: FGFR3 IS A STRONG HSP90 CLIENT: IMPLICATION FOR THERAPEUTIC MANIPULATION…….29

2.1 ABSTRACT……...…….30

2.2 INTRODUCTION……..30

2.3 MATERIALS AND METHODS……32

2.4 RESULTS…….…..36

2.5 DISCUSSION…….……54

2.6 SUPPLEMENTAL DATA……..……58

CHAPTER 3: CONCLUSIONS AND FUTURE DIRECTIONS……...61

3.1 CONCLUSIONS……...……..…61

3.2 FUTURE DIRECTIONS……...……..…63

3.3 SUMMARY……...……..68

APPENDIX: PRELIMINARY TEST OF HSP90 CHAPERONE COMPLEX MODULATION IN PRECLINICAL MODELS OF ACHONDROPLASIA…...…69

A.1 ABSTRACT……..….69

A.2 INTRODUCTION……..…...69

A.3 MATERIALS AND METHODS……..…… 73

A.4 RESULTS…….……..…76

A.5 DISCUSSION……...……..…84

REFERENCES…….…….……..93

LIST OF FIGURES

CHAPTER 1

Figure 1.1 *Physical manifestations of achondroplasia*……..……..…5

Figure 1.2 *FGFR3 signal transduction*…….……9

Figure 1.3 *Architecture and zones of the growth plate*……...……11

Figure 1.4 *Potential targets for therapeutic intervention*…….....…17

Figure 1.5 *The protein folding energy landscape*…….……..19

Figure 1.6 *An example the role of chaperones in the folding of kinases*……22

Figure 1.7 *Examples of structurally diverse Hsp90 inhibitors*……...…….28

CHAPTER 2

Figure 2.1 *FGFR3 associates with Hsp90 and Cdc37*……...…..38

Figure 2.2 *FGFRs differentially associate with Hsp90 complexes*……...…..41

Figure 2.3 *FGFR3 requires Hsp90 function for stability*…….....44

Figure 2.4 *Hsp90 inhibition results in FGFR3 ubiquitination*……47

Figure 2.5 *Loss of Hsp90 function reduces FGFR3 bioactivity*…..……...…...52

Figure 2.S1 *Summary of mass spectrometry data*…….….58

Figure 2.S2 *Supplementary data*……....59

APPENDIX

Figure A.1 *Organ culture genotype versus phenotype*……..…..…88

Figure A.2 *Modulation of metatarsal and tibia growth*……..….89

Figure A.3 *Effect of 17-AAG on metatarsal growth*……....……90

Figure A.4 *Characterization of CA-FGFR3 genotype versus phenotype*…….91

Figure A.5 *Genetic cross of Actin-CHIP and CA-FGFR3*…….…….92

LIST OF ABBREVIATIONS

AKT	v-akt murine thymoma viral oncogene homolog
BFA	brefeldin A
bp	base pair
CA	constitutively active
c-Cbl	Cas-Br-M (murine) ecotropic retroviral transforming sequence
Cdc37	cell division cycle 37
CHIP	C-terminus of heat shock protein 70
CK2	casein kinase 2
CNP	C-type natriuretic peptide
DMSO	dimethyl sulfoxide
EGFR	epidermal growth factor receptor, also known as ErbB1
ErbB2	avian erythroblastic leukemia viral oncogene homolog 2, also Her2
ERK	extracellular signal-related protein kinase
FGF	fibroblast growth factor
FGFR	fibroblast growth factor receptor
FRS2	fibroblast growth factor receptor substrate 2
GFP	green fluorescent protein
HDAC	histone deacetylase
Hop	Hsp70/Hsp90 organizing protein
Hsp	heat shock protein
IP	immunoprecipitation

kDa	kilodalton
KD	kinase dead
MAPK	mitogen-activated protein kinase
MDM2	murine double minute 2
MTT	methylthiazolyldiphenyl-tetrazolium bromide
NPR-B	natriuretic peptide receptor-B
NQO1	NAD(P)H/quinone oxioreductase 1
OMIM	online mendelian inheritance in man
PP5	protein phosphatase 5
SBMA	spinal bulbar muscular atrophy, also known as Kennedy's disease
STAT	signal transducer and activator of transcription
TDII	thanatophoric dysplasia Type II (FGFR3 K650E)
TRP	tetratricopeptide
WT	wild type

ACKNOWLEDGEMENTS

This work would not be possible without the love and support (since the day we met) of my best friend and husband Aaron Rowden and my furry study-buddy companion Jasmine. Also a significant amount of love and support came from my family Alison, Bob, Heather and Luke Laederich, as well as Charlie Rowden's little, and not so little, kicks. Support also came from my friends Mahta Nili, Katannya Kapeli and Eric Stoffregen and the other graduate students of my class.

The many hours of mentoring from my advisor Bill Horton made this work possible and greatly expanded my education. The Horton lab members Catherine Degnin, Greg Lunstrum and Paul Holden mentored me in experimental designs and made the lab an interesting place to work. Thanks also for mentoring from the post docs Connie Shung, Jackie Wirz, Kohtaro Tanaka, Bill Hooker as well as other professors at the Shriners Hospital. The professors of OHSU contributed significantly to my education with special thanks to Jackie Shannon, Chris Corless and most significantly Rachel Dresbeck. Molly Kulesz-Martin, Colleen Sweeney and Kermit Carraway helped me with mentoring and by believing in me.

My thesis advisory committee (Linda Musil, Bill Skach, Phil Stork) provided invaluable feedback, guidance and intellectual challenges that guided the Chapter 2 and my conceptual understanding of this dissertation.

I would also like to acknowledge and honor the mice for giving up their life for science.

ABSTRACT

Fibroblast growth factor receptor 3 (FGFR3) is an important regulator of growth and differentiation, whose aberrant activation by mutation causes a number of genetic diseases including skeletal diseases and cancer. I found that FGFR3 strongly associates with Hsp90 chaperone complexes. Hsp90 function has become a drug target for several diseases because it can be modulated using small molecule inhibitors to alter the stability of disease-causing proteins. This dissertation details the experiments characterizing the role of Hsp90 chaperone complexes in FGFR3 and FGFR family stability, and examines the use of Hsp90 inhibitors in pre-clinical models of FGFR3-mediated disease. Chapter 1 outlines the background on FGFR3 and its role in disease, the function of Hsp90 chaperone complexes and the use of small molecule inhibitors of Hsp90. Chapter 2 summarizes data characterizing the role of Hsp90 chaperone complexes in the stability of FGFR3 and the FGFR family. This chapter documents that FGFR3 is an inherently unstable protein that constitutively requires Hsp90 function for stability. In contrast, other FGFRs interact with Hsp90 more weakly and react differently to inhibition of Hsp90 function. Inhibition of Hsp90 function using small molecule inhibitors such as 17-AAG induces the ubiquitination and degradation of FGFR3. In addition to Hsp90, FGFR3 can form complexes with Hsp70, Cdc37 and CHIP suggesting that the function of these proteins could also serve as future drug targets. Chapter 3 summarizes the work presented here, its significance and limitations as well as the future directions branching

from this work. The appendix outlines some preliminary studies performed in pre-clinical models of achondroplasia including metatarsal and tibia organ cultures, as well as an *in vivo* experiment in mice that genetically manipulates Hsp90 complexes using transgenic overexpression of the chaperone-specific ubiquitin ligase CHIP. In summary, the work presented here establishes Hsp90 function as a necessary component of FGFR3 stability and implicates the use of Hsp90 inhibitors in diseases driven by FGFR3 function. The role of FGFR3 in cancer, combined with the positive results of Hsp90 inhibitors in cancer clinical trials, warrants the examination of Hsp90 inhibitors in cancers driven by FGFR3. However, the therapeutic potential to modulate Hsp90 function to treat skeletal diseases remains to be determined and will require more detailed analysis in pre-clinical models to determine effective drug delivery to chondrocytes, as well as the role of Hsp90 function within the skeletal growth plate.

CHAPTER 1

INTRODUCTION AND BACKGROUND

1.1 Overview

Spontaneous germ-line and somatic gain-of-function mutations in Fibroblast growth factor receptor 3 (FGFR3) give rise to genetic diseases including skeletal growth disorders and cancers [1-3]. The ability of these mutations to cause these phenotypically different disorders has stimulated interest in understanding their pathologies and the possibility to use similar approaches for treatment. Because achondroplasia (OMIM 100800) is an autosomal dominant disease that manifests as an increase in the kinase activity of FGFR3, targeting the activity and stability of FGFR3 is a valid therapeutic approach and is similar to those used to target oncogenic FGFR3 in cancer. However, none of the therapeutics designed to target FGFR3 in cancer have yet successfully been applied to treat FGFR3 mediated skeletal disorders.

While performing preliminary experiments for another project I discovered that FGFR3 strongly interacts with members of the Hsp90 chaperone system which are known drug targets in cancer. I hypothesized that, like select other proteins, FGFR3 or mutated FGFR3 may be a strong Hsp90 client and that small molecule inhibitors of Hsp90 could alter the function and stability of FGFR3 in disease. Thus, the following body of work focused on understanding the potential of manipulating Hsp90 chaperone complexes to control the function and stability of FGFRs as a potential treatment strategy for achondroplasia as well as a prognostic indicator of Hsp90 inhibitors in cancer.

The following chapters outline the experiments characterizing the role of chaperones in the stability of FGFR3 and their significance in a molecular and therapeutic context. This chapter gives an overview followed by an introduction to the biology of FGFRs and Hsp90 chaperone systems. Chapter 2 compares and contrasts the interaction of FGFR3, mutant FGFR3 and the FGFR family with members of the Hsp90 chaperone system and characterizes the ability of Hsp90 inhibitors to modulate the stability of FGFR3. Chapter 3 summarizes the findings and significance of this body of work as a framework for understanding the benefits and limitations of targeting chaperones systems in FGFR3 diseases as well as an outline of some future directions that stem from this work. The appendix discusses several different preliminary experiments testing if Hsp90 inhibitors are effective in targeting FGFR3 function in pre-clinical models of achondroplasia.

1.2 Fibroblast Growth Factor Receptor 3 and Disease [1]*

**Introduction section 1.2 as well as figures 1.2, 1.3 and 1.4 were adapted from the review entitled "Achondroplasia: pathogenesis and implications for future treatment" by M. Laederich and W. Horton, 2010 [1]*

Achondroplasia is by far the most common form of dwarfism in humans and the prototype of the human chondrodysplasias [4]. Its clinical phenotype has been recognized for centuries and the notion that it reflects a disturbance of cartilage-mediated (endochondral) bone growth has existed for about 100 years. However, it was not until mutations of the transmembrane receptor Fibroblast Growth Factor Receptor 3 (FGFR3) were identified in the mid-1990s that the molecular pathogenesis of achondroplasia began

to be unraveled. Indeed, considerable progress has been made in elucidating FGFR3 as a key negative regulator of endochondral ossification and in delineating the functional impact of disease causing mutations on growth plate chondrocyte biology. Potential targets for therapeutic intervention have been identified for achondroplasia, and pilot studies have been carried out in mouse models of achondroplasia. This review will examine recent progress in understanding how FGFR3 mutations interfere with bone growth, the application of this knowledge to preclinical trials in mice and the implications of this research for future therapy of children with achondroplasia.

Clinical manifestations of achondroplasia [5]

The primary clinical manifestation of achondroplasia is short stature with an average adult height of 112-136 cm for females and 118-145 cm for males [5]. Short stature stems from a disproportionate reduction in linear bone growth that affects the long bones, especially proximally, more severely resulting in rhizomelic shortening of the limbs (pictured in Figure 1.1) [4]. Other clinical features, some of which lessen with age, include a large head with frontal bossing, midface hypoplasia, joint laxity, limited elbow extension, trident shaped hands and bowed legs. Altered neurologic function may develop due to reduced spinal canal circumference and spinal cord compression which can lead to hypotonia, obstructive apnea, respiratory problems and sudden death in infants and small children, and numbness and loss of control of the bladder or bowel in adults. Additionally, other symptoms may include obesity, dental crowding and otitis media (middle ear infection). People with achondroplasia have normal intelligence;

however, recurrent episodes of otitis media can lead to hearing loss that may interfere with language development [6].

The prevalence of achondroplasia in the United States has an observed range of about 1/17,000 to 1/28,000 live births [7]. Life expectancy is significantly reduced by an average of ten years due to accidental death, heart disease or neurological complications from the disease [8]. Despite the fact that the achondroplasia mutation (discussed below, G380R) is found in some cancers and likely plays an oncogenic role in cancer development, there has been no reported increase of cancer incidence in people with achondroplasia. However, reports have found that a similar transmembrane mutation in FGFR4 (G388R)—present in 50% of the world's population permitting large scale analysis—causes a small but significant increase in cancer development [9]. Thus, detecting a small increase of cancer incidence in the achondroplasia population may be limited by the relatively low disease incidence of achondroplasia and cannot be discounted.

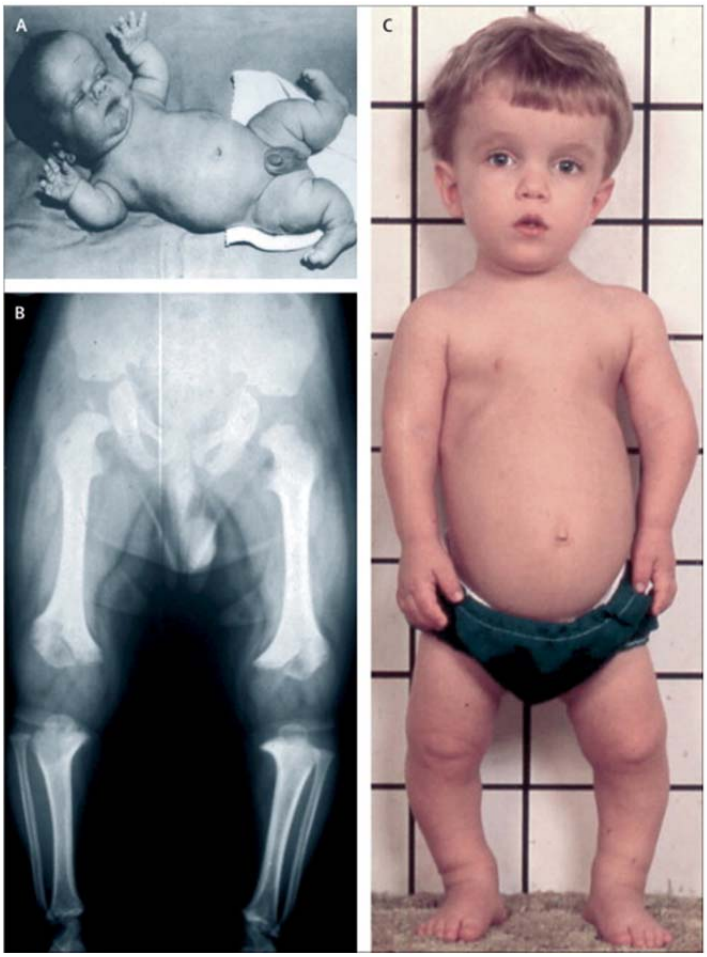

Figure 1.1 *Physical manifestations of achondroplasia. Reproduced with permission from Horton et al. 2007 [4]*. A. An infant with achondroplasia demonstrating trident hands with short fingers, frontal bossing, macrocephaly and rhizomelia of the limbs. B. Example radiograph of child with achondroplasia demonstrating disproportionate shortening of the femur relative to the tibia, as well as rounded iliac bones. C. A 3-year old child with achondroplasia displaying an altered phenotype from that of the infant with a reduction in skin folds and frontal bossing, and an increase in rhizomelic bone shortening.

Fibroblast Growth Factor Receptor 3

To understand the rationale behind the therapeutic strategies that have been proposed for achondroplasia, it is necessary to briefly discuss the genetic basis of the condition and the biology of FGFR3.

Genetics

Achondroplasia is inherited as an autosomal dominant trait. However, mapping its genetic locus was hindered by the paucity of multigenerational families needed to establish linkage as most cases arise from a new mutation to nonachondroplastic parents. Nevertheless, it was mapped to the distal short arm of chromosome 4 in 1994 and heterozygous mutations were discovered in FGFR3 shortly afterwards [10-13]. Essentially all patients with the classical features of achondroplasia have the same glycine to arginine substitution at position 380 (G380R), which maps to the transmembrane domain of the receptor. Additional FGFR3 mutations were subsequently detected in thanatophoric dysplasia, hypochondroplasia and other disorders whose clinical phenotypes qualitatively resemble achondroplasia [4, 14, 15]. Despite an initial debate about the functional consequences of these mutations, analysis of mice in which FGFR3 was knocked out, or in which FGFR3 bearing the achondroplasia mutation was overexpressed, revealed that disease-causing mutations lead to gain of receptor function

[16-18]. These observations also established FGFR3 as an important negative regulator of endochondral bone growth.

Receptor

FGFR3 is one of four high affinity FGF receptors (FGFR1–4) [2, 19, 20]. It functions as transmembrane receptor tyrosine kinase possessing an extracellular ligand-binding domain, a transmembrane domain and an intracellular split tyrosine kinase domain (Figure 1.2). Alternative splicing of the proximal extracellular domain generates 'b' and 'c' isoforms, which are expressed in a tissue specific manner and affect ligand specificity; the c isoform is predominantly expressed in skeletal tissues.

Activation

Like other FGFRs, FGFR3 is activated by FGF ligands released from cells near the FGFR3-bearing target cells. These ligands are often referred to as canonical or paracrine FGFs; they include FGF 1–10, 16–18, 20 and 22 [21]. The physiologic ligand(s) for FGFR3 is (are) not known, although FGFs 2, 4, 9 and especially 18 are the best candidates based on their distribution of expression and ability to bind and activate FGFR3, and the phenotypes of mice lacking these ligands [2, 22-24]. Heparin or heparan sulfate proteoglycans are required for FGF–FGFR3 interactions and likely influence binding specificity and ligand localization. The current dogma holds that canonical FGFs binding to their cognate FGFRs induce dimerization of receptors, leading to transactivation of the receptors' tyrosine kinase activity and transphosphorylation of key tyrosine residues within the receptors' kinase domain [19, 25-28]. Signals are propagated

by the recruitment of signaling molecules to these phosphorylated residues or to closely linked docking proteins, namely Fibroblast Growth Factor Substrate 2 (FRS2), which binds to the receptor and provides additional tyrosine residues that are phosphorylated in response to receptor activation.

Signaling

A number of signaling pathways have been detected downstream of FGFR3 activation, including the signal transducer and activator of transcription (STAT), mitogen activated protein kinase (MAPK), and phospholipase Cγ pathways, the first two receiving the most attention (Figure 1.2) [19, 29-33]. STAT signals are thought to inhibit chondrocyte proliferation, whereas MAPK signals not only negatively influence proliferation but also disrupt terminal differentiation and postmitotic matrix synthesis [31, 34-36]. Gene expression studies suggest that FGFR3 signals through multiple pathways that downregulate growth-promoting molecules, leading to reduced proliferation and differentiation of chondrocytic cells in growing bones [37, 38].

Consequences of the mutation

As noted earlier, the mutations that cause achondroplasia act by exaggerating the negative regulatory functions of FGFR3 on endochondral ossification [4, 28, 39]. To understand how this occurs, one must consider the impact of the mutation on the receptor itself and that on the growing skeleton.

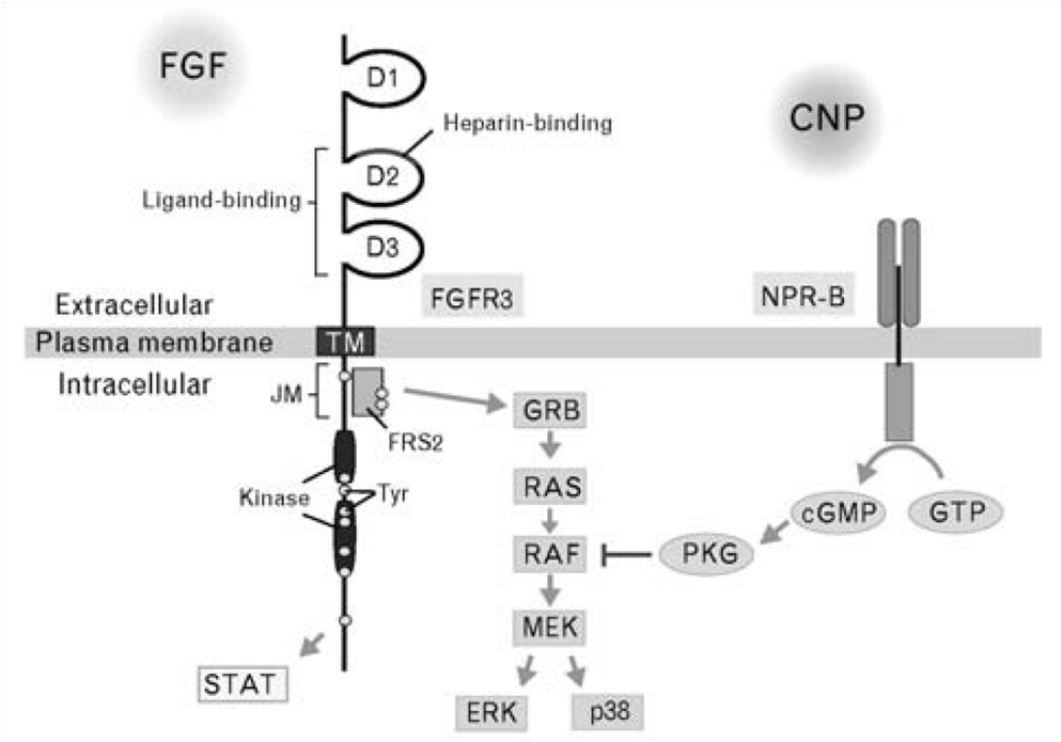

Figure 1.2 *FGFR3 signal transduction.* FGF and heparin binding to the extracellular domain of FGFR3 induce dimerization, kinase activation and transphosphorylation of tyrosine residues, leading to activation of downstream signaling pathways such as STAT. Membrane-bound FRS2 constitutively associates with the intracellular juxtamembrane domain of FGFR3, is phosphorylated by the receptor upon activation and serves as scaffolding platform for signal transduction cascades through the MEK/ERK/p38 pathway. CNP binding to NPR-B induces the generation of the second messenger cGMP, which activates PKG, leading to attenuation of the MEK pathway via RAF.

Impact on the receptor

The achondroplasia mutation maps to the transmembrane domain of the receptor. It has been proposed that the amino acid substitution stabilizes the receptor dimer, although this finding has been challenged [40, 41]. Another mechanism involves delayed turnover of activated receptor, which can lead to an increase in overall signal output. For instance, Monsonego-Ornan [42] and colleagues have suggested that the achondroplasia mutation slows receptor internalization, leaving it on the surface to signal. Others have described a defect in c-Cbl-mediated receptor ubiquitination that delays trafficking of mutant FGFR3 to lysosomes for degradation [43, 44]. Similarly, Ben-Zvi *et al*. have suggested that SOCS3 (suppressor of cytokine signaling 3) induced in response to exaggerated STAT1 signals may prolong the survival of mutant FGFR3 [45].

Impact on the growing skeleton

Endochondral ossification is responsible for both the formation and linear growth of most of the skeleton (Figure 1.3). However, the negative regulatory influence of FGFR3 is exerted mainly in the growth phase, in which it reduces the rate of cartilage template formation and turnover necessary for bone elongation. Most evidence to date suggests that FGFR3 inhibits both the proliferation and terminal differentiation of growth plate chondrocytes and synthesis of extracellular matrix by these cells [2, 46, 47]. This inhibitory function is consistent with its expression in cells exiting the cell cycle. However, it is also proposed that FGFR3 induces premature terminal differentiation, reducing the number of cells that contribute to template synthesis [36, 48].

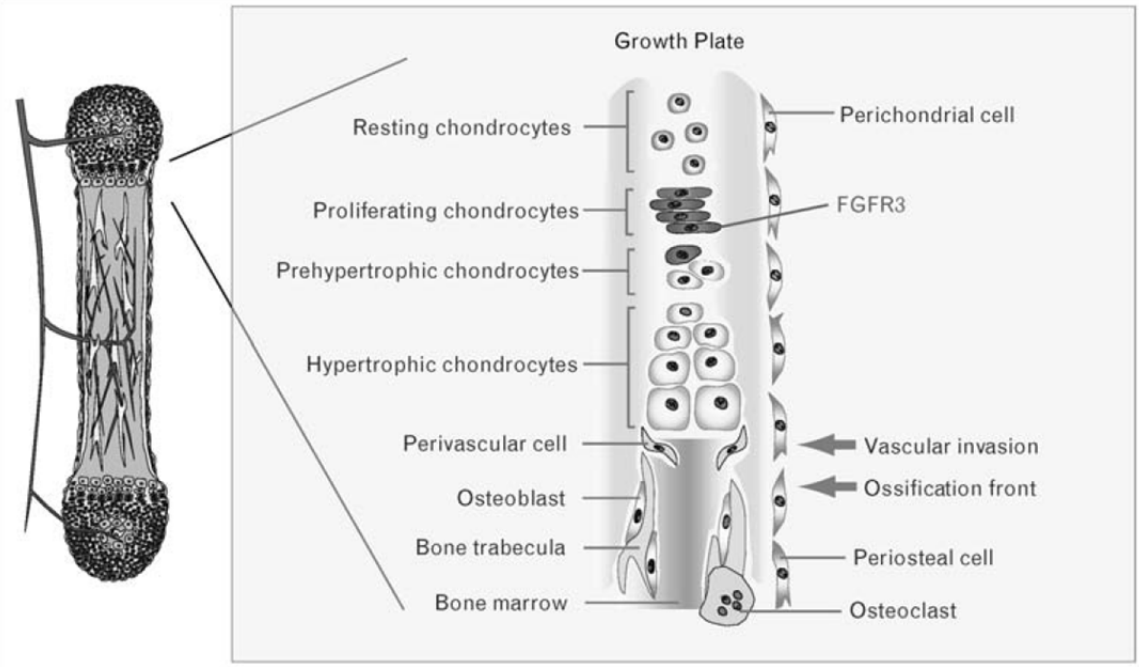

Figure 1.3 *Architecture and zones of the growth plate.* Linear bone growth results from chondrocyte proliferation and differentiation sequentially through the growth plate zones. FGFR3 is primarily expressed in proliferating chondrocytes, in which it tightly regulates proliferation and transition to terminal differentiation. Some FGFR3 is expressed in prehypertrophic chondrocytes, in which mutant FGFR3 dysregulates their differentiation and matrix secretion.

Alteration of downstream signal

While all of the pathways that normally propagate FGFR3 signals presumably transmit the exaggerated output of the mutant receptors, there is evidence that the extracellular signal-related protein kinase (ERK) and p38 arms of the MAPK pathway are especially important. Indeed, transgenic mouse strains in which expression of constitutively active MEK1 and MEK6 was targeted to cartilage displayed 'achondroplastic' skeletal phenotypes; MEK1 and MEK6 lie upstream of ERK and p38 phosphorylation cascades and activate these downstream targets [35, 49]. Additionally, humans with mutations in proteins involved in the RAS/MAPK pathway that cause constitutive activation of this pathway demonstrate reduced growth and craniosynostosis, further supporting that activation of this pathway plays a role in human skeletal disorders [50, 51]. MAPK signals that slow bone growth are subject to downregulation by the signaling cascade activated by C-type natriuretic peptide (CNP) [28, 52]. Indeed, genetic manipulation of this pathway up or down in mice leads to skeletal overgrowth or undergrowth, respectively, and overexpression of CNP ameliorates dwarfism in achondroplastic mutant mice as discussed in more detail below [52, 53].

CNP is one of three structurally related peptides that were originally defined in the context of regulating blood pressure and volume [54]. Through interaction with its receptor, natriuretic peptide receptor-B (NPR-B), CNP induces accumulation of intracellular cGMP. Signals downstream of NPR-B intersect with MAPK signals downstream of FGFR3 at the level of RAF1 (Figure 1.2), antagonizing the growth-

inhibiting effects of FGFR3 [55, 56]. Both CNP and NPR-B are expressed in the proliferative and prehypertrophic zones of the growth plate, setting up a potential autocrine or paracrine regulatory circuit [57]. Of interest, inactivating mutations of NPR-B are responsible for the dwarfing condition acromesomelic dysplasia, type Maroteaux (OMIM 602875) [58].

Therapeutic targeting of Fibroblast Growth Factor Receptor 3

Many nonsurgical strategies aimed at reducing excessive FGFR3 output have been entertained as possible treatments to stimulate linear bone growth in achondroplasia. They include strategies to interfere with FGFR3 synthesis, block its activation, inhibit its tyrosine kinase activity, promote its degradation, and antagonize its downstream signals (Figure 1.4). Many have been borrowed conceptually from the cancer treatment field, which is not surprising because the genetic lesions leading to achondroplasia and FGFR3-related skeletal disorders are identical to those found in FGFR3-driven cancers. Three of the proposed therapeutic strategies have progressed beyond the discussion phase and merit more attention here: chemical inhibition of FGFR3 tyrosine kinase activity, antibody blockade of FGFR3 activation, and CNP-mediated antagonism of FGFR3 downstream signals.

Fibroblast Growth Factor Receptor 3 kinase inhibitors

The rationale behind this approach is that FGFR3's kinase activity is critical for its activation and signal output; chemical inhibition of its kinase activity should block its inhibitory output and restore bone growth. The strategy has been successful for many

oncogenic kinases [59]. Aviezer *et al*. reported synthesis of an inhibitor selective for FGFR3 compared with FGFR1 [60]. The compound reconstituted normal growth in cultured limb bones from a knock-in mouse model of achondroplasia. However, this success has not been extended to live mice.

Antibody blockade

On the basis of the successful results from treating breast cancer patients with trastuzumab, this strategy was proposed for achondroplasia [60]. Trastuzumab (trade name Herceptin) is a humanized monoclonal antibody to the extracellular domain of the HER2/neu (ErbB2), a transmembrane receptor overexpressed on the surface of about 15–30% of breast cancer cells [61]. HER2 transmits mitogenic signals to the cancer cells in the absence of external mitogens, and trastuzumab reverses the adverse effects of the overactive receptor. Rauchenberger *et al*. described generation of a comparable antibody to FGFR3 that effectively blocked ligand-induced FGFR3 activation; however, there have been no subsequent reports on its capacity to stimulate bone growth *in vivo* [62].

Of note, activating FGFR3 mutations are relatively common in bladder cancer, in which they are thought to promote proliferation and survival of the tumor cells [63]. Blocking antibodies similar to those just described have been used successfully to reduce proliferation in cells derived from these tumors, further supporting the utility of this approach to reducing FGFR3 output [64-66].

C-type natriuretic peptide antagonism of Fibroblast Growth Factor Receptor 3 signals

The therapeutic potential of CNP-mediated antagonism of FGFR3 downstream signals was first demonstrated in genetic crosses of transgenic mice overexpressing CNP in the growth plate [52]. When these mice were crossed with transgenic mice overexpressing mutant FGFR3 (achondroplasia mutant G380R) in the growth plate the achondroplastic phenotype was reversed. These experiments were then followed by transgenic overexpression of CNP in the liver to continuously and systemically dose the mice with CNP, which has a short half-life (2.6 minutes) and requires constant administration [67, 68]. These mice displayed increased bone growth suggesting that systemic administration of CNP via the circulation could be used to increase bone length. In a final set of experiments, recombinant CNP was delivered using a continuous infusion system in wild-type and transgenic achondroplastic mice [69]. Systemic administration of recombinant CNP also ameliorated the achondroplastic phenotype as well as increased the bone growth of wild-type mice without any overt side effects. Taken together, these series of experiments support the notion that CNP administration may be a safe and valid treatment for bone growth disorders in humans; however, future work is needed to define the long-term side effects of CNP administration *in vivo*.

Other possible treatment strategies

Although not directed at mutant FGFR3, at least two other strategies have been explored to downregulate the consequences of similar activating mutations of FGFR2.

Apert syndrome, a classic and severe form of craniosynostosis, is commonly caused by the S252W mutation of FGFR2, which utilizes many of the same signaling pathways as FGFR3 to propagate its signals. Shukla *et al*. utilized RNA interference to knock-down expression of the mutant FGFR2 allele [70]. They generated a transgenic mouse strain that produced a short-hairpin RNA (shRNA) that reduced expression of transcripts from the mutant FGFR2 allele. When these mice were crossed with mice harboring a S252W FGFR2 allele and exhibiting features of Apert syndrome, the craniosynostosis phenotype was rescued. A similar approach targeted to the mutant FGFR3 allele in achondroplasia merits consideration, although delivery of an RNA interference vector to growth plate chondrocytes represents a challenge.

Based on evidence that FGFR2 transmits signals through MAPK:MEK:ERK as much as FGFR3 does, this group administered the MEK chemical inhibitor U0126 to the Apert syndrome mice prenatally and during the early postnatal period [70]. The treatment partially ameliorated the craniosynostosis without obvious complications. These results raise the possibility of taking advantage of a similar strategy for achondroplasia, with the caution that MEK inhibition could affect many signaling pathways in addition to FGFR3 pathways [71].

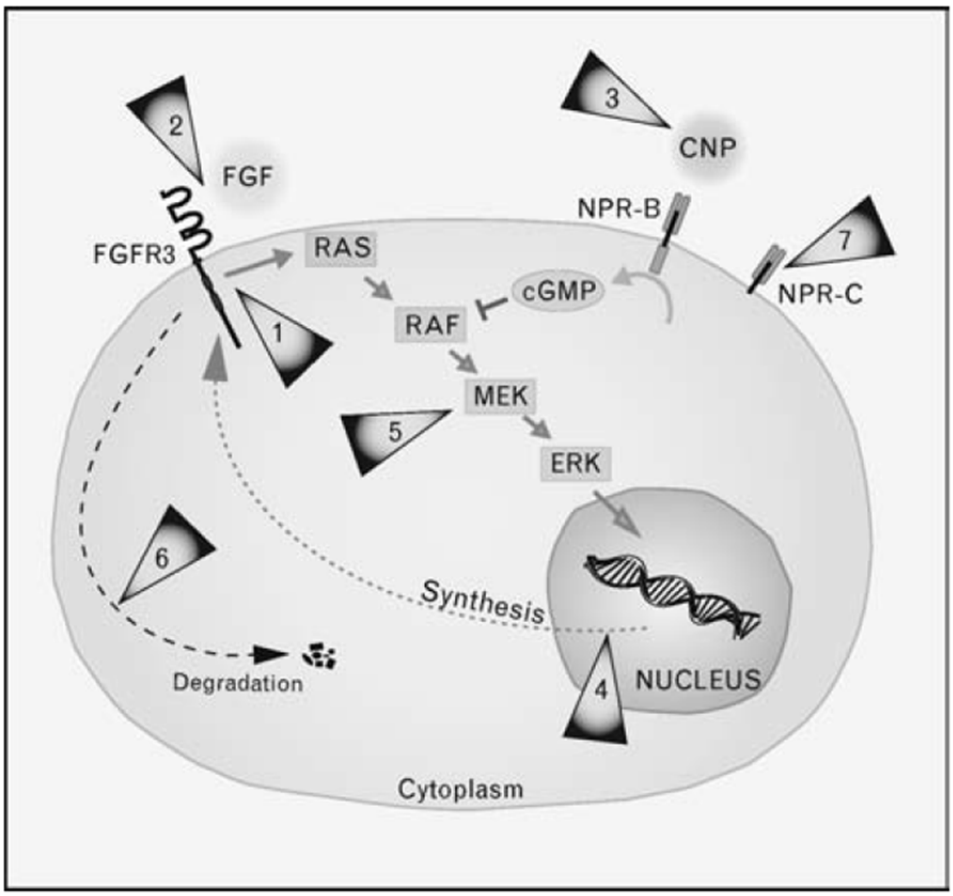

Figure 1.4 *Potential targets for therapeutic intervention* 1. FGFR3 tyrosine kinase activity 2. Ligand-mediated receptor activation 3. CNP-mediated antagonism of signals downstream of the receptor 4. Expression or synthesis of mutant FGFR3 5. Kinase mediators of MAPK signaling pathway 6. Degradation of activated receptor 7. Interference with CNP decoy receptor NPR-C. See text for discussion.

1.3 The Hsp90 Chaperone System

The role of chaperones in protein folding\

Protein folding within the crowded environment of a cell requires the input of energy to overcome the energy barriers of incorrect conformations and to prevent irreversible unfolding [72]. As proteins fold they settle into lower energy conformations which may not form the functional higher-energy native state of the protein (a conceptualized image of folding states relative to energy levels is pictured in Figure 1.5) [73]. Proteins that settle into non-native lower energy states may gain or lose function, become unstable and prone to degradation, or become aberrantly stable and form toxic aggregates within the cell. These improper folding states can lead to disease [74]. Examples of diseases caused by protein misfolding and aggregation include Parkinson's, Alzheimer's and polyglutamine diseases. Collectively these diseases appear to stem from a low energy non-native folding state of the protein that is prone to aggregation leading to cellular toxicity through unclear mechanisms.

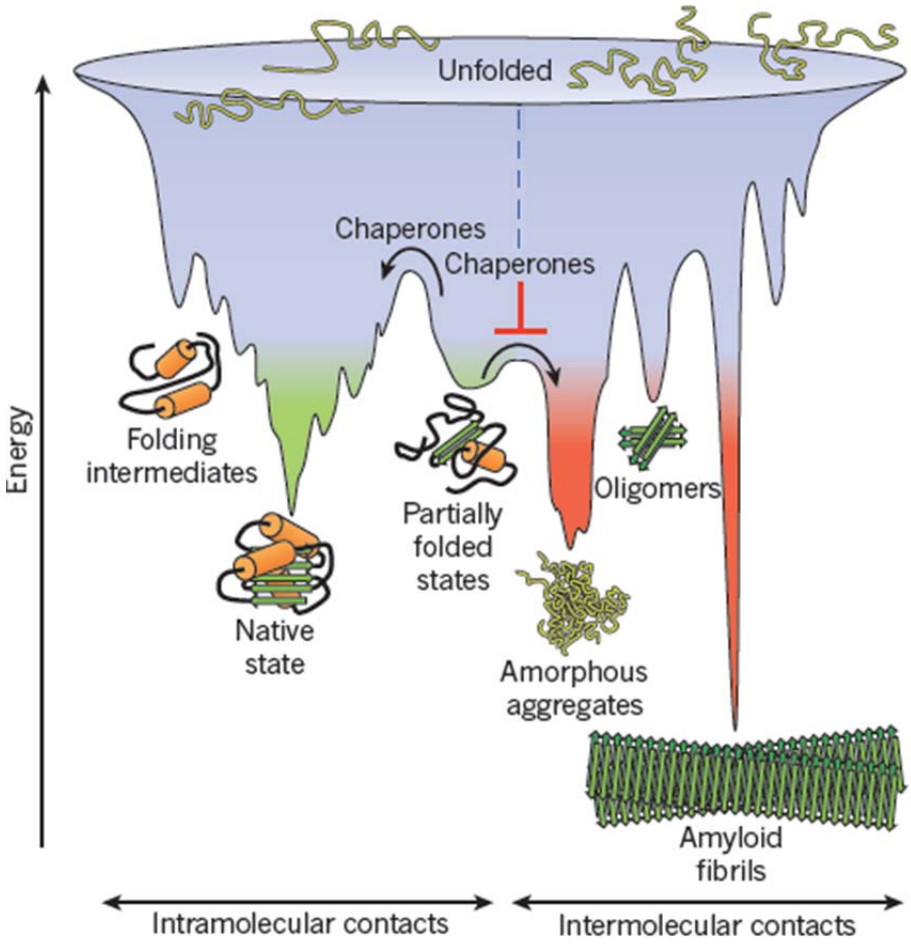

Figure 1.5 *The protein folding energy landscape. Reproduced with permission from Hartl et al. [73].* Unfolded proteins proceed through a number of lower energy folding intermediates until they are kinetically trapped into a lower energy state (illustrated by energy "wells"). This state may represent the native folded protein, or may instead be an unfolded intermediate or partially folded state. The partially folded state is prone to aggregation and may form toxic species if chaperones do no not prevent this by binding to them. Alternatively chaperones may input energy to fold proteins into their native state to create a functional wild-type protein. Strong Hsp90 clients dwell in the partially folded state.

To overcome the challenges of protein folding, a significant percentage of the proteome is dedicated to specialized proteins that facilitate folding: chaperones. General chaperones such as Hsp70 and Hsp40 bind to unfolded regions of a "client" protein by recognizing hydrophobic patches not exposed in the folded state; binding prevents client aggregation and is often followed by conformational changes that promote folding. Specialized "cochaperone" proteins may facilitate the recognition and recruitment of unfolded proteins to chaperones. The full mechanism and series of events by which chaperones and cochaperones recognize and fold clients is not clear. However, *in vitro* studies and experiments in yeast suggest that folding proceeds through a cycle of chaperone and cochaperone binding events that can vary for different types of clients [75-79]. An example of a chaperone binding cycle is illustrated in Figure 1.6, which includes common chaperones known to play a role in kinase folding including Hsp40, Hsp70, Hop, Cdc37 and Hsp90 [77, 80-82]. The minimal proteins needed to fold some kinases *in vitro* include Hsp40, Hsp70, Hsp90, Cdc37, as well as the kinase that phosphorylates and activates Cdc37, casein kinase-2 (CK2) [77]. Further detail is provided in the following sections on the chaperones discussed in this dissertation and their role in protein folding and disease.

Modulation of protein folding has been investigated as a therapeutic approach for genetic diseases stemming protein misfolding [83]. In some cases, a mutation may cause partial or complete protein unfolding leading to degradation and a loss-of-function function phenotype. Such is the case for the most common mutation causing cystic fibrosis, in which a mutation causes the protein to be recognized as misfolded by chaperones resulting in protein degradation and disease. Use of chemical chaperones to refold the protein or manipulation of chaperone complexes to favor the folded state can restore the stability and functional location of the mutant protein *in vitro* [84, 85]. In other cases, mutations can cause aberrant stabilization of a disease causing protein through the action of chaperones [86-88]. In this case, such as with oncogenic kinases in cancer, inhibiting the function or association of chaperone complexes with the mutant protein can cause protein degradation and amelioration of disease. The latter case is most relevant to this dissertation as mutant FGFR3 demonstrates increased stability and was investigated for its ability to associate with chaperone complexes.

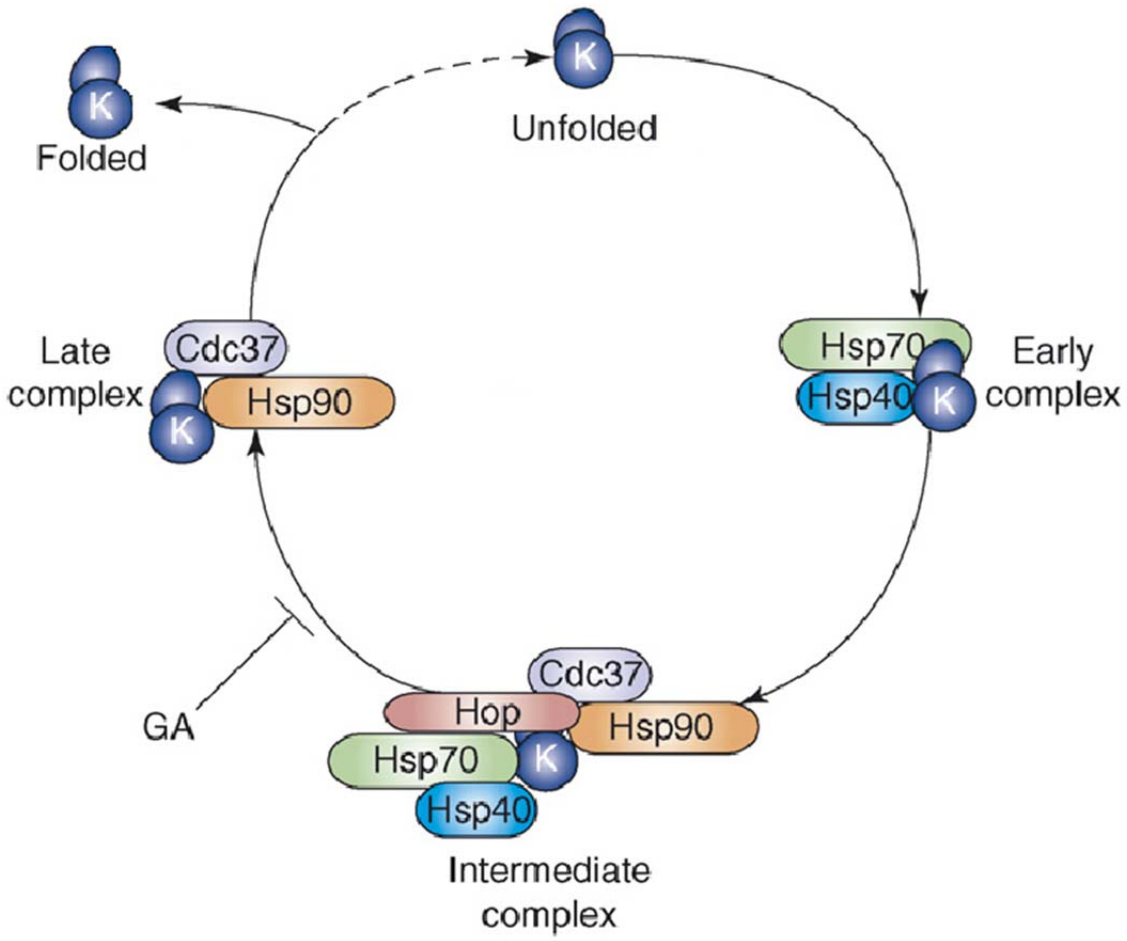

Figure 1.6 *An example of the role of chaperones in the folding of kinases. Reproduced with permission and modified from Caplan et al. [74].* The unfolded protein kinase is first recognized by Hsp70 and Hsp40 to create an early complex that may partially fold the kinase or simply prevent its aggregation [70, 75]. The cochaperone Hop facilitates association of Hsp90 and Cdc37 with Hsp70 and Hsp40 [68]. Hsp90 ATPase activity stimulates the formation of a more folded 'late complex' which can be inhibited by geldanamycin (GA) [73]. Strong Hsp90 clients dynamically cycle or dwell in the late complex, whereas weak Hsp90 clients are released from Hsp90 and Cdc37 fully folded. Cdc37 must be phosphorylated by CK2 for this reaction to proceed [70].

Hsp90 stabilizes metastable proteins

Hsp90 is specialized chaperone that facilitates the initial folding of proteins as well as the sustained folding of select metastable proteins termed “strong clients” [89]. Hsp90 is relatively poor at recognizing unfolded proteins and binding is facilitated by cochaperones (such as Cdc37 and Hop) that deliver clients after they have interacted with Hsp70, which is a more general chaperone involved in recognizing newly synthesized proteins [76-78]. Hsp90 consists of an N-terminal ATP and client binding domain, a middle client binding domain and a c-terminal dimerization domain [90, 91]. Cochaperones can bind to any of these domains and influence client binding or the ATPase cycle of Hsp90. Hsp90 chaperoning activity is intimately tied to ATP hydrolysis, but it is also influenced by client binding which, together with cochaperones, propagates structural rearrangements facilitating client folding and release [79, 92, 93]. Additionally, Hsp90 function can be influenced by a number of posttranslational modifications including acetylation, nitrosylation and phosphorylation [94-97].

Hsp90 stabilizes a large number of strong clients (>200), most of which play key roles in signal responsiveness or signal transduction [97, 98]. Because of its diverse clientele, Hsp90 function can influence many arms of cellular physiology, including apoptosis, proliferation and stress responses [97, 99]. Furthermore, Hsp90 has been implicated in facilitating some genetic diseases because disease-causing mutations can destabilize a protein converting it into a strong Hsp90 client; this has been observed for several gain-of-function mutations in oncogenes implicating Hsp90 function as a drug target in cancer

[97, 100-102]. The observation that Hsp90 facilitates the stability of mutant proteins is the cornerstone of its renowned role as a buffer of phenotypic variation in several model organisms [103]. These studies implicate the ability of Hsp90 to stabilize mutant proteins as a way to preserve the function of metastable mutant proteins that otherwise would be degraded, thereby masking loss-of-function phenotypes as well as permitting gain-of-function phenotypes. Because of these observations, manipulation of Hsp90 function to alter the stability and function of disease-causing proteins has the potential to treat some genetic diseases.

The kinase-specific cochaperone Cdc37

Cdc37 is a specialized Hsp90 cochaperone that facilitates recruitment and folding of kinase clients [104]. In addition, Cdc37 can act as a chaperone independent of Hsp90 and can promote the folding of proteins that are not kinases [105, 106]. Structural studies indicate that Cdc37 makes direct contacts with both Hsp90 and the client protein, with data supporting contacts of Cdc37 with the N-lobe of kinases [107-111]. The association of Cdc37 with the client and Hsp90 decreases the ATPase activity of Hsp90, which promotes client binding [112]. The ability of Cdc37 to interact with client proteins requires phosphorylation by casein kinase 2 (CK2) [113-115]. Phosphorylated Cdc37 can be dephosphorylated when it is bound to Hsp90 by the cochaperone phosphatase PP5, thereby inactivating Cdc37/Hsp90 chaperone activity [116]. The biological signaling events that lead to CK2 mediated phosphorylation of Cdc37 and PP5 dephosphorylation are not understood. An example of the role of Cdc37 in Hsp90 client binding in the

folding cycle is given in Figure 1.6 [81]; however, specific details remain unknown and likely vary by client [79]. Because of its role in facilitating kinase stability, Cdc37 has become a drug target in cancer [117].

The E3 ubiquitin ligase CHIP

CHIP is an E3-ubiquitin ligase initially discovered in a screen for proteins containing a tetratricopeptide repeat (TRP) motif, a motif that plays a key role in chaperone interactions [118]. It was initially demonstrated that the TRP motifs of CHIP are necessary for binding to both Hsp90 and Hsp70 and that the U-box domain of CHIP contains E3-ubiquitin ligase activity able to induce the ubiquitination and degradation of unfolded client proteins [119]. While CHIP has been identified as the primary ubiquitin ligase linking chaperones to the proteasome system, it is clear from studies using knockout mice that CHIP function can be compensated for by other ubiquitin ligases [120]. Ubiquitination by CHIP can also influence the trafficking of proteins and lead them to a degradative fate in the lysosome [121, 122].

As the major ubiquitin ligase facilitating the degradation of unfolded Hsp90/Hsp70 clients, the role of CHIP in the pathology of several diseases has been examined. Cancers frequently contain oncogenic mutant proteins that are strong Hsp90 clients which are abnormally stable and thereby promote cancer cell proliferation, survival or both. The ability of CHIP, and other ubiquitin ligases such as c-Cbl and MDM2, to promote the ubiquitination and degradation of Hsp90 clients proteins can be prevented by the association of Hsp90 with the client, and influences by the binding and release

kinetics of Hsp90 [101, 123, 124]. Inhibition of Hsp90 function using small molecule inhibitors restores the ability of clients to be ubiquitinated and degraded. Similarly, overexpression of CHIP in tissue culture experiments frequently leads to increased ubiquitination and degradation of Hsp90 clients, although the overexpression of ubiquitin ligases may decrease their specificity for substrates. An overexpression study of CHIP *in vivo* has also been performed to determine if the ability of CHIP to shuttle misfolded proteins to the proteasome can prevent aggregation diseases mediated by Hsp90 clients. In this study, a mouse model of spinal and bulbar muscular atrophy (SBMA) which expresses an aggregation-prone polyglutamine-expanded androgen receptor, had an increase in the age of disease onset when crossed with a transgenic mouse overexpressing CHIP [125]. Similar results were observed when the mice were treated with Hsp90 inhibitors [126]. These results suggest that overexpression of CHIP *in vivo* may mimic treatment with Hsp90 inhibitors, and underscores the important role of CHIP in protein homeostasis.

Hsp90 inhibitors

Before their mechanism of action was elucidated, Hsp90 inhibitors were first identified as naturally occurring antibiotics produced in microorganisms such as the well-studied bacteria *Streptomyces hygroscopicus* [127]. The discovery that some of these antibiotics were able to reverse the phenotype of cells transformed with oncogenic viruses led to the identification that they were Hsp90 inhibitors [128]. This began with the benzoquinone ansamycins class of inhibitors (geldanamycin, macbecin and

herbimycin), which could inhibit the transforming activity of oncogenic kinases such as Src without affecting their kinase activity [128, 129]. This enigma was resolved by the generation of columns covalently bound with the inhibitor geldanamycin, which affinity purified Hsp90 [130]. It was subsequently demonstrated that inhibiting Hsp90 function rapidly destabilizes client proteins, thereby inactivating them [130]. The identification of Hsp90 as the target of geldanamycin led to the many studies characterizing other structurally diverse classes of Hsp90 inhibitors, Hsp90 clients, the role of Hsp90 in the cell, and ultimately the use of Hsp90 inhibitors in clinical trials.

Although a number of different Hsp90 inhibitors have been characterized (including synthetically generated inhibitors) the most important and well-studied inhibitor has remained geldanamycin and its derivatives (structures of important Hsp90 inhibitors are illustrated in Figure 1.7). Geldanamycin competitively binds to the ATP binding pocket of Hsp90, preventing ATP hydrolysis and chaperone function thereby destabilizing Hsp90 clients via ubiquitin-mediated degradation. Unfortunately, geldanamycin is hepatotoxic in pre-clinical studies and very insoluble [131]. However, it was discovered early on that the 17-carbon of geldanamycin could be chemically modified without abolishing its activity [130]. This led to the generation of less toxic geldanamycin analogs including 17-AAG (tanespimycin) as well as a water soluble analog 17-DMAG. Translation of Hsp90 inhibitors into the clinic has been accelerated by the observations that they are selectively taken up and retained in cancer cells relative to normal tissue, that cancer cells are hypersensitive to Hsp90 inhibitors and these inhibitors can prevent chemotherapeutic resistance caused by oncogenic pathway switching [132-134].

Currently over 18 different Hsp90 inhibitors have been tested in dozens of clinical trials up to Phase III [135, 136]. Some success has been reported, but optimization of drug pharmacodynamics, dose, and delivery is still needed to reduce side effects and improve therapeutic effects [97].

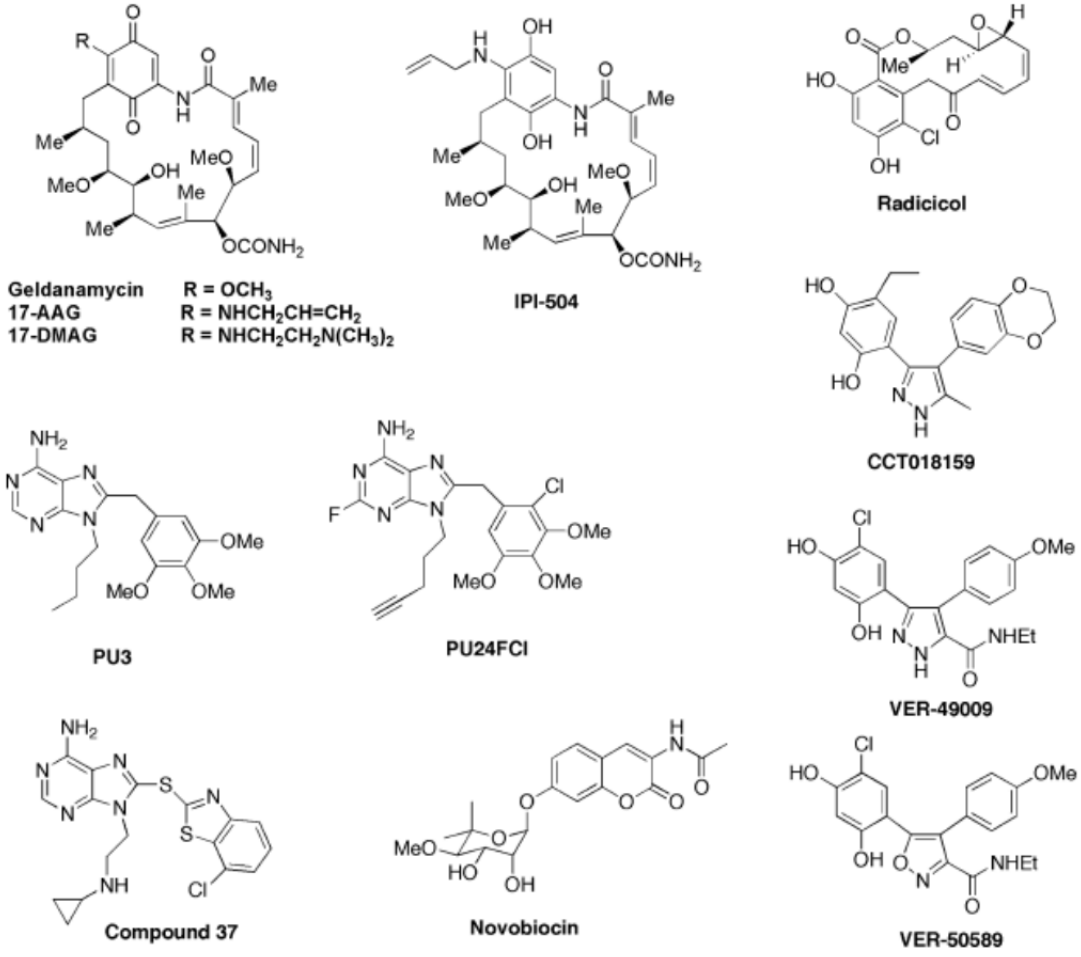

Figure 1.7 *Examples of structurally diverse Hsp90 inhibitors. Reproduced with permission from the manuscript of Workman et al. [121].*

CHAPTER 2

FIBROBLAST GROWTH FACTOR RECEPTOR 3 (FGFR3) IS A STRONG HEAT SHOCK PROTEIN 90 (HSP90) CLIENT: IMPLICATIONS FOR THERAPEUTIC MANIPULATION

Melanie B. Laederich[1,2], Catherine R. Degnin[1], Gregory P. Lunstrum[1], Paul Holden[1,3] and William A. Horton[1,3]

From the Research Center of Shriners Hospital for Children, Portland Oregon[1] and the Departments of Cell & Developmental Biology[2] and Molecular & Medical Genetics[3], Oregon Health & Science University, 3101 SW Sam Jackson Park Road, Portland, Oregon 97239

This Chapter was accepted for publication by the Journal of Biological Chemistry, April 12th 2011 [137]. MBL designed and performed all experiments and wrote the paper. WAH, CRD, GPL and PH assisted in experimental design and paper writing and/or editing. CRD also provided supplemental data figure 2.S1.B.

2.1 Abstract

Fibroblast growth factor receptor 3 (FGFR3) is a key regulator of growth and differentiation whose aberrant activation causes a number of genetic diseases including achondroplasia and cancer. Hsp90 is a specialized molecular chaperone involved in stabilizing a select set of proteins termed clients. Here we delineate the relationship of Hsp90 and its co-chaperone Cdc37 with FGFR3 and the FGFR family. FGFR3 strongly associates with these chaperone complexes and depends on them for stability and function. Inhibition of Hsp90 function using the geldanamycin analog 17-AAG induces the ubiquitination and degradation of FGFR3 and reduces the signaling capacity of FGFR3. Other FGFRs weakly interact with these chaperones and are differentially influenced by Hsp90 inhibition. The Hsp90-related ubiquitin ligase CHIP is able to interact and destabilize FGFR3. Our results establish FGFR3 as a strong Hsp90 client and suggest that modulating Hsp90 chaperone complexes may beneficially influence the stability and function of FGFR3 in disease.

2.2 Introduction

Fibroblast growth factor receptors (FGFRs) are responsible for coordinating numerous developmental and cellular processes such as cellular differentiation and growth [19]. Germline and somatic mutations in FGFRs give rise to genetic disorders of skeletal development and cancer [2, 138], which reflect increased or misregulated FGFR signals. FGFR3 is mutated or abnormally expressed in the most common form of human dwarfism, achondroplasia, and cancers, notably superficial bladder cancer and multiple myeloma [63, 139]. Interestingly, identical mutations are found in bone growth disorders

and cancer, suggesting that they share common pathogenetic features and may respond to similar therapeutic approaches [1].

Hsp90 is a molecular chaperone that is abundantly and ubiquitously expressed within cells [89, 140]. It is involved in initial protein folding as well as in stabilizing proteins with unstable domains. For kinases, the dedicated co-chaperone Cdc37 helps recruit and control Hsp90 association with the folding complex. Some kinases depend on Hsp90 constitutively for their stability; these "strong clients" include ErbB2 and AKT [141, 142]. Others require Hsp90 only when rendered constitutively active by mutation, i.e., EGFR and B-RAF [100, 102]. Inhibition of Hsp90 function using small molecule inhibitors alters chaperone complex composition and promotes the association of E3-ubiquitin ligases such as Carboxyl terminus of Hsp70 Interacting Protein (CHIP), leading to client ubiquitination and degradation [143].

Many Hsp90-stabilized kinases are oncogenic, which has led to the development of Hsp90 inhibitors for cancer therapy. Indeed, geldanamycin derivatives such as 17-AAG and other Hsp90 inhibitors have progressed to Phase II clinical trials [135]. Hsp90 inhibitors have also been investigated in preclinical models of genetic diseases of mutated Hsp90 clients, such as the androgen receptor in spinal and bulbar muscular atrophy (SBMA, Kennedy disease) [126, 144].

Here we define the relationship of FGFR3 and the FGFR family with Hsp90 and its co-chaperone Cdc37. Our data establish FGFR3 as a strong Hsp90 client in contrast to the other FGFR family members. Inhibition of Hsp90 function alters the chaperone

complexes associated with FGFR3 and reduces the receptor's stability and signaling capacity. Our results suggest that Hsp90 is an important regulator of FGFR3 function and that Hsp90 inhibitors may be useful for treating FGFR3 mediated diseases.

2.3 Materials and Methods

Reagents and Cell lines- The following antibodies and reagents were purchased from Santa Cruz Biotechnology: FGFR1 (C-15), FGFR2 (C-17), FGFR3 (C-15), FGFR3 (B9), FGFR4 (C-16), EGFR (528), EGFR (1005), Neu (3BS), Neu (CB11), Hsp90 (F-8), Hsp70 (W27), Cdc37 (C-11), FRS2 (H91), pERK (E-4), ERK1 (K-23), Normal Rabbit and Mouse IgG, Goat Anti-Mouse IgM HRP. Other antibodies include Sigma Cytoplasmic Anti-FGFR3 (F-0425, used for untagged immunoprecipitation), Sigma Actin (A-2066), Invitrogen V5 (R96025), Abcam GFP (ab290), Cell Signaling pFRS-α Y196 (3864) and phospho-FGFR (3471), Covance Anti-ubiquitin P4D1 (MS-257P), Biomol Anti-Polyubiquitin FK1 (PW8805) and BD Biosciences PY20 (610000). The generation of TREX tet-on cell lines was performed following the manufacturer's instructions (Invitrogen). Cell lines and transfections were created with plasmids containing mouse FGFR1-4 (IIIc form) and human ErbB1 and ErbB2. FLAG-CHIP was kindly provided by Gen Sobue [125]. Mutagenesis was performed using the QuickChange Site Directed mutagenesis kit (Stratagene). The specific residue number for the swapping mutations is as follows for human sequence (if different, the mouse amino acid number is shown in parenthesis): FGFR1 D554G, FGFR2 D557G (D576G),

FGFR3 G533D (G527D), FGFR3 G548D (G542D), FGFR4 E543G (E540G). Chimeric kinase domain FGFR3/FGFR2 receptors were generated using PCR and blunt ligation. The boundaries used to define the kinase domains were modeled after the manuscript of Chen *et al.* [20]. The human amino acid boundaries are (the corresponding mouse amino acids are in parenthesis): FGFR3 kinase domain L457-D758 (L451-D752), FGFR2 kinase domain Y466-E767 (Y485-E786), FGFR3 N-lobe/hinge L457-N562 (L451-N556), FGFR2 N-lobe/hinge Y466-N571 (Y485-N590), FGFR3 C-lobe/kinase insert L563-D758 (L557-D752), FGFR2 C-lobe/kinase insert L572-E767 (L591-E786).

The generation of the COS7 stable cell lines has been previously described [43]. Because the effective dose of 17-AAG (InvivoGen) is affected by cell number [145], all HEK 293 (293) based cell lines were plated at 2 x 10^5 cells/cm^2 and RT112 cells plated at 2.4 x 10^5 cells/cm^2. Celastrol, PD173074 and Radicicol were purchased from Calbiochem. Quercetin and cycloheximide were purchased from Sigma. Brefeldin A and lactacystin were purchased from Enzo. FGF2 and FGF9 were purchased from R&D Systems. Moosa Mohammadi generously provided us with FGF1. Biotinylation reagents were obtained from Thermo Scientific: EZ-link Sulfo-NHS-SS-BIOTIN (21331) and NeutrAvidin Agarose Resin (2920).

Immunofluorescence- Cells were treated as indicated, fixed in 4% paraformaldehyde for 20 minutes, mounted with PermaFluor (Thermo) and imaged by confocal microscopy.

Immunoprecipitation- Cells either transiently transfected or induced with tetracycline for 48 hours (or as notated), were treated with drugs as indicated, rinsed in 1x PBS and

immunoprecipitation was performed as described by Sweeney *et al.* [146], with the replacement of inhibitors with 1x Roche Complete Protease Inhibitors and Sigma Phosphatase Inhibitor Cocktail 2. For denaturing immunoprecipitation, cells were prepared following the protocol by VanSlyke *et al*. with slight modification [147]. Briefly, cells were rinsed 1x in PBS and lysed in SDS denaturation buffer (5 mM Tris-HCl, 5 mM EDTA, 5 mM EGTA, 0.6% SDS, 10 μM iodoacetamide, 200 μM PMSF, 1x Roche Protease Inhibitor Cocktail). Lysates were incubated at 100° C for 3 minutes and passaged through a QIAshredder (QIAGEN). The lysates were then diluted with 2.5 volumes of immunoprecipitation dilution buffer (100 mM NaCl, 20 mM sodium borate, 15 mM EDTA, 15 mM EGTA, 0.7% BSA, 1.2% TX-100, 10 μM iodoacetamide, 200 μM PMSF) and centrifuged to remove insoluble protein. Samples were immunoprecipitated following standard protocol. Following electrophoresis and transfer to PVDF membranes, membranes were treated for 30 minutes at 4° C in denaturing buffer [148] (6 M guanidine-HCl, 20 mM Tris-HCl pH 7.5, 5 mM 2-mercaptoethanol), rinsed well and processed as a normal western.

Biotinylation- RT112 cells were rinsed in PBS and labeled for 20 minutes at 4° C on ice with 250 μg/mL Sulfo-NHS-SS-BIOTIN (Thermo Scientific). Cells were washed 3x in TBS and then incubated in complete media (RPMI + 10% FBS) with either 1 μM 17-AAG or DMSO for indicated times at 37° C. Cells were lysed, protein quantified and equal amounts were affinity purified with avidin agarose beads.

Half-life determination- For cycloheximide experiments, cells were treated as indicated in the presence of 100 μM cycloheximide. Cells were lysed, immunoprecipitated and subjected to western analysis. For ^{35}S half-life determination, transfected 293 cells were subjected to pulse chase analysis as previously described with the addition of DMSO or 1 μM 17-AAG in the chase [44]. For BFA experiments, cells were pulsed (25 minutes) and chased in the presence of 6 μg/mL BFA. Half-lives were calculated by subtracting background densitometry (captured from phosphor screen) and fitting to a one-phase decay curve using GraphPad software.

Mass Spectrometry- 1D SDS–PAGE bands were subjected to in-gel digestion with trypsin. Identification of tryptic peptides was performed by liquid chromatograph-mass spectrometer equipped with an electrospray ionization source. Proteins were identified from MS/MS spectra by a database search of the identified peptides using the software provided with the instrumentation.

Cell viability and signaling assays- Serum starvation of the RT112 cell line was in DMEM, while the Hela cells were starved in DMEM + 0.1% FCS. For MTT proliferation assays, cell lines were plated at appropriate densities (RT112 $1x10^4$, Hela $7.5x10^3$, RCS $5x10^3$ cells per well) in a 96-well dish and incubated overnight. Drugs or vehicle were added as indicated and a MTT assay was performed (Roche). For FGF experiments, cells were pretreated with 17-AAG for 4 hours before the addition of growth factor.

2.4 Results

FGFR3 interacts with Hsp90 and co-chaperones. To screen for proteins that interact with activated FGFR3, we transiently transfected GFP tagged constitutively activated FGFR3 (CA-FGFR3, K650E mutation of thanatophoric dysplasia type II) or GFP alone into 293 cells [14]. Immunoprecipitation (IP) of FGFR3 pulled-down multiple species of the receptor and other distinct bands (Figure 2.1A). Prominent bands from several replicates were identified by N-terminal sequencing and mass spectrometry as the chaperones Hsp90 and Hsp70 (Figure 2.1A and Figure 2.S1A). Improved separation of the IgG heavy chain band subsequently revealed a 50 kDa band containing fragments of the kinase specific co-chaperone Cdc37 by mass spectrometry (Figure 2.S1A, B).

These results were confirmed by coimmunoprecipitation and western blotting, which consistently showed that Hsp90 and Cdc37 immunoprecipitated with wild-type (WT-FGFR3), CA-FGFR3 and kinase dead FGFR3 (KD-FGFR3, K508A) (Figure 2.1B) [149]. Although Hsp70 was frequently pulled-down nonspecifically in negative controls, it was usually enriched in FGFR3 specific pull-downs (Figure 2.1A and 2.1E). In the reverse immunoprecipitation, Hsp90 pulled-down immature (120 kDa) and mature (130 kDa) forms of WT-, CA- and KD-FGFR3 suggesting that Hsp90 can interact with the receptor throughout its maturation and trafficking in the secretory pathway (Figure 2.1C) [150]. Immunoprecipitation of Cdc37 and blotting for FGFR3 revealed that Cdc37, unlike Hsp90, interacted more strongly with CA-FGFR3 (Figure 2.1D). The tighter association was with the 120 kDa immature high mannose endoplasmic reticulum (ER) form of the

mutant receptor, in contrast to the 130 kDa cell surface form, suggesting that that the chaperone complexes associating with immature CA-FGFR3 may be enriched in Cdc37.

To determine if Hsp90 interacts with endogenous FGFR3, FGFR3 was immunoprecipitated from RT112 bladder cancer cells, which express high levels of wild-type FGFR3 [151]. The immunoprecipitation pulled-down Hsp90 and Cdc37 and was enriched for Hsp70 (Figure 2.1E). In the reverse immunoprecipitation, Hsp90 pulled-down endogenous FGFR3 but not the weak Hsp90 client EGFR (Figure 2.1F). These data demonstrate that FGFR3 can interact with Hsp90 chaperone complexes regardless of whether the receptor is expressed endogenously (Figure 2.1E) or exogenously with a C-terminal tag (Figure 2.1A-GFP, Figure 2.1B-V5) or untagged (Figure 2.S2A).

Hsp90 inhibitors typically interfere with the Hsp90:client interactions [152, 153]. Indeed, a concentration-dependent decrease of Hsp90 coimmunoprecipitating with FGFR3 was detected for the two structurally dissimilar Hsp90 inhibitors 17-AAG and radicicol, which correlated with their affinities for Hsp90 (Figure 2.1G) [154, 155]. Celastrol, an inhibitor of the Cdc37/Hsp90 interaction, also disrupted binding, while quercetin, which alters Hsp90 complexes but not Hsp90 client binding, did not disrupt Hsp90 coimmunoprecipitation [156, 157].

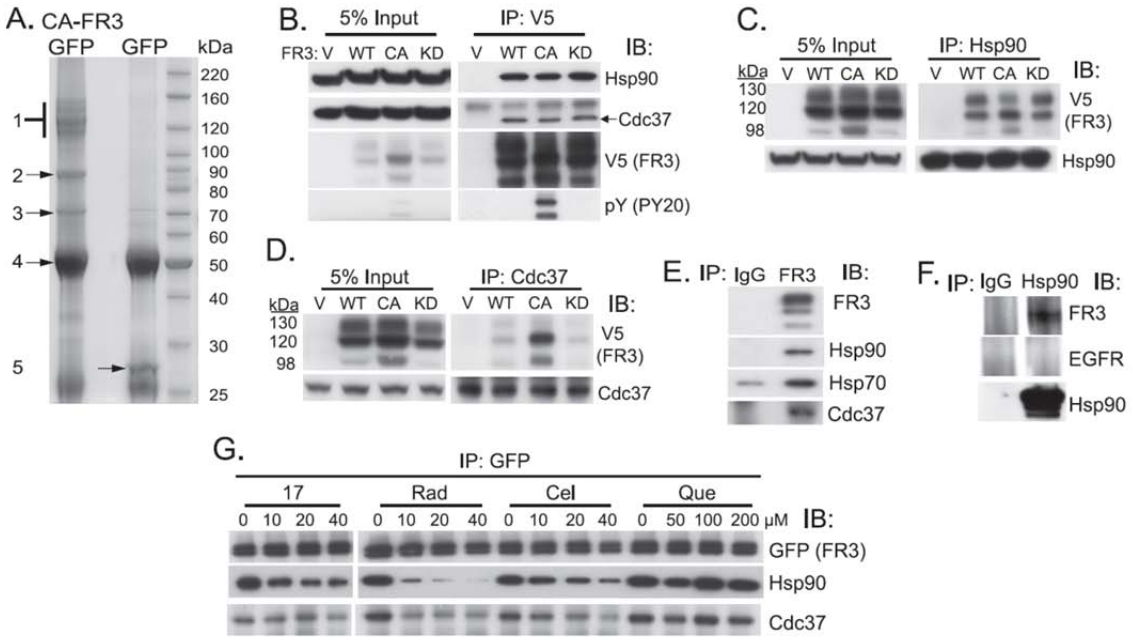

Figure 2.1 *FGFR3 associates with Hsp90 and Cdc37*. *A.* Coomassie stain of immunoprecipitated CA-FGFR3-GFP or GFP from 293 cells. 1-FGFR3; 2-Hsp90A/B; 3-Hsp70; 4-IgG heavy chain; 5-GFP. *B.* Immunoprecipitation (IP) of transfected V5 tagged WT-, CA- or KD-FGFR3 and immunoblotting (IB) for Hsp90, Cdc37, V5 (FR3) or phosphotyrosine (PY20) in 293 cells. *C.* IP of endogenous Hsp90 and blot for transfected FGFR3 (V5) in 293 cells. *D.* IP of endogenous Cdc37 and blot for transfected FGFR3 (V5) in 293 cells. *E.* IP of endogenous FGFR3 (FR3) from RT112 cells and blot for Hsp90, Hsp70 and Cdc37. IgG-rabbit IgG used as control. *F.* IP of Hsp90 from RT112 cells and blot for FGFR3 and EGFR. IgG-mouse IgG used as control. *G.* 293 cells inducibly expressing WT-FGFR3-GFP were treated for 1 hour with increasing concentrations of Hsp90 inhibitors (17: 17-AAG, Rad: radicicol, Cel: celastrol, Que: quercetin), immunoprecipitated for GFP and blotted as indicated.

FGFRs differentially associate with Hsp90 complexes. Hsp90 interacts with kinase clients through their kinase domain [89, 153]. Because the amino acid sequence for this domain is highly conserved for FGFR family members (Figure 2.2A), we tested if other FGFRs interact with Hsp90 and Cdc37. When untagged FGFRs (with the exception of FGFR4 due to lack of an immunoprecipitation antibody) were expressed and immunoprecipitated with receptor specific C-terminal antibodies, Hsp90 readily pulled-down (Figure 2.S2A). FGFR3 consistently pulled-down more Hsp90 in these experiments; however, no direct comparison could be made due to differences in the affinities of the receptor specific antibodies. For a more accurate comparison, we tagged the receptors with a C-terminal V5 epitope. Expression and immunoprecipitation of equal amounts of lysate revealed that FGFR3 associated more strongly with Hsp90 than the other FGFRs (Figure 2.2B). Similarly, Cdc37 pulled-down more strongly with FGFR3 and was faintly observed for FGFR1 and FGFR4 but not for FGFR2.

The kinase domain αC-ß4 loop is important for Hsp90 binding to some kinases, notably the EGFR/ErbB family of receptor tyrosine kinases [142, 158]. Binding is favored by the lack of negatively charged residues in the loop. In fact, the presence of a single aspartic acid residue in the loop distinguishes the weak client EGFR from the strong client ErbB2, which has a glycine in the same position. Sequence alignment of the FGFRs alongside EGFR and ErbB2 shows that the FGFRs lack negatively charged residues in this loop and have a glycine in the key position (Figure 2.2A). To test if this glycine residue plays a similar role in the FGFR3:Hsp90 interaction as it does for the ErbB2:Hsp90 interaction, we mutagenized FGFR3 glycine G533 to an aspartic acid and

compared the two receptor proteins in pull-down assays. Mutation of this residue did not disturb Hsp90 or Cdc37 association with FGFR3 (Figure 2.2C).

Further examination of the N-terminal lobe of the FGFR's kinase domain revealed a difference that could potentially explain the differential binding of Hsp90 to FGFRs. Residue 548 in the adjacent FGFR3 β4-β5 loop is a glycine in contrast to aspartic acid in FGFR1 and FGFR2 or glutamic acid in FGFR4 (Figure 2.2A). We mutated this residue to aspartic acid in FGFR3 and to glycine in the other FGFRs (Figure 2.2D). Swapping of these residues did not significantly alter the binding pattern except for that of FGFR4 which decreased rather than increased binding.

To narrow down the binding region of Hsp90 and Cdc37 to FGFR3 and to confirm its specific association with the kinase domain, we carried out domain swapping experiments between FGFR3 and the weakest Hsp90 binder FGFR2. Swapping of the entire kinase domain of FGFR2 into FGFR3 prevented strong association of Hsp90 and Cdc37 with chimeric FGFR3 (Figure 2.2E). Interestingly, the chimeric kinase receptor displayed an increase in its apparent steady state stability and altered the ratio of biosynthetic species to mimic that of FGFR2. Further swapping of the individual lobes of the kinase domain revealed that Hsp90 and Cdc37 did not bind to the FGFR3 chimera with FGFR2's N-lobe/hinge, but did bind to FGFR3 containing the FGFR2 C-lobe/kinase insert. These results indicate that Hsp90 and Cdc37 strongly bind to the N-lobe/hinge of FGFR3. Taken together, our results suggest that Hsp90 binding to FGFRs is distinct from the EGFR family as has been observed for other Hsp90 kinase clients [159, 160].

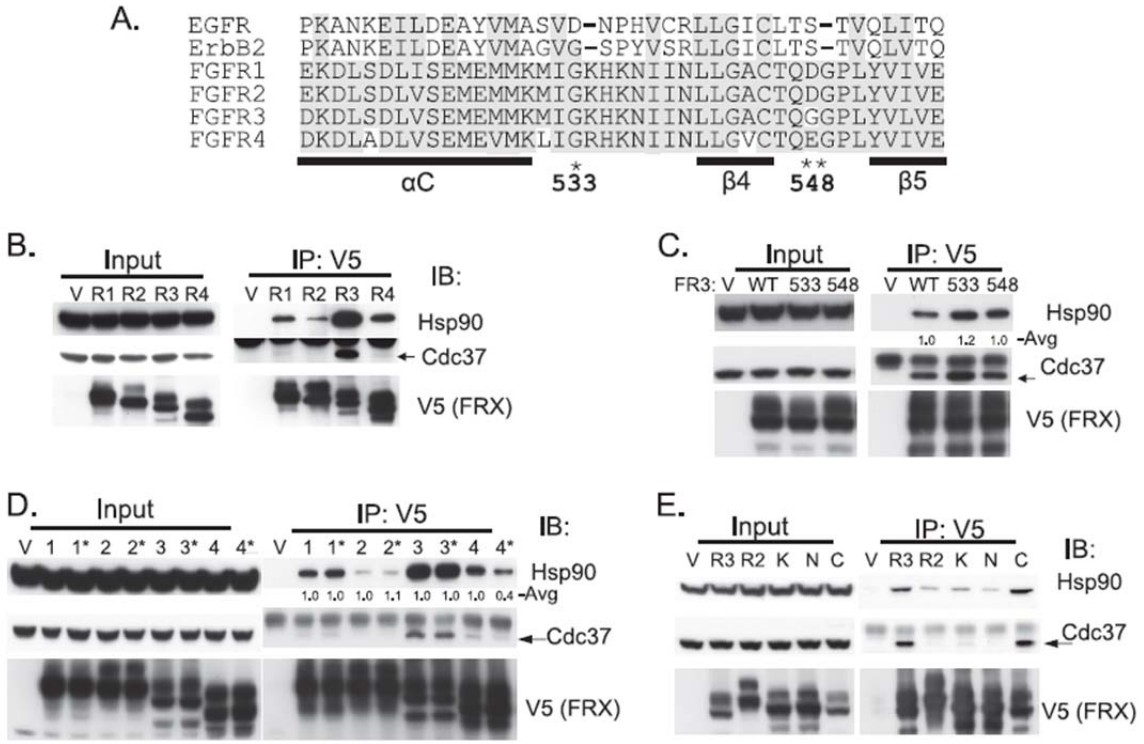

Figure 2.2 *FGFRs differentially associate with Hsp90 complexes*. *A.* Sequence alignment of part of the EGFR, ErbB2 and FGFR family kinase domains. Grey shading indicates identical/related residues. Boxed and * marks the conserved glycine (FGFR3 G533 in human). ** indicates a negatively charged residue (G548) absent in FGFR3 relative to the other FGFRs. Secondary structures are identified below by black boxes based on the analysis by Chen *et al* [20]. *B.* Transfection of empty vector (V) or FGFR1-4 V5 in 293 cells followed by V5 IP and blotting. Arrow denotes the Cdc37 band running just below the IgG heavy chain. *C.* Transfection in 293 cells of empty vector (V), WT-FGFR3 (WT), G533D FGFR3 (533) or G548D FGFR3 (548) followed by IP and blotting. -Avg indicates the averaged ratio of the amount of Hsp90 pull-down by mutated receptor relative to the wild-type receptor. *D.* 293 transfection of empty vector (V) or FGFR1-4 with a swapping mutation of the respective residue found in FGFR3 (548) as indicated by an asterisk (R1/2 D to G, R4 E to G, R3 G to D). *E.* 293 transfection followed by IP and blotting of FGFR3 (R3), FGFR2 (R2) or chimeras FGFR3/kinase-FGFR2 (K), FGFR3/N-lobe-hinge-FGFR2 (N) and FGFR3/C-lobe-kinase insert-FGFR2 (C).

FGFR3 requires Hsp90 function for stability. Altering the chaperone:client interaction through inhibition of Hsp90 function rapidly destabilizes strong Hsp90 client proteins [89]. To determine the dependence of FGFR3 stability on Hsp90 function, we examined endogenous receptor stability in the presence of 17-AAG. FGFR3 stability was compared to that of the strong and weak clients ErbB2 and EGFR, respectively, which are also endogenously expressed in the RT112 cells. FGFR3 was rapidly destabilized by 17-AAG, even more so than ErbB2 (Figure 2.3A). A comparison of untagged, stably induced receptors in 293 cells showed that FGFR3 is less sensitive to 17-AAG than ErbB2, but more sensitive than EGFR (Figure 2.S2B). These results suggest that cellular context may influence the dependence of FGFR3 stability on Hsp90, as has been reported for other Hsp90 clients [141]. Confocal imaging of FGFR3-GFP revealed decreased fluorescence after addition of 17-AAG (Figure 2.3B) further supporting the need of Hsp90 function for FGFR3 stability.

To further document the loss of FGFR3 stability associated with Hsp90 inhibition and to exclude that it is mediated by Hsp90 effects on transcription and translation, we performed ^{35}S pulse-chase half-life analysis. A substantial decrease in FGFR3 half-life was consistently observed in the presence of Hsp90 inhibitors when the receptor was expressed either transiently (Figure 2.3C) or stably (Figure 2.S2D). This reduction was dose dependent (Figure 2.S2D). These results were validated for endogenous FGFR3 in RT112 cells. Because immunoprecipitation of FGFR3 in the RT112 cells pulled-down a non-specific radioactively labeled band, which confounded interpretation, cycloheximide was used to determine the half-life in this cell line. The half-life of FGFR3 was

decreased by 50%, from 4 to 2 hours in the presence of 17-AAG (Figure 2.3D). Originally we hypothesized that CA-FGFR3 would be destabilized by 17-AAG more than WT-FGFR3. Although we found a variable response depending on the cell line tested, CA-FGFR3 was destabilized less than WT-FGFR3 in three paired transfection experiments (WT-FGFR3 destabilized by an average of 51 ± 3% of vehicle and CA-FGFR3 31 ± 7%). In contrast, in our stable COS7 cell lines, where adaptation to CA-FGFR3 results in a similar half-life for the two receptors, the half-life decreased to a similar degree (Figure 2.S2D). These findings support the idea that like ErbB2, FGFR3 is a strong Hsp90 client and requires Hsp90 function for stability even when constitutively activated.

Pulse-chase analysis was used to assay the half-lives of the other FGFRs in the presence of 17-AAG (Figure 2.3E). As for FGFR3, the half-life of FGFR4 decreased in response to Hsp90 inhibition. FGFR1 displayed a small increase, while FGFR2 showed a modest increase in half-life. Although rare, an increase in half-life in response to Hsp90 inhibition has been reported [161, 162]. The trend we detected for half-life is consistent with what we observed for Hsp90 binding (Figure 2.2B). Despite differences in experimental conditions, i.e. cell type and means of receptor expression, FGFR3 was consistently more sensitive to 17-AAG mediated destabilization than the other FGFRs with FGFR2 as the most resistant.

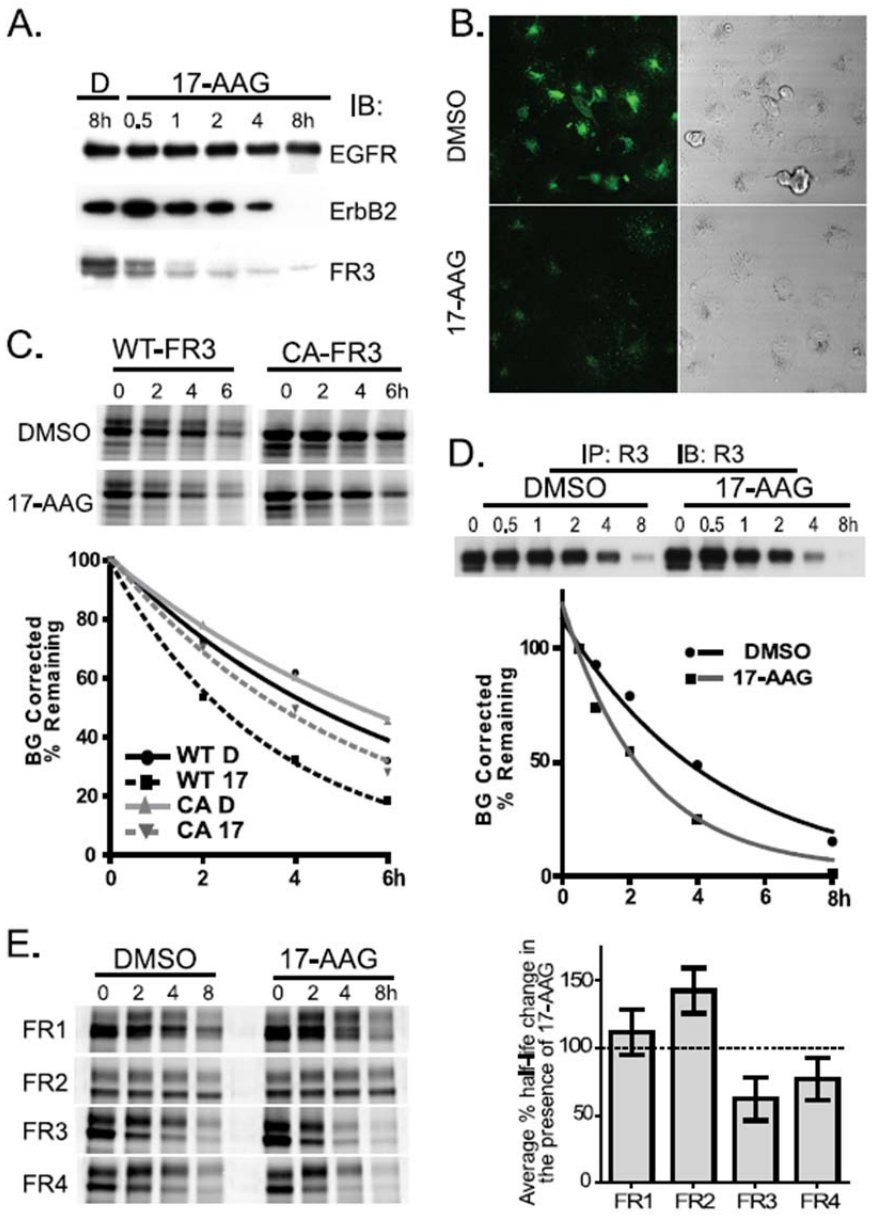
A.
D
17-AAG
IB:
8h 0.5 1 2 4 8h
EGFR
ErbB2
FR3
B.
DMSO
17-AAG
C.
WT-FR3
CA-FR3
0 2 4 6
0 2 4 6h
DMSO
17-AAG
BG Corrected % Remaining
WT D
WT 17
CA D
CA 17
D.
IP: R3 IB: R3
DMSO
17-AAG
0 0.5 1 2 4 8
0 0.5 1 2 4 8h
BG Corrected % Remaining
DMSO
17-AAG
E.
DMSO
17-AAG
0 2 4 8
0 2 4 8h
FR1
FR2
FR3
FR4
Average % half-life change in the presence of 17-AAG
FR1 FR2 FR3 FR4

Figure 2.3

Figure 2.3 *FGFR3 requires Hsp90 function for stability*. *A.* Time course of 1 μM 17-AAG or vehicle (DMSO, D) in whole cell lysates from RT112 cells. *B.* Immunofluorescence of stably expressed WT-FGFR3-GFP in COS7 cells in the presence of DMSO or 1 μM 17-AAG for 3 hours. *C.* ^{35}S half-life of transfected WT-FGFR3 and or CA-FGFR3 in 293 cells in the presence or absence of 1 μM 17-AAG. The graph represents background subtracted densitometry relative to the percentage remaining at time 0. *D.* Cycloheximide half-life analysis of immunoprecipitated and blotted FGFR3 in the presence or absence of 0.5 μM 17-AAG in RT112. The graph represents background subtracted band densitometry expressed as the percent remaining relative to 0.5 hour. *E.* Representative ^{35}S pulse chase half-life analysis scan of transfected FGFR1-4 V5 in 293 cells and chased in the presence or absence of 1 μM 17-AAG. Graph represents the average percent change in half-life in response to 1 μM 17-AAG relative to DMSO control. Error bars are +/- standard deviation (*n*=3).

Inhibition of Hsp90 results in ubiquitin-mediated degradation of FGFR3. Inhibition of Hsp90 function alters co-chaperone complex composition and promotes the incorporation of E3-ubiquitin ligases, leading to client ubiquitination and degradation [143]. To determine if FGFR3 undergoes ubiquitination after Hsp90 inhibition, we treated RT112 cells with 17-AAG and immunoprecipitated FGFR3 under denaturing conditions. FGFR3 displayed a time dependent increase in total ubiquitination after 17-AAG treatment but not with vehicle control (Figure 2.4A). A coincidental decrease in total FGFR3 levels was observed at later time points. These results are consistent with the observed decrease in half-life and are characteristic of strong Hsp90 clients.

We next determined if 17-AAG induces ubiquitination of other FGFR family members. For direct comparison, tagged FGFRs were transfected and immunoprecipitated under denaturing conditions following treatment with 17-AAG for 1 hour. FGFR3 and FGFR4 displayed increases in polyubiquitination, with FGFR1 showing a small increase and FGFR2 showing no response (Figure 2.4B). Although not comparable among receptors, similar trends were observed in response to 17-AAG treatment for untagged receptors (Figure 2.S2C). These responses to Hsp90 inhibitors echo the observed relative associations of Hsp90 with the receptors and the changes in half-life in response to Hsp90 inhibition.

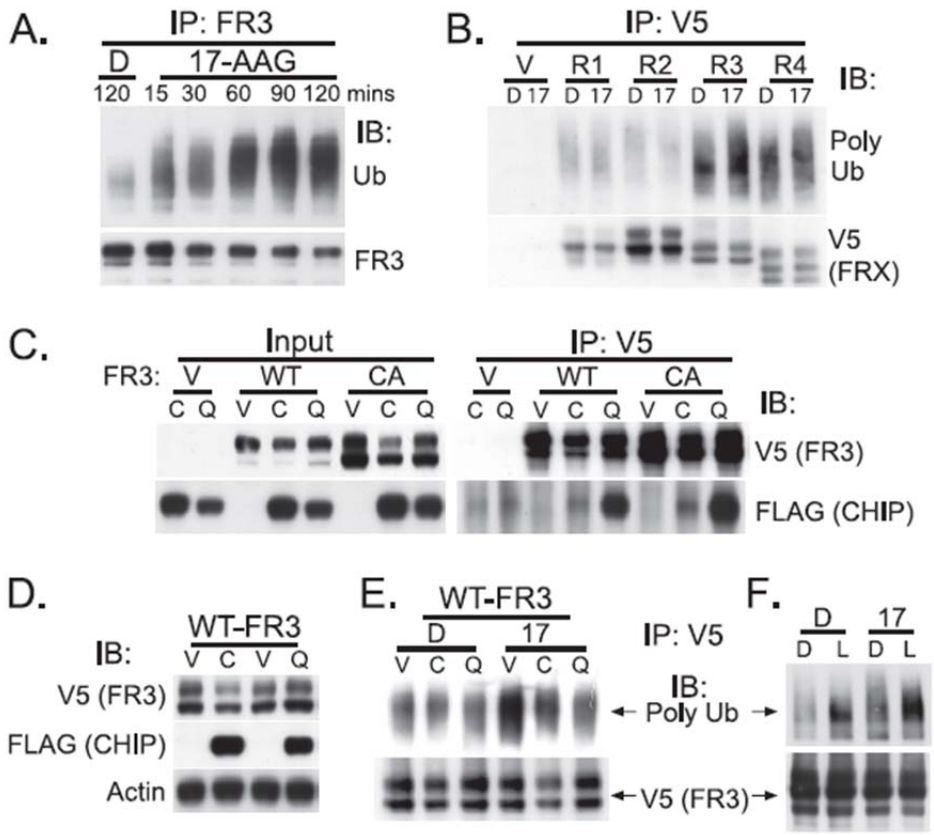

Figure 2.4 *Hsp90 inhibition results in FGFR3 ubiquitination*. *A.* Time course of total ubiquitin blotting of immunoprecipitated FGFR3 from RT112 in the presence of 0.5 μM 17-AAG or DMSO (D) for the indicated times. *B.* Transiently expressed V5 tagged FGFR1-4 (R1-R4) in 293 cells for 48 hours. Cells were treated for 1 hour with 1 μM 17-AAG (17) or vehicle (D) followed by IP and blotting for polyubiquitin (Poly Ub). *C.* Cotransfection (24 hours) of WT- or CA-FGFR3-V5 with empty vector (V), CHIP-FLAG (C) or H260Q-FLAG (Q) in 293 cells, followed by V5 IP and probed as indicated. *D.* Equal protein loaded from whole cell lysates of cotransfected (48 hours) WT-FGFR3-V5 with CHIP-FLAG (C), H260Q-FLAG (Q) or empty vector (V) *E.* 293 cells were cotransfected with WT-FGFR3-V5 and empty vector (V), CHIP-FLAG (C) or H260Q-FLAG (Q). After 24 hours cells were treated for 1 hour with 1 μM 17-AAG or DMSO followed by IP and polyubiquitin blotting (Poly Ub). *F.* Transfection and IP of WT-FGFR3-V5 in the presence of 5 μM lactacystin (L) or vehicle (D-DMSO) for 5 hours, with the last hour in the presence of 1 μM 17-AAG (17) or vehicle (D-DMSO).

CHIP can interact and influence the stability of FGFR3. CHIP is an E3-ubiquitin ligase that binds to the C-terminal tail of Hsp70 and Hsp90 and catalyzes the ubiquitination of client proteins [143]. Upon treatment with an Hsp90 inhibitor, Hsp90 complexes incorporate CHIP leading to client ubiquitination and degradation. We were unable to convincingly detect endogenous CHIP in FGFR3:Hsp90 coimmunoprecipitations, which we attributed to the technical limitations of the available antisera (data not shown). Thus, we performed coimmunoprecipitation studies with transiently expressed FGFR3 and FLAG-tagged CHIP. As a control we used dominant-negative H260Q-CHIP-FLAG (H260Q), which has a mutated E2 interaction site thereby preventing ubiquitin conjugation but not client binding [163]. After immunoprecipitation of FGFR3, CHIP-FLAG was barely detectable above background but the catalytically inactive H260Q-CHIP immunoprecipitated with both WT- and CA-FGFR3 (Figure 2.4C). Increased detection of H260Q in coimmunoprecipitations has been reported for other Hsp90 clients such as ErbB2 and has been attributed to "enzymatic trapping" of H260Q-CHIP [164].

We next examined the extent to which CHIP can destabilize FGFR3 by cotransfecting CHIP or H260Q with WT-FGFR3 for 48 hours. WT-FGFR3 was destabilized when co-transfected with CHIP but not H260Q (Figure 2.4D). Our working model predicts that this destabilization results from CHIP-mediated ubiquitination of FGFR3, and that this would be enhanced by Hsp90 inhibition. To test this prediction, CHIP or H260Q was cotransfected with WT-FGFR3 in the presence or absence of 17-AAG for 24 hours (Figure 2.4E). We did not observe an increase in ubiquitination upon cotransfection with

CHIP, presumably due to a rapid destabilization of this ubiquitinated population over the 24 hours of cotransfection. Most significantly however, H260Q did not destabilize FGFR3 and protected it from 17-AAG induced ubiquitination (Figure 2.4E). Although other ubiquitin ligases can compensate for ubiquitination of Hsp90 clients in the absence of CHIP [120, 165], our results suggest that as for many Hsp90 clients, CHIP can affect FGFR3 stability.

CHIP targeted proteins are commonly reported to be degraded by proteasomes [143]. Adding the proteasomal inhibitor lactacystin to FGFR3 enhanced receptor polyubiquitination and this effect was further enhanced by the addition of 17-AAG (Figure 2.4F). These findings are consistent with a role for the proteasome in the degradation of FGFR3 in response to 17-AAG.

Hsp90 inhibition reduces FGFR3 signaling output. As receptors typically initiate signaling from the cell surface, we next asked if inhibition of Hsp90 function destabilizes FGFR3 residing at this location. Surface receptors of RT112 cells were biotinylated, incubated with or without 17-AAG and analyzed following affinity purification of biotin labeled proteins. Inhibition of Hsp90 accelerated degradation of biotinylated FGFR3 (Figure 2.5A) as was also observed for the strong client ErbB2 but not for the weak client EGFR. These data suggest that Hsp90 inhibitors effectively reduce the cell surface population of FGFR3.

Some mutations directly activate FGFR3 kinase activity eliminating the need for the receptor to dimerize or reach the cell surface for signaling. To determine if Hsp90

inhibitors can destabilize intracellularly retained receptors, we carried out ^{35}S pulse-chase analysis of FGFR3 in the presence of brefeldin A (BFA), which prevents anterograde trafficking from the ER thereby trapping newly synthesized and labeled FGFR3. A chase in the presence of 17-AAG and BFA showed reduced stability of this population of FGFR3 over time (Figure 2.5B). We also observed a progressive increase in the molecular weight of FGFR3, presumably due to continued exposure of the retained receptor to glycosylating enzymes residing in the ER as a consequence of the BFA blockade.

One would expect the decreased FGFR3 levels resulting from Hsp90 inhibition to be accompanied by reduced FGFR3 signal output. To confirm this expectation, we assayed FRS2 and ERK1/2 for phosphorylation as proximal and distal readout markers of MAP kinase signaling respectively in RT112 cells. Both FRS2 and ERK1/2 were constitutively phosphorylated in the absence of FGF stimulation despite serum starvation for 20 hours (Figure 2.5C). Treatment with 17-AAG for 1.5 hours abolished phosphorylation of both markers and also significantly reduced phosphorylation after 10 minutes of ligand stimulation (Figure 2.5C).

As the viability of RT112 cells depends on FGFR3 function, we reasoned that destabilization of FGFR3 by Hsp90 inhibitors would reduce their viability [65]. MTT assays, which measure respiring cells and over time reflect a combination of proliferation and survival, were performed in the presence of increasing concentrations of inhibitors (Figure 2.5D). A dose dependent reduction in cell viability was observed for 17-AAG.

These cells showed a similar response to radicicol and to the FGFR kinase inhibitor PD173074.

We next asked if Hsp90 inhibition alters the responses of other cell types to FGF stimulation. Hela cells undergo growth arrest when serum starved; they display a proliferative response when subsequently treated with serum or FGF and assayed by MTT. This response was ablated by treating cells with 100 nM 17-AAG 4-hours prior to, and during the 3-day exposure to FGF1 (Figure 2.S2E). This protocol had minimal effects on the mitogenic response to serum stimulation.

Finally, we examined rat chondrosarcoma (RCS) cells, which like chondrocytes reduce proliferation in response to FGF stimulation. They display a reduction in proliferation as measured by reduced viability and proliferation in response to FGF9 over 48 hours as previously reported [166]. Low concentrations of 17-AAG blocked this reduction in a dose-dependent manner (Figure 2.5E). As expected inhibition of FGFR3 kinase activity with PD173074 also increased proliferation. Similar results were seen with FGF2 (Figure 2.S2F). We conclude that Hsp90 inhibitors can block FGFR3 signal output and can modulate FGFR3 signaling pathways and even reverse its growth inhibitory signals.

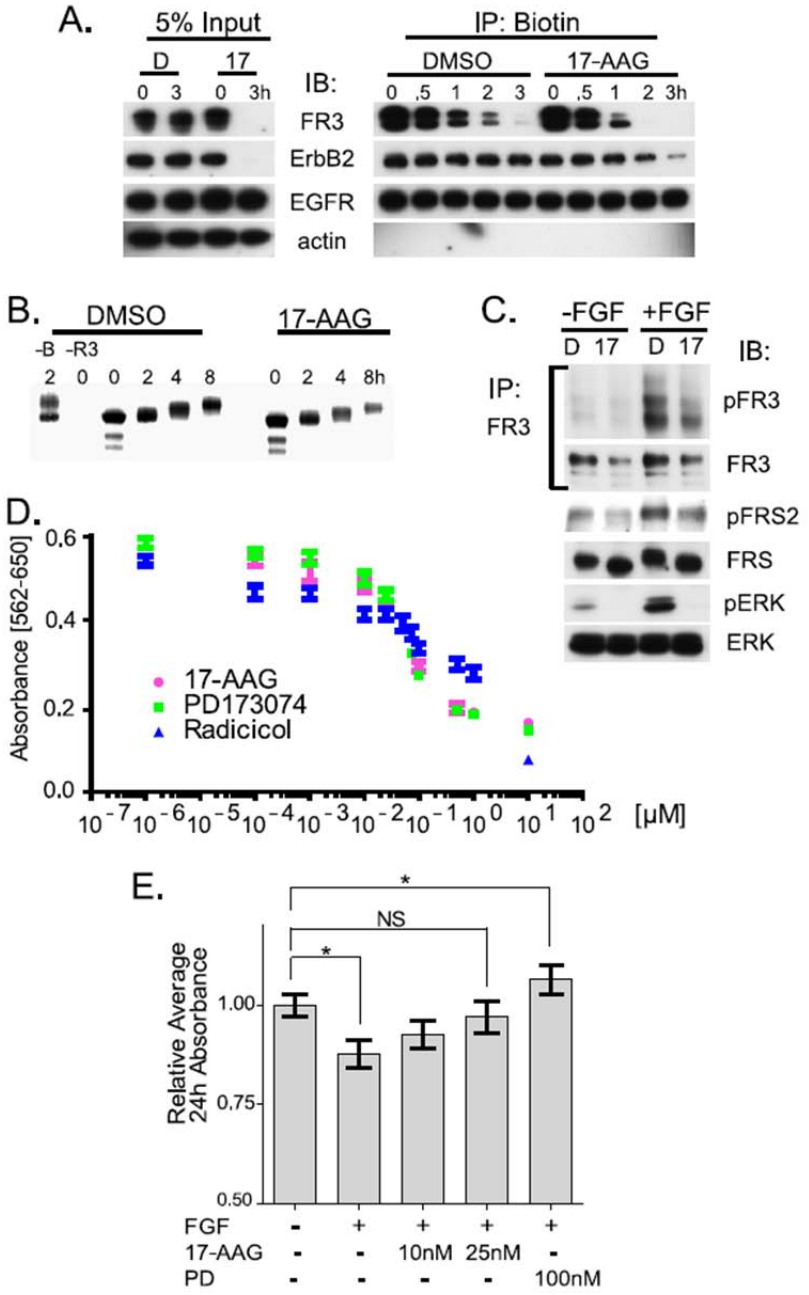
A.
5% Input
IP: Biotin
D
17
DMSO
17-AAG
IB:
FR3
ErbB2
EGFR
actin
B.
DMSO
17-AAG
-B
-R3
C.
-FGF
+FGF
IP:
FR3
pFR3
FR3
pFRS2
FRS
pERK
ERK
D.
Absorbance [562-650]
17-AAG
PD173074
Radicicol
[μM]
E.
Relative Average 24h Absorbance
NS
FGF
17-AAG
PD
10nM
25nM
100nM

Figure 2.5

Figure 2.5 *Loss of Hsp90 function reduces FGFR3 bioactivity*. *A.* RT112 cell surface proteins were biotinylated and then chased in 1 μM 17-AAG (17) or DMSO (D) for indicated times, affinity purified and blotted as indicated. Actin exposure serves as a control for cell surface specific biotinylation. *B.* ^{35}S pulse chase of transfected WT-FGFR3-V5 in 293 cells in the presence of BFA (-B is no BFA control) and DMSO (D) or 1 μM 17-AAG (17). –R3 is empty vector control. *C.* Serum starved RT112 incubated with 1 μM 17-AAG (17) or DMSO (D) for 1.5 hours and then treated with FGF1 for 10 minutes. *D.* MTT assay in RT112 cells after 48 hours of growth in the presence of increasing concentrations of inhibitors. *E.* RCS cells were pretreated for 4 hours with DMSO, 17-AAG, or PD173074 (PD) and then stimulated with 50 ng/mL FGF9 in the continued presence of the drugs for 48 hours. Data is graphed relative to the average vehicle absorbance (no FGF, DMSO). * indicates statistical significance by two-tailed paired t-test ($p<0.01$). NS. Not statistically different. Error bars are +/- Std. Dev.

2.5 Discussion

The data presented here establish FGFR3 as a strong Hsp90 client. The degree to which FGFR3 is stabilized by Hsp90 is underscored by the rapid degradation of both intracellular and cell surface receptors and a subsequent loss in signal output following Hsp90 inhibition. FGFR3's dependence on Hsp90 contrasts with that of the other FGFR family members that interact and respond to 17-AAG differently. Overall, our findings provide a new context for understanding FGFR3 biology and for treating FGFR3-related disease.

We found that Hsp90 association was stronger for FGFR3 compared to other FGFRs although their stability was also influenced by Hsp90 inhibition. We consistently observed a hierarchy of destabilization by 17-AAG treatment, with FGFR3>FGFR4>>FGFR1>>>FGFR2. Interestingly, FGFR2 exhibited little binding to Hsp90 but its half-life was increased in the presence of 17-AAG, a phenomenon that has been reported for other proteins and may illustrates the variable nature of Hsp90:kinase interactions and/or indirect responses [161, 167].

We detected similar binding of Hsp90 to WT-, CA-, and KD-FGFR3 as has been observed for strong Hsp90 clients, such as ErbB2, that interact with Hsp90 independent of activation [153]. In contrast to ErbB2, however, we observed that addition of a negatively charged residue into the αC-β4 loop of FGFR3 did not disrupt binding to Hsp90 or Cdc37. This finding illustrates the multifactorial association of Hsp90 chaperone complexes with kinases [89]. Along these lines, it has been suggested that

Hsp90 binding may be linked to kinase dimer formation [168, 169]. Indeed, given the collective observations that Hsp90/Cdc37 chaperone complexes interact with key regions of the N- and C-terminal lobes of kinases [89, 107, 158], and recent insights into the asymmetric nature of FGFR kinase domain trans-phosphorylation [170], it is conceivable that Hsp90 may play a role in asymmetric FGFR3 kinase dimer formation or its regulation.

We observed physiologic responses to Hsp90 inhibition in two cell types that we attribute largely to antagonism of FGFR3 signaling due to receptor destabilization. In the first case, bladder cancer RT112 cells, which are dependent on FGFR3 output for proliferation and survival, exhibited a dose-dependent decline in viability in response to both 17-AAG and radicicol. The response was remarkably similar to that following treatment with the FGFR tyrosine kinase inhibitor PD173074. RCS cells display a cellular phenotype similar to proliferating growth plate chondrocytes, including expression of endogenous FGFR3 and an antiproliferative response to FGF stimulation [166]. We found that pre-treatment with 17-AAG blunted the FGF-mediated inhibition of proliferation, increasing cellular growth in a dose-dependent fashion. This result is consistent with a direct effect on FGFR3 stability, although we cannot exclude that it was mediated by Hsp90 stabilized pathways unrelated to FGFR3.

We have previously reported that activated FGFR3 is degraded in lysosomes and is directed into this pathway by c-Cbl-mediated ubiquitination [43]. In fact, we observed that FGFR3 bearing gain-of-function mutations progress through this pathway less

efficiently than WT-FGFR3. Our current results suggest FGFR3 may also be degraded through a proteasomal pathway that utilizes the CHIP ubiquitin ligase and is buffered by Hsp90 stabilization. Little is known about the coordination of these two pathways, but it is conceivable that mutant receptors that escape c-Cbl-mediated degradation are stabilized by Hsp90 and Cdc37 making them susceptible to chaperone inhibitor mediated degradation. FGFR3 would not be unique as a substrate for both pathways as similar properties have been reported for the Ron tyrosine kinase [152]. Furthermore, CHIP has the capacity to target proteins for lysosomal degradation in addition to its role in proteasomal targeting [122].

While we have established in detail that FGFR3 is a client of Hsp90, others have proposed this relationship for FGFR1 and FGFR3. For example, a proteomics screen for proteins that interact with the dimerized transmembrane and intracellular domains of FGFR1 detected Hsp90 and Cdc37 [171]. A report that Hsp90 inhibitors destabilize oncogenes implicated in synovial sarcoma included FGFR3 as a kinase that responds to Hsp90 inhibition [172]. Most recently, subtypes of FGFR3-driven multiple myeloma were shown to be sensitive to a new Hsp90 inhibitor [173]. This study reported that both WT- and CA-FGFR3 interact with Hsp90 and are sensitive to Hsp90 inhibitors. Thus, our findings are consistent with and expand on previously described observations.

Our findings implicate Hsp90 in the pathogenesis of diseases resulting from activating FGFR3 mutations. It follows that Hsp90 inhibition could be an effective therapeutic strategy in these diseases, notably certain cancers and achondroplasia. The use of Hsp90

inhibitors for cancer is not new, as they are being investigated as a means to down regulate multiple oncogenic kinases [135]. Cancers in which oncogenic mutations of FGFR3 are detected, such as superficial bladder cancer and multiple myeloma, would be potential candidates for this strategy.

In contrast to cancer, the potential application of this therapeutic strategy to achondroplasia is novel although it has been used to target mutant proteins for degradation in another genetic disease [144]. SBMA is a slowly progressive muscle disease that results from a polyglutamine expansion in the androgen receptor, a known Hsp90 client protein [126]. Hsp90 inhibitor treatment of mice modeling SBMA reduced the cellular accumulation of the mutant receptor and ameliorated most of the clinical disease establishing the paradigm for this therapeutic approach. We are currently pursuing similar studies in mouse models of achondroplasia.

2.6 Supplemental Data

A.

Protein	Band	Percent Coverage	Protein ID	Accession	Representative Peptides
FGFR3	1	41	Fibroblast growth factor receptor 3 [mus musculus]	46877057	CPAAGNPTPSISWLK DGTGLVASHR DLVSCAYQVAR DVHNLDYYK
Hsp90 alpha	2	34	HSP90AA1 Heat shock protein HSP90-alpha	153792590	APFDLFENR CLELFTELAEDKENYK DLVILLYETALLSSGFSLEDPQTHANR DNSTMGYMAAK
Hsp90 beta	2	41	HSP90AB1 Heat shock protein HSP90-beta	20149594	ADLINNLGTIAK APFDLFENK CLELFSELAEDKENYK DLVVLLFETALLSSGFSLEDPQTHSNR
Hsp70	3	45	HSPA1B;HSPA1A Heat shock 70 kDa protein 1	167466173	AFYPEEISSMVLTK AQIHDLVLVGGSTR CQEVISWLDANTLAEKDEFEHK DAGVIAGLNVLR
Hsc70	3	8	HSPA8 Isoform 1/2 of Heat shock cognate 71kDa protein	5729877	DAGTIAGLNVLR SQIHDIVLVGGSTR
Cdc37	Fig S1B	20	Hsp90 co-chaperone Cdc37	5901922	LKELEVAEGGK LQAEAQQLR SMPWNVDTLSK LGPGGLDPVEVYESLPEELQK

B.

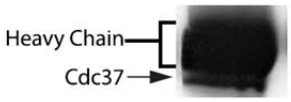

Figure 2.S1 *Summary of mass spectrometry data A.* Table summarizing the mass spectrometry data obtained from Figures 2.1A and 2.S1B. If desired more detailed information regarding this data can be obtained by contacting the authors. *B.* Coomassie staining of a gel where Cdc37 separation from the heavy chain of the antibody was resolved.

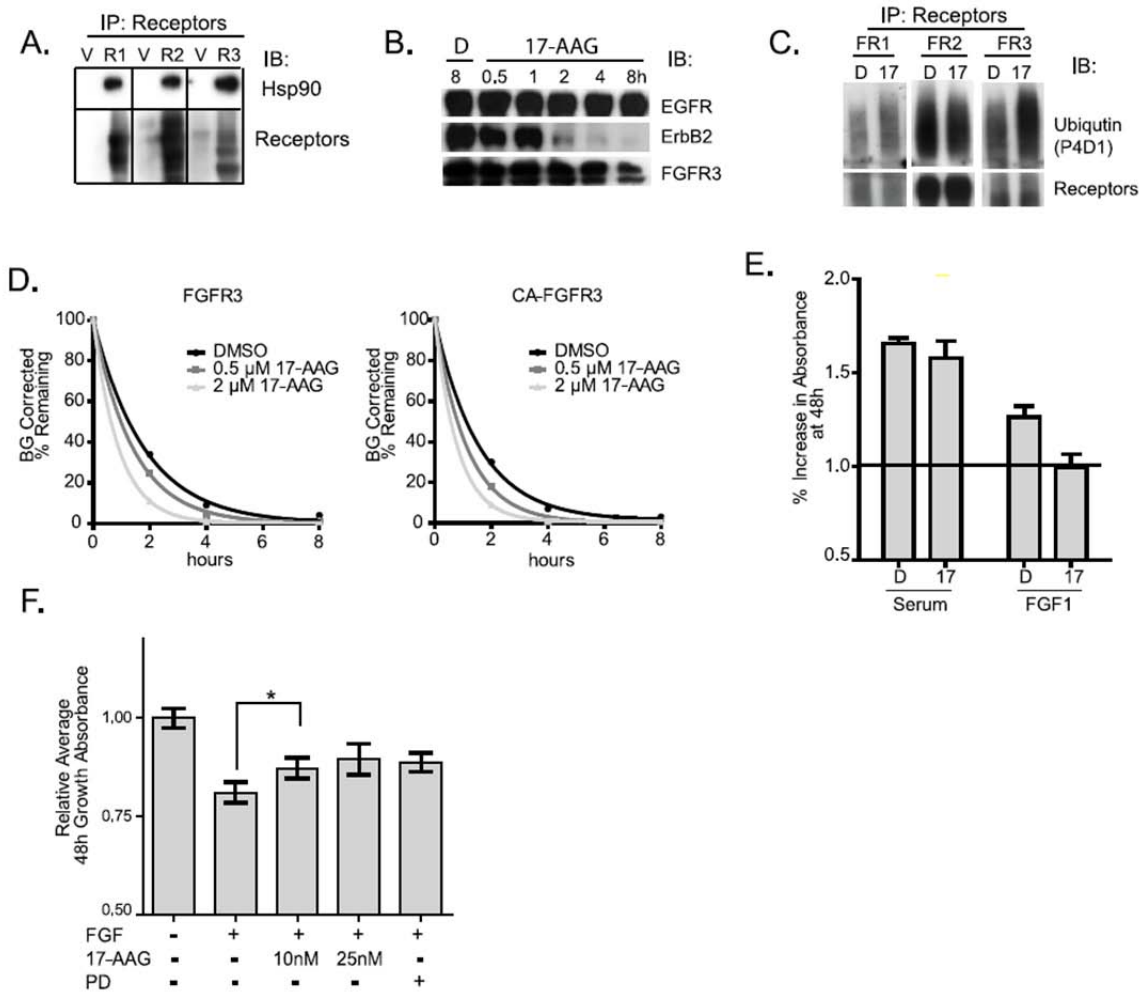
A.
IP: Receptors
V R1 V R2 V R3
IB:
Hsp90
Receptors
B.
D
17-AAG
8 0.5 1 2 4 8h
IB:
EGFR
ErbB2
FGFR3
C.
IP: Receptors
FR1 FR2 FR3
D 17 D 17 D 17
IB:
Ubiqutin (P4D1)
Receptors
D.
FGFR3
CA-FGFR3
BG Corrected % Remaining
DMSO
0.5 μM 17-AAG
2 μM 17-AAG
hours
E.
% Increase in Absorbance at 48h
D 17 D 17
Serum
FGF1
F.
Relative Average 48h Growth Absorbance
FGF
17-AAG
PD
10nM
25nM

Figure 2.S2

Figure 2.S2 *Supplemental Data.* *A.* Untagged transiently transfected FGFRs or empty vector control (V) were immunoprecipitated with sera specific to their c-terminus and blotted as indicated in 293 cells. Note, FGFR3 antibodies consistently demonstrated the weakest affinity relative to the other FGFR antibodies, with FGFR2's antibody having the highest affinity, further underscoring the inability of lane comparison. Antibodies were not able to IP mouse FGFR4. *B.* 293 inducible cell lines expressing indicated receptors for 48 hours were treated for indicated times in DMSO (D) or 1 μM 17-AAG and equal amounts of whole cell lysate were subjected to western analysis. *C.* Blotting of total ubiquitin from untagged FGFR1-3 transiently expressed in 293 cells and subjected to denaturing immunoprecipitation. Note, lanes cannot be compared between receptors due to differences in antibody affinities. *D.* Graphical analysis of COS7 cells stabling expressing wild-type or CA FGFR3-GFP were subjected to ^{35}S pulse labeling and chased in the presence of increasing concentration of 17-AAG as indicated. *E.* MTT assay of Hela cell proliferation in response to the indicated mitogenic stimulus (10% serum, 25 ng/ml FGF1) after 48 hours of growth in the absence (DMSO, D) or presence of 100 nM 17-AAG (17) (cells were pre-treated with drug for 4 hours before the addition of mitogenic stimulus). All values are relative to the average absorbance measured at Day 0 (set equal to 1). Error bars represent standard deviation. *F.* MTT assay of RCS cell proliferation after 48 hours of incubation in the absence or presence of 20 ng/ml FGF2, and treatment (from four hours before growth factor addition) with increasing concentrations of 17-AAG (10 and 25 nM) or 100 nM PD173074. * indicates statistical significance as defined by a two-tailed paired t-test ($p<0.01$).

CHAPTER 3

CONCLUSIONS AND FUTURE DIRECTIONS

The central goal of this dissertation research was to determine if the initially observed association of Hsp90 with FGFR3 was specific and if it could serve as a therapeutic target to increase linear bone growth in achondroplasia. Using a variety of experimental approaches, I determined that Hsp90 associated with the kinase domain of FGFR3 and that this was required for its stability. The therapeutic relevance of this interaction was examined in several preliminary studies in pre-clinical models of achondroplasia with little success (detailed in the appendix). The following section will briefly review these conclusions, their limitations and the knowledge contributed to the field during the course of these studies.

3.1 Conclusions

The work presented in Chapter 2 defined the association and role of Hsp90 in FGFR3 stability and function. FGFR3, regardless of its activation state, associated with Hsp90 and cochaperone Cdc37 by immunoprecipitation studies. The kinase domain of FGFR3 is required for its interaction with Hsp90, and specific sequences within the N-lobe/hinge of the kinase domain are necessary for the ability of FGFR3 to strongly associate with Hsp90. These results are in contrast to those found for other FGFRs, which appear to bind Hsp90 weakly. Treatment of FGFR3-containing cell lines with the Hsp90 inhibitor 17-AAG resulted in increased ubiquitination of FGFR3 and reduced its half-life at both

the cell surface and when trapped in the endoplasmic reticulum. FGFR3 was also able to associate with dominant negative CHIP by co-immunoprecipitation studies, suggesting that CHIP can associate with FGFR3 complexes and that it likely plays a role in the ubiquitination of FGFR3 in response to Hsp90 inhibitors. Taken together, these results establish FGFR3 as a strong Hsp90 client.

These results are the first in-depth analysis of the interaction of FGFR3 and the FGFR family with Hsp90 and cochaperones. These experiments clearly define a new therapeutic strategy to target FGFR3 stability in diseases such as cancer and achondroplasia, and warrant further examination of the mechanisms through which the differential association of Hsp90 with the FGFRs alters receptor signaling and biological output. These experiments are complicated by the fact that inhibition of Hsp90 function can affect many different aspects of cellular physiology [97]. However, they also reveal that FGFR3 function is intimately tied to the dynamics of cellular physiology that affect Hsp90 function via post translation modifications (described below). Future work with FGFR3 mutants unable to bind to Hsp90 may be used to elucidate the *in vivo* significance of the integration of these pathways and to further define the molecular role of Hsp90 on FGFR3 biological function.

The appendix outlines several preliminary experiments testing Hsp90 complex modulation in pre-clinical models of achondroplasia. Metatarsal and tibia cultures from our CA-FGFR3 mouse models recapitulated the disease phenotype in culture, but Hsp90 inhibitors did not alleviate the retardation of linear growth in heterozygote or

homozygous bones. A genetic test of Hsp90 complex modulation by cross of the CA-FGFR3 mice with mice overexpressing CHIP did not counteract the reduced growth of the CA-FGFR3 mice. While these were negative results, there are a number of limitations preventing us from concluding that Hsp90 inhibitors are ineffective for the treatment of achondroplasia. Because of the preliminary nature of these experiments, they were limited in their statistical power due to experimental design limitations and restricted man-power. These limitations prevented finding an optimal dose and detection of small changes. Negative results raise questions into the many barriers that face pre-clinical models of achondroplasia such as the feasibility of delivering drugs to avascular tissues, the pharmacodynamics properties of the drug, the doses needed and its frequency of administration, and the age at which to begin treatments.

3.2 Future Directions

The studies presented in this dissertation indicate that the stability and signaling capacity of FGFR3 is dependent on its interaction with functional Hsp90. These observations raise a number of questions about the biological consequence of this interaction on both molecular and therapeutic levels. The following section outlines some future directions that could be pursued from the work presented in this dissertation.

Determining the structural rationale for differential dependence of FGFRs on Hsp90

The dramatic difference of the association of Hsp90 with the four members of the FGFR family provides an ideal model to study the structural differences contributing to Hsp90 binding. A number of attempts have been made to identify a binding motif or a

structural rationale within kinase domains to explain why strong clients associate with Hsp90, however, there has been little reproducible success [106-109, 111, 142, 158, 160, 174]. Although the FGFR family contains a high degree of homology, especially within the kinase domain (~90%), their interaction and dependence on Hsp90 function is clearly varied. Comparison of the highly homologous FGFR family members is likely to provide more detailed insight then comparison of less similar proteins.

The data presented in Chapter 2 (Figure 2.2) narrowed down the N-lobe/hinge region of the kinase domain as the primary site determining Hsp90 binding; however, I was unable to identify the precise residue(s) within that region responsible for Hsp90 binding, and further work with the mutants unable to bind to Hsp90 will elucidate if this observation is direct or indirect. Further mutagenesis studies to determine the residues contributing to Hsp90 association coupled with crystal structure analysis of all four FGFR kinase domains would provide insight into how Hsp90 discriminates between these similar proteins. Other experiments involving NMR and/or small angle X-ray scattering (ideally in conjunction with the crystal structures) could be designed to study binding or allosteric changes of the kinase domain due Hsp90 association. These studies could be further expanded to include Cdc37.

Understanding the structure/binding relationship between FGFR3 and Hsp90 would also permit prediction as to whether disease-causing kinase mutations found in other FGFRs would enhance their stability dependence on Hsp90 function. As kinase domains are well conserved, this information may allow us to predict if N-lobe mutations in other

kinases increase Hsp90 dependence and sensitivity to Hsp90 inhibitors. Structural insight may also provide new targets for drug design. This information would be of interest to a wide audience, not only to those studying kinases, but also to those studying Hsp90 and chaperones in general.

Oncogenic FGFR3 as a prognostic indicator of Hsp90 inhibitors in cancer

Gain-of-function mutations or overexpression of FGFR3 is observed in several types of cancer with the most frequently reported including bladder cancer and multiple myeloma [3]. FGFR3 expression levels and mutational status have been analyzed as an indicator of disease severity, outcome, recurrence and drug responses in these cancers [175-178]. The identification of FGFR3 as a strong Hsp90 client suggests that cancers dependent on FGFR3 may be more sensitive to Hsp90 targeted therapies, providing a rationale to stratify prognostic response to these therapies relative to FGFR3 status. Additionally, as is currently done with other Hsp90 clients and the induction of the heat shock response, FGFR3 protein stability or activity could be examined as an indicator of pharmacodynamic responses to Hsp90 inhibitors in tumors after treatment. While multiple myeloma has successfully undergone a number of clinical trials with Hsp90 inhibitors, most frequently in combination with proteasome inhibitors, its response to Hsp90 inhibitors in relationship to FGFR3 mutational or overexpression status has not been evaluated [179, 180]. Furthermore, bladder cancer has not been exclusively tested for Hsp90 inhibitory efficacy in clinical trials, however, there are now studies indicating that Hsp90 inhibitors are effective against bladder cancer *in vitro* [137, 181].

About 70% of bladder cancers contain mutations that constitutively activate FGFR3, making it an ideal platform for testing targeted therapies [182]. Multiple studies have demonstrated that targeting FGFR3 using small molecule inhibitors or blocking antibodies can block bladder cancer proliferation and sensitize cells to apoptosis [65, 66, 183-186]. Because FGFR3 is a strong Hsp90 client, bladder cancer represents a solid tumor that is uniquely (and molecularly uniformly) enriched with a strong Hsp90 client that promotes proliferation and survival, increasing the potential of a successful Hsp90 inhibitor response and as a model system for analyzing molecular responses.

Several pre-clinical studies could be performed to determine if Hsp90 inhibitors are likely to be effective in bladder cancer treatment. Bladder cancer cell lines could be further tested for the ability of Hsp90 inhibitors to induce apoptosis, inhibit cell cycle progression, alter signal transduction, and reduce motility and invasiveness. An assessment of the length (pulse) of treatment needed to induce these responses should be made to provide insight into dosing schemes *in vivo*. Studies in mouse xenografts could be used to determine the ability of Hsp90 inhibitors to reduce tumor volume, decrease proliferation, induce apoptosis, decrease vasculature or increase hypoxia. These studies may elucidate the feasibility and facilitate the design of a clinical trial in bladder cancer depending on the Hsp90 inhibitor chosen, and the mode of delivery (systemic, versus direct delivery into the bladder).

Regulation of FGFR3 stability by post-translational modifications of Hsp90: HDAC6

Hsp90 function is modulated by numerous post-translational modifications including acetylation, serine/threonine/tyrosine phosphorylation and S-nitrosylation [97]. To date, the most therapeutically relevant posttranslational modification of Hsp90 is acetylation. Acetylation of Hsp90 reduces its ability to chaperone client proteins, resulting in client destabilization and degradation [96, 187-189]. Histone deacetylase (HDAC) inhibitors increase the acetylation of Hsp90, thereby decreasing the function of Hsp90 and destabilizing clients. Furthermore, HDAC inhibitors are in numerous cancer clinical trials and have demonstrated synergy with many first line therapies used in cancer treatment [190].

HDAC6, a predominantly cytosolic HDAC, plays the major role in removing acetyl groups from cytosolic Hsp90 [191]. Understanding the role of HDAC6 in FGFR3 stability, as well as the potential for HDAC inhibitors to modulate FGFR3 stability, is a question of both molecular and therapeutic relevance. Studies to test the role of HDAC6 function in FGFR3 stability would ideally be performed in bladder cancer cell lines testing the association of HDAC6 with the FGFR3/Hsp90 complexes, the consequence of HDAC6 knockdown on FGFR3 stability, and the ability of HDAC inhibitors to destabilize FGFR3 protein levels and thus signaling output.

The therapeutic relevance of this topic extends beyond the potential therapeutic application of HDAC inhibitors in the treatment of FGFR3-related diseases. It may also provide a molecular rationale for the long-observed cancer preventative properties of

broccoli consumption. Consumption of broccoli is strongly associated with a reduced risk for developing of some types of cancer including bladder cancer [192-195]. A naturally occurring HDAC inhibitor found in broccoli, sulforaphane, has demonstrated effectiveness in inhibiting HDAC6 function and in inducing destabilization of Hsp90 clients [196-198]. Understanding what role HDAC6 plays in FGFR3 stability may provide a molecular rationale for the decreased prevalence of bladder cancer in broccoli consumers. These studies could lead to clinical trials of HDAC inhibitors not only for the treatment of bladder cancer, but more importantly for its prevention.

3.3 Summary

In conclusion, the kinase domain of FGFR3 is uniquely dependent on its interaction with Hsp90 chaperone complexes for proper stability. This information provides new insight into the unique requirement of Hsp90 for FGFR3 signal transduction and implies that FGFR3 signaling is influenced by the signals that regulate Hsp90 function. Future work will further elucidate the significance of this interaction in FGFR3 biology and disease, and may lead to future therapeutic methods to manipulate FGFR3 mediated processes in skeletal growth and cancer.

APPENDIX

PRELIMINARY TEST OF HSP90 CHAPERONE COMPLEX MODULATION IN PRE-CLINICAL MODELS OF ACHONDROPLASIA

A.1 Abstract

Fibroblast Growth Factor Receptor 3 (FGFR3) is an important regulator of linear bone growth and a number of activating mutations in FGFR3 give rise to skeletal diseases. In Chapter 2, I reported that FGFR3 is a strong Hsp90 client and that therapeutically relevant Hsp90 inhibitors can reduce the stability and thus function of FGFR3 in tissue culture. Here I perform some preliminary experiments to test the ability of Hsp90 inhibitors to modulate linear bone growth in pre-clinical models. I found no significant increase in linear bone growth from the Hsp90 inhibitor 17-AAG in *ex-vivo* organ cultures or in a pilot trial of 17-AAG injection in CA-FGFR3 mice. A genetic cross of our CA-FGFR3 mouse with a mouse overexpressing the E3-ubiquitin ligase CHIP, which should destabilize strong Hsp90 clients such as FGFR3, showed no significant increase in linear bone growth. Further research is needed to determine if modulation of Hsp90 chaperone complexes could be an effective therapy for FGFR3 mediated skeletal disease.

A.2 Introduction

Gain-of-function mutations in the receptor tyrosine kinase FGFR3 give rise to a series of dominantly inherited skeletal diseases uniformly characterized by a reduction in linear bone growth [2]. The most common of these diseases is achondroplasia, which results

from a mutation in the transmembrane of FGFR3 (G380R) [13]. Studies have suggested several different mechanisms by which the G380R mutation results in increased activation including an increase in the propensity of the receptor to dimerize, increased stability of the receptor and increased transphosphorylation capacity [42, 43, 199]. In addition to skeletal diseases, somatic activating mutations of FGFR3 have also been found in cancer where they promote proliferation and survival [3]. However, the targeting agents designed to counteract the activity of FGFR3 in cancer have not successfully been translated to the treatment of achondroplasia.

Before the genetic lesion causing achondroplasia was identified, several therapeutic approaches were exploited to increase growth [60]. Subcutaneous injections with growth hormone were found to increase height, however the effectiveness was minimal and responsiveness wears off over the span of a few years [200]. Limb lengthening surgical procedures have been used to increase height over time, but this procedure has a number of complications including a significant risk for infection [201]. While limb lengthening may increase height, it does not improve other manifestations of achondroplasia including spinal stenosis or respiratory problems [60, 67]. An effective therapy to normalize bone growth in achondroplasia has yet to be identified.

The preclinical systems used to test the effectiveness of treatments for achondroplasia rely primarily on mouse models and organ cultures of bones. Several different mouse models have been generated to mimic the achondroplastic phenotype [202]. Our lab uses a mouse model that expresses a knock-in of the point mutation that causes thanatophoric

dysplasia type II (K650E, CA-FGFR3) [203]. Thanatophoric dysplasia is more severe (embryonic lethal) than achondroplasia and is caused by a point mutation in the kinase domain that constitutively activates FGFR3 to a stronger degree than the transmembrane achondroplasia mutation [204]. This mouse serves as a model for the less severe disease of achondroplasia because the knock-in CA-FGFR3 mRNA levels are reduced due to the placement of the Neo selection cassette, thus permitting a viable phenotype similar to that of an achondroplasia (G380R) transgenic mouse [203]. The benefit of using this mouse is that while the kinase activity is increased to a greater degree it is likely done so from a lower amount of protein (due to lower mRNA expression levels) than the achondroplasia mouse, thus increasing the probability of observing a change when protein stability is therapeutically targeted.

Recently I discovered that FGFR3 is a strong client of the chaperone Hsp90 and requires Hsp90 function for proper stability and function (Chapter 2). Inhibiting Hsp90 chaperone function using small molecule inhibitors such as 17-AAG reduces the stability and signaling capacity of FGFR3 thereby suggesting that targeting Hsp90 function may be a valid approach for treating FGFR3 gain-of-function diseases. Indeed, Hsp90 function has been validated as a therapeutic drug target in several diseases including cancer and neurodegenerative diseases [205]. FGFR3 mutated or over-expressing cancers are strong candidates for Hsp90 inhibitor drug targeting. However, the possibility of using Hsp90 inhibitors to treat skeletal disorders arising from identical gain-of-function mutations remains an open question. The possibility exists that the same altered responses of cancer cells to Hsp90 inhibitors may exist for cells expressing CA-

FGFR3, thereby making them selectively more able to take up and respond to Hsp90 inhibitors. However, because achondroplasia is characterized by a reduction in linear bone growth, using Hsp90 inhibitors to increase cellular proliferation is the opposite biological response targeted by the inhibitor in cancer. Although Hsp90 can target multiple pathways especially those promoting growth, we found that it was possible to prevent FGF-mediated reductions in proliferation in a chondrocyte tissue culture model, thereby suggesting it may be possible to use Hsp90 inhibitors to increase linear bone growth *in vivo* (Chapter 2, Figure 2.5E and 2.S2F).

In addition to Hsp90 inhibitors, genetic overexpression and manipulation of Hsp90 complexes has been used to conceptually validate them as drug targets. In the laboratory of Dr. Gen Sobue, mice were generated that ubiquitously overexpressed the E3-ubiquitin ligase CHIP, which is responsible for inducing the ubiquitination and degradation of Hsp90 client proteins [125]. These mice were then crossed with a pre-clinical model of an aggregation-prone Hsp90 client (the androgen receptor with a polyglutamine repeat) in a disease model of spinal and bulbar muscular atrophy (SMBA). Cross of the SMBA mice with transgenic mice overexpressing CHIP slowed disease progression and improved overall disease burden. The response to CHIP overexpression was similar to that observed when they injected SMBA mice with 17-AAG [126]. In both cases, this group demonstrated *in vivo* that 17-AAG treatment and CHIP overexpression induced the degradation of the disease causing Hsp90 client and reduced the onset and severity of disease. These results suggest that overexpression of CHIP *in vivo* may indicate the responsiveness of diseases to Hsp90 inhibitors.

Here I characterized several pre-clinical models recapitulating the ability of FGFR3 to reduce linear bone growth and test the ability of the Hsp90 complex modulation to reverse this growth. I characterized the ability of 17-AAG to prevent FGF induced reductions in linear bone growth in *ex vivo* organ cultures as well as its ability to correct reduced growth in organ cultures from our CA-FGFR3 mice (CA-FGFR3, K650E knock-in) [203]. I also performed a pilot trial to characterize the measurable parameters of our CA-FGFR3 mice and tested if injection with 17-AAG affected growth. Finally, I crossed the CA-FGFR3 mice with a transgenic mouse overexpressing CHIP, to determine if overexpression of CHIP can push FGFR3 towards a degradative fate and promote bone growth *in vivo*.

A.3 Materials and Methods

Metatarsal and Tibia Culture- 17-AAG was purchased from InvivoGen, dissolved in DMSO to a concentration of 50 mg/ml and stored at -20° C. Metatarsals and tibias were dissected and cultured following the methods of Mukherjee *et al*. with slight modification [206]. Briefly, E15.5 embryos were dissected out and placed in 1 x PBS containing 0.05 mg/ml gentamycin. Within 1 hour of fetal dissection, the three center metatarsals were isolated from each embryo and placed in one well of a 24-well dish containing 0.5 ml of metatarsal culture media which was composed of MEM Alpha+GlutaMAX-1 media (GIBCO) supplemented with 0.05 mg/ml ascorbic acid, 0.05 mg/ml gentamycin, 1 mM β-glycerophosphate and 0.2% Bovine Serum Albumin. The perichondrium was left undisturbed. Post dissection, metatarsals were incubated at 37° C overnight before the

media was replaced with 1 ml of experimental culture media (Day 0). Metatarsals were imaged using a Nikon inverted microscope fitted with a Nikon digital camera. Tibias were imaged using a Leica MZFLIII Fluorescent Stereoscope. All images were taken with a snapshot of a stage micrometer (2 mm ruled to 0.01 mm) for digital pixel to length conversion. Image J was used to digitally measure the bones in a series of two measurements, one from the blunt end of the bone to the middle and the other from the middle to the pronged edge. FGF2 and FGF18 were purchased from R&D and FGF18 was from Biovision. CNP was purchased from Calbiochem.

Pilot treatment of CA-FGFR3 mice with 17-AAG- CA-FGFR3 mice (thanatophoric dysplasia type II, K650E) were obtained from Chu-Xia Deng [203]. Genotyping was performed on genomic DNA isolated from ear punched skin. Genotyping PCR was performed using the following primers, which (due to intron 5 and 6 deletions) give a 500 base pair (bp) band for a wild-type allele and a 350 bp band for the knock-in allele: 5'GGCTCCTTATTGGACTCGC and 5'TCACTGCCTAGAATGGCTGTC. The PCR was performed with USB HotStart-IT Taq Master Mix (2x) with the following PCR conditions: 1. 98° C, 30 seconds 2. 98° C, 10 seconds 3. 59° C, 30 seconds 4. 72° C, 30 seconds 5. Repeat steps 2-4, 35 times 6. 72° C, 10 minutes 7. 4° C, hold. Mice were measured (tail length and weight) and treated three times a week via intraperitoneal injection with 25 mg/kg of 17-AAG in DMSO from week 2 through week 8 of life. Mice were anesthetized for X-rays using a cocktail provided by the Department of Comparative Medicine at OHSU (7.5 mg ketamine, 1.5 mg xylazine 0.25 mg acepromazine per ml of water). X-rays were taken on a Faxitron X-ray machine (40

volts, for 20 seconds) at 4, 6 and 8 weeks. X-rays were scanned and measured relative to a ruler placed on the X-ray using Image J.

Genetic cross of TDII with actin-CHIP- The actin-CHIP BDF1 mice were obtained from Gen Sobue [125]. Male homozygous actin-CHIP BDF1 mice were crossed with female heterozygous CA-FGFR3 C57BL6 mice. Genotyping for the CHIP allele was determine using the primers 5'CATCTCAGAAGAGGATCTGTG and 5'GGTCGAGGGATCTTCATAAG and PCR performed with USB HotStart-IT Taq Master Mix (2x) with the following PCR conditions: 1. 94° C, 2 minutes 2. 94° C, 30 seconds 3. 60° C, 1 minute 4. 72° C, 1 minute 15 seconds 5. Repeat step 2-4, 35 times 6. 72° C, 10 minutes 7. 4° C, hold. To distinguish between homozygous and heterozygous alleles for the CHIP allele, DNA was quantified using a Thermo Scientific Nano Drop and diluted to 10 ng/μl and subjected to quantitative real-time PCR. The following optimized primer set was used which primes a 153 base pair (bp) fragment within the coding region of the transgene for human CHIP: 5'GGAGCAGGGCAATCGTCTG and 5'GCCAGGGCCTGCTCGTG. GAPDH was used to normalize the samples with the following primers: 5'CCACCCAGAAGACTGTGGAT and 5'TTCAGCTCTGGGATGACCTT. Reactions were carried out with a final volume of 25 μl of 1x IQ SYBR Green Supermix (Biorad) with 40 ng DNA, 300 nM Primers. Primer efficiencies were calculated using serial dilutions and linear regression, and were used to calculate the relative amount of DNA compared to control samples using the Pfaffl method [207]. Tail lengths and weight were measured every other week beginning at weaning, week 3 of age.

A.4 Results

Ex vivo organ culture treatments with 17-AAG

Establishment of a dissection protocol. To determine the effect of Hsp90 inhibitors on linear bone growth in *ex vivo* organ cultures, I established a dissection protocol for metatarsals from wild-type C57BL6 mice based off the methods of Mukherjee *et al.* [206]. Dissection of wild-type metatarsals revealed significant variability in growth due to several dissection related factors which were normalized in future dissections. These factors included the temperature and length of time of the dissection from the 15.5 day embryo, the post-dissection quality of the perichondrium or the method used to remove it, extraneous tissue or cells that influenced the culture media and drug concentrations and trauma to the cartilaginous anlage during dissection. As illustrated in Figure A.1A, the metatarsals exhibit a clear cartilaginous anlage which, over time, develops a hypertrophic clearing yielding to ossification. While I found that the linear growth of the metatarsals was consistent over time, I did not find the onset of appearance or expansion rate of the ossification center to consistently correlate to days post dissection (data not shown). This may have been related to the position of the three metatarsals in the foot. Therefore, all measurements focused on linear growth.

Metatarsal and Tibia Cultures correlate FGFR3 genotype to phenotype. After establishing a reproducible dissection protocol, I characterized the growth phenotypes of metatarsal dissected from the CA-FGFR3 (K650E knock-in) achondroplasia mouse model [203]. As illustrated in Figure A.1B, at dissection Day 0 the metatarsals had

similar length, which increased linearly with time and in relationship to genotype. Linear regression revealed that the growth rates correlated with genotype, with wild-type metatarsals growing the fastest (73.4 μm/day), and the heterozygous and homozygous metatarsals growing slower (51.5 and 48.3 μm/day, respectively). Unlike the length, the widths of the metatarsals were significantly different from one another at Day 0, with homozygous metatarsals significantly wider than wild-type (Figure A.1C).

In addition to metatarsals, I characterized the growth phenotype of tibias from the CA-FGFR3 mice to maximize the yield from each embryo (6 metatarsals and 2 tibias per embryo). Tibia culture protocols are similar to those of metatarsal cultures, and the tibias adapted well to the established protocol. Tibias cultured at day 15.5 were at a more advanced stage of development and had well-established ossification centers. Unlike the metatarsals, tibias had significantly different lengths at Day 0 relative to their genotype (Figure A.1D, y-intercept). Tibia cultures grew with a rate directly related to genotype (wild-type 165, heterozygous 122, homozygous 94 μm/day), thus permitting distinction between all three genotypes. Thus, tibia cultures represented a better model to study the FGFR3 phenotype to genotype correlation. However, due to the yield of tibias (2 per animal), using metatarsals gave more statistical power (6 per animal). Experiments were initially performed with only the metatarsals, and later experiments were performed with both.

Responsiveness of organ cultures to FGF requires heparin. Several studies have published that addition of FGF to *ex vivo* organ cultures results in a reduction of linear

growth through FGFRs, presumably FGFR3. I was not able to reproducibly observe a reduction in growth after administration of FGFs as published in the protocol by Mukherjee *et al*. [206]. While it seemed that increased concentrations of FGFs were negatively impacting growth it was not dose responsive and highly variable (Figure A.2A, left). Further reading suggested that others had used 10 μg/ml heparin with FGF stimulation in metatarsals [31]. Addition of heparin reduced the FGF response variability and produced dose responsive reductions in metatarsal linear growth to FGFs (Figure A.2A). Interestingly, heparin alone caused an increase in linear growth (Figure A.2B). It is likely that excess heparin may disrupt FGF signaling in the growth plate causing an increase in linear growth. The lowest concentration of heparin tested was 10 μg/ml, which facilitated consistent responses to FGFs and was used in future experiments. In addition to FGF2, I found that FGF18, a more relevant FGF found in the growth plate, reduced the linear growth of the metatarsals (Figure A.2C). It appeared to affect the growth of the metatarsals more than that of FGF2, perhaps reflecting a higher affinity of FGFR3 for this growth factor. This observation is consistent with reports in the literature that FGF18 knockout and FGFR3 knockout have similar phenotypes, and thus are likely responsible for the reduction in linear growth observed in these cultures [16, 23]. As a positive control for the induction of linear bone growth above that of basal rates, I found that the addition of CNP (no heparin) to both metatarsal and tibia cultures increased linear bone growth (Figure A.2D, E).

Metatarsal cultures tolerate low nM levels of 17-AAG. Several dose curves were performed to determine the optimal working dose of 17-AAG. Because inhibition of

Hsp90 function can target multiple pathways, and because many of these pathways promote growth, determining an appropriate dose is critical. Indeed, concentrations of 17-AAG at or above 100 nM caused a reduction or complete stop in metatarsals growth (Figure A.2E). Unfortunately, due to unknown reasons, a significant variability in response made it difficult to determine a precise concentration to use between 1 and 100 nM. While 25 nM or 50 nM caused no effect in one experiment it could be observed to slightly negatively impact growth in other experiments. Further experiments were proposed to refresh drug at lower does daily, however, this was highly toxic even at low nM concentrations and an optimal dose for this type of experiment was not determined (data not shown). Despite these unanswered possibilities, at no concentration of 17-AAG did I observe a statistically significant increase in linear growth compared to the DMSO control when added to basally growing metatarsals.

25 nM 17-AAG does not prevent FGF induced reductions in linear bone growth. To determine if 17-AAG was able to prevent an FGF induced reduction in linear growth, metatarsals were allowed to recover overnight from their dissection and then treated with media containing 17-AAG and FGF2/heparin. 17-AAG was unable to prevent an FGF2 induced reduction in linear bone growth (Figure A.3A). Likewise, pre-treatment with 17-AAG for 24 hours before the addition of FGF2/heparin did not prevent a FGF2 reduction in growth (Figure A.3B).

17-AAG does not rescue TDII metatarsal or tibia growth. To determine if 17-AGG was able to increase growth in metatarsals from mice expressing CA-FGFR3, metatarsals

were treated with 25 μM 17-AAG over the course of the culture. 17-AAG appeared to slightly decreased wild-type metatarsal growth but did not effect CA-FGFR3 metatarsal growth (Figure A.3C). Similar results were seen for tibia cultures (Figure A.3D). This observation may indicate that CA-FGFR3 induces altered responses to Hsp90 inhibitors. Further research is needed to determine the significance of this observation.

Establishing experimental parameters in a pilot trial of 17-AAG in CA-FGFR3 mice

A preliminary study was performed to estimate the technical parameters needed to conduct a thorough investigation of the effect of 17-AAG treatment in the CA-FGFR3 mice. This pilot study was based on a similar study performed by Waza *et al*. [126]. The goal of this pilot trial was to gauge the technical feasibility and cost of performing a larger trial, to determine the best phenotypes to measure and their statistical variability, and to determine an appropriate dosing scheme.

Rationale of initial dosing scheme. We modeled our dosage scheme to target FGFR3 in the growth plate as was performed previously by Waza *et al.* to target the androgen receptor in the central nervous system [126]. Because 17-AAG was able to target the androgen receptor in the central and peripheral nervous system, which has reduced absorbance of 17-AAG due to the poor ability of 17-AAG to traverse the blood-brain barrier [208], and because there were no apparent side effects on the growth of these animals, we choose to similarly treat our achondroplastic mice with three weekly intraperitoneal injections of 25 mg/kg.

Phenotype genotype correlations and observations. Although the experiments were performed blinded with respect to genotype, phenotypes became apparent as the mice grew preventing true blinding (Figure A.4A). X-rays permitted clear visualization and measurement of tibia and femur lengths which correlated with genotype (Figure A.4B). It was observed that the homozygous mice were hypersensitive to the anesthesia and several did not recover. Wild-type and heterozygous mice had similar weights which increased rapidly once weaned, while the homozygous mice were significantly smaller and had a reduction in weight after weaning, suggesting that they had difficulty transitioning to hard food despite the fact that all mice were placed on wet food post weaning (Figure A.4C). Tail length accurately reflected genotype and was used as the primary experimental parameter (Figure A.4D). When whole litters were compared to each other variations in litter size significantly affected offspring size early on but this effect disappeared quickly, especially after weaning (data not shown). This observation may be of significance for future experiments attempting to dose offspring as litter size may effect competition for food, growth, or dose of medication depending on delivery method.

TDII mice were not responsive to 25 mg/kg 17-AAG. Analysis of genotype versus treatment revealed no significant increase in tail length from treatments with 17-AAG (Figure A.4E). To control for sex specific differences in growth, female mice, for which we had a larger number of animals, also did not show any change with treatments (data not shown). X-rays were measured and analyzed for femur length but did not show a statistically significant change in femur length upon treatment (data not shown).

Genetic cross of the CA-FGFR3 and actin-CHIP mice

Others have reported that overexpression of CHIP can destabilize Hsp90 clients and induce their ubiquitination and degradation [143]. Similar to that observed for other Hsp90 clients, we observed that CHIP was able to interact with and destabilize FGFR3 in tissue culture models (Chapter 2, Figure. 2.4). Some of our experiments suggested that CA-FGFR3 was more sensitive to CHIP overexpression (Figure A.5A). The ability of CHIP overexpression to destabilize Hsp90 clients has also been demonstrated *in vivo* by crossing an Hsp90 client disease model (SMBA) to a transgenic mouse overexpressing CHIP [125]. In this mouse CHIP is overexpressed from an actin promoter leading to significant expression of CHIP in all tissues tested. This approach theoretically eliminates most problems arising from a pharmaceutical approach such as finding an appropriate dose of the drug, cellular uptake of the drug, metabolic breakdown of the drug, cellular absorbance of the drug or drug reaching target tissues. Because our previous pre-clinical models were confounded with determination of the appropriate dose of 17-AAG without causing toxicity, we crossed our mouse model of achondroplasia with that of the mouse line overexpressing actin-CHIP.

Establishment and observations of the actin-CHIP line. The actin-CHIP transgenic mouse line was kindly provided to us by Dr. Gen Sobue and was reestablished at the OHSU Transgenic Core using embryos at the two cell stage. Although no overt phenotype was previously reported, it was clear that the actin-CHIP mice were different

than wild-type BDF1 mice. Homozygous mice had large ears with a prominent ridge extending horizontally across the back of the ear. Male actin-CHIP mice aged differently than the parental line and became mottled grey on their back with increased age. It was also noted that the offspring of the mixed background cross were prone to lethally aggressive fighting in the males, significantly more than that observed in the BDF1 or C57BL6 lines.

Rationale and observations for crosses. We modeled our experimental crosses after that done by Adachi *et al.* [125]. In this publication they crossed their disease mouse model, which was on a C57BL6 background, to the actin-CHIP BDF1 transgenic line. Similar to their design, we crossed our TDII C57BL6 mice with the actin-CHIP BDF1 (Figure A.5B)

Actin-CHIP does not rescue the TDII phenotype. To determine if overexpression of CHIP rescues the CA-FGFR3 phenotype, I crossed homozygous actin-CHIP BDF1 mice to heterozygous CA-FGFR3 C57BL6 mice to produce offspring that contained one copy of the actin-CHIP allele in the presence or absence of a CA-FGFR3 allele (depicted in Figure A.5B). These crosses generated 89 mice with roughly the expected Mendelian ratios (Figure 5C). Tail lengths and weight were monitored weekly. Analysis of female tail length revealed no significant change in the rate of growth for the CA-FGFR3 mice containing an actin-CHIP allele (Figure A.5D).

A.5 Discussion

This appendix outlined some preliminary experiments to gauge the therapeutic potential of modulating Hsp90 complexes to alter FGFR3 mediated reductions in linear bone growth *in vivo*. In contrast to our observations in tissue culture models where 17-AAG treatment could alter proliferation in response to FGFs (Chapter 2 Figure 2.5E and 2.S2F), I was unable to demonstrate that treatment with 17-AAG or CHIP overexpression was able to increase bone growth in these models. The lack of response in these preliminary experiments may reflect a number of possibilities including fundamental molecular differences between these models, technical and statistical barriers to determine the optimal dose or to detect change *in vivo*, or dosing scheme of 17-AAG.

An important difference between the tissue culture and *in vivo* models is that both of the tissue culture lines previously tested (RCS and Hela) were not only immortalized but also transformed. Because Hsp90 function is closely integrated with several aspects of cellular physiology that may be altered in transformed cells including metabolism and stress, its function in transformed cells may be more active and constant and thus rendering more easily inhibited and observed. Others have documented that the activity of Hsp90 in cancer is upregulated relative to non-transformed cells [132, 209]. This may explain why the role of Hsp90 in FGF responses may be observable in our tissue culture models rather than in non-transformed tissue. Additionally, cellular responses to 17-AAG are facilitated by the enzyme NAD(P)H/quinone oxioreductase (NQO1) which converts 17-AAG to a more potent dihydroquinone form [210, 211]. It is possible that

non-transformed chondrocytes lack expression of this enzyme, in which case other Hsp90 inhibitors may be more effective in targeting Hsp90. Furthermore, if CA-FGFR3 altered the expression of this enzyme in chondrocytes it may explain the differential sensitivities observed in the CA-FGFR3 organ cultures to 17-AAG (Figure A.3C, D). Future studies should include an analysis of NQO1 expression levels in chondrocytes and/or examine the ability of other Hsp90 inhibitors to affect chondrocyte growth.

In addition to the molecular differences in these models, there are major differences in the technical and statistical experimental set-up and power. With the tissue culture model, it was possible to plate tens of thousands of cells in 96-well dishes with many replicates. The experiments could be performed in a matter of days and were easily optimized for growth factor and drug concentrations. In contrast, dissection of metatarsals and tibias was time consuming and inherently variable. Although this variability was controlled for as much as possible, it was impossible to completely remove thereby increasing the number of samples required to detect a significant change. Therefore, small changes may exist but would have been undetectable due to this inherent variability.

A serious limitation to these experiments is to find a dose of 17-AAG at which FGFR3 is destabilized without negatively affecting other Hsp90 clients necessary for promoting growth. Thus, lack of a response could be due to an inadequate concentration of 17-AAG or too high of a concentration that inhibits growth. It is possible that no such optimal concentration exists *in vivo*, due to the presence of stronger Hsp90 clients that

promote growth of the growth plate. If the window of concentration is narrow, it is unlikely that a treatment with an Hsp90 inhibitor could be dosed properly in humans.

To ask this question genetically and independent of the problems arising from administration and dosing of 17-AAG, we performed a cross of the CA-FGFR3 line with the transgenic actin-CHIP mice. This experiment was modeled after the work done by Adachi *et al.*, where a CHIP transgene dosage effect was observed to improve disease in SMBA mice by reducing the protein levels of the disease causing Hsp90 client. Although the rationale for CHIP to destabilize client protein levels in these two diseases is similar, the natures of these two diseases are quite distinct. It is possible that the results observed in the SMBA mouse models are due to a broader role of Hsp90 in the pathology of polyglutamine related diseases, or in the stress response of cells to Hsp90 inhibitors [205]. Furthermore, the co-chaperone makeup is different for the client proteins of these two diseases, in that FGFR3 is a kinase specific client which also contains the co-chaperone Cdc37. Other studies in cancer models have shown that inhibiting Hsp90 function is necessary to destabilize Hsp90 clients using CHIP overexpression [101, 123]. Some of my preliminary data suggested that combining CHIP overexpression with 17-AAG treatment synergized to destabilize CA-FGFR3, more so than that observed for wild-type FGFR3 (Figure A.5A). Further work could answer this possibility by crossing the CA-FGFR3 mouse with actin-CHIP in the presence and absence of an Hsp90 inhibitor.

Taken together, these results suggest that the use of Hsp90 inhibitors to treat achondroplasia and other skeletal disease mediated by FGFR3 are unlikely to be effective. However, the results shown here are preliminary and warrant further, more rigorous, investigation. Some future investigations could include experiments with optimized (less toxic, more potent) Hsp90 inhibitors, in utero treatment strategies or combination of CHIP overexpression with Hsp90 inhibition. These studies have also established the usefulness of CA-FGFR3 metatarsal and tibia cultures to recapitulate the disease phenotype *in vitro* as a pre-clinical model for FGFR3 disease.

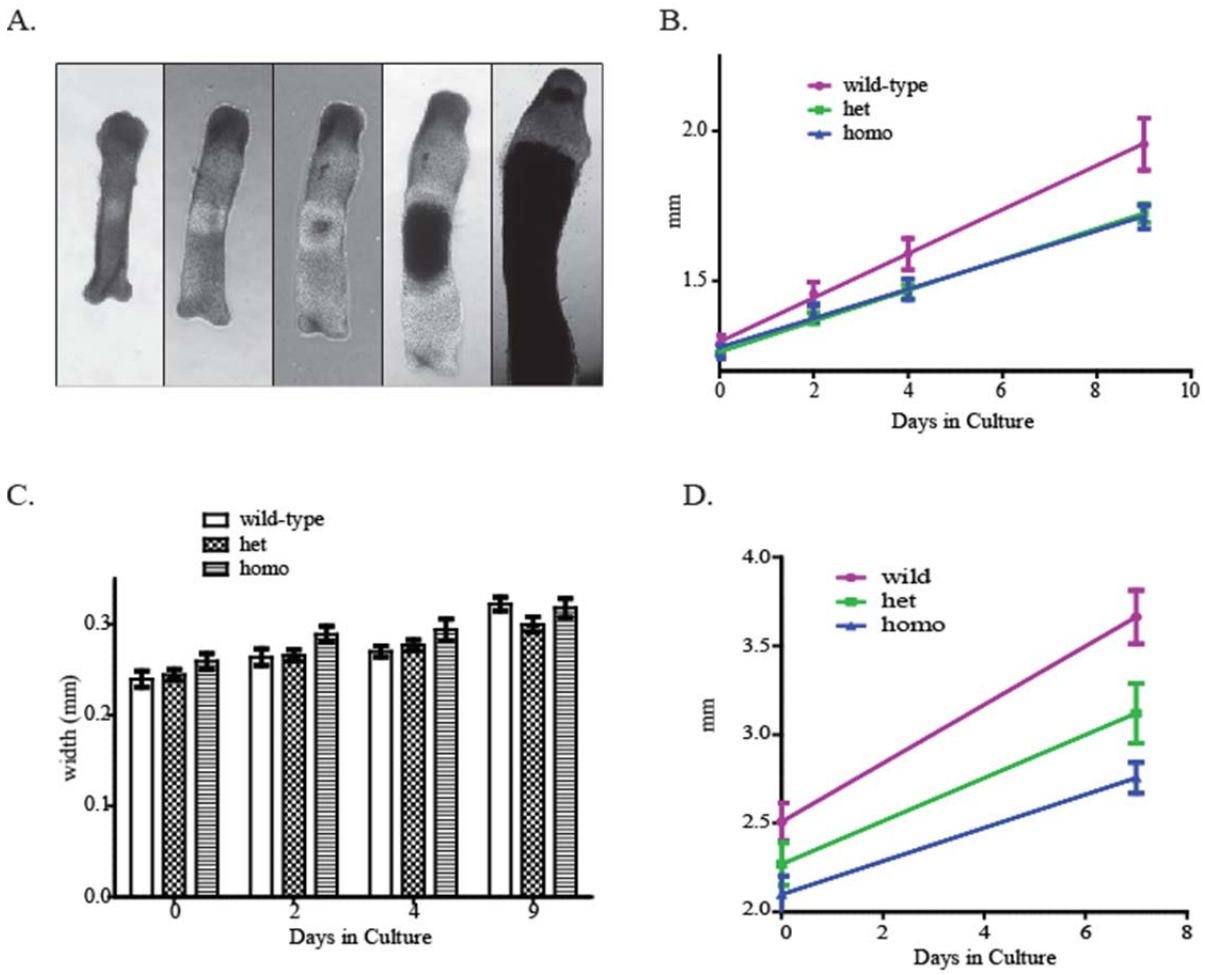

Figure A.1 *Organ culture genotype versus phenotype.* A. Representative image of *ex vivo* metatarsal development. B. Growth rate of CA-FGFR3 metatarsals versus genotype. C. Metatarsal genotype versus width over time. D. Growth rate of CA-FGFR3 tibias versus genotype.

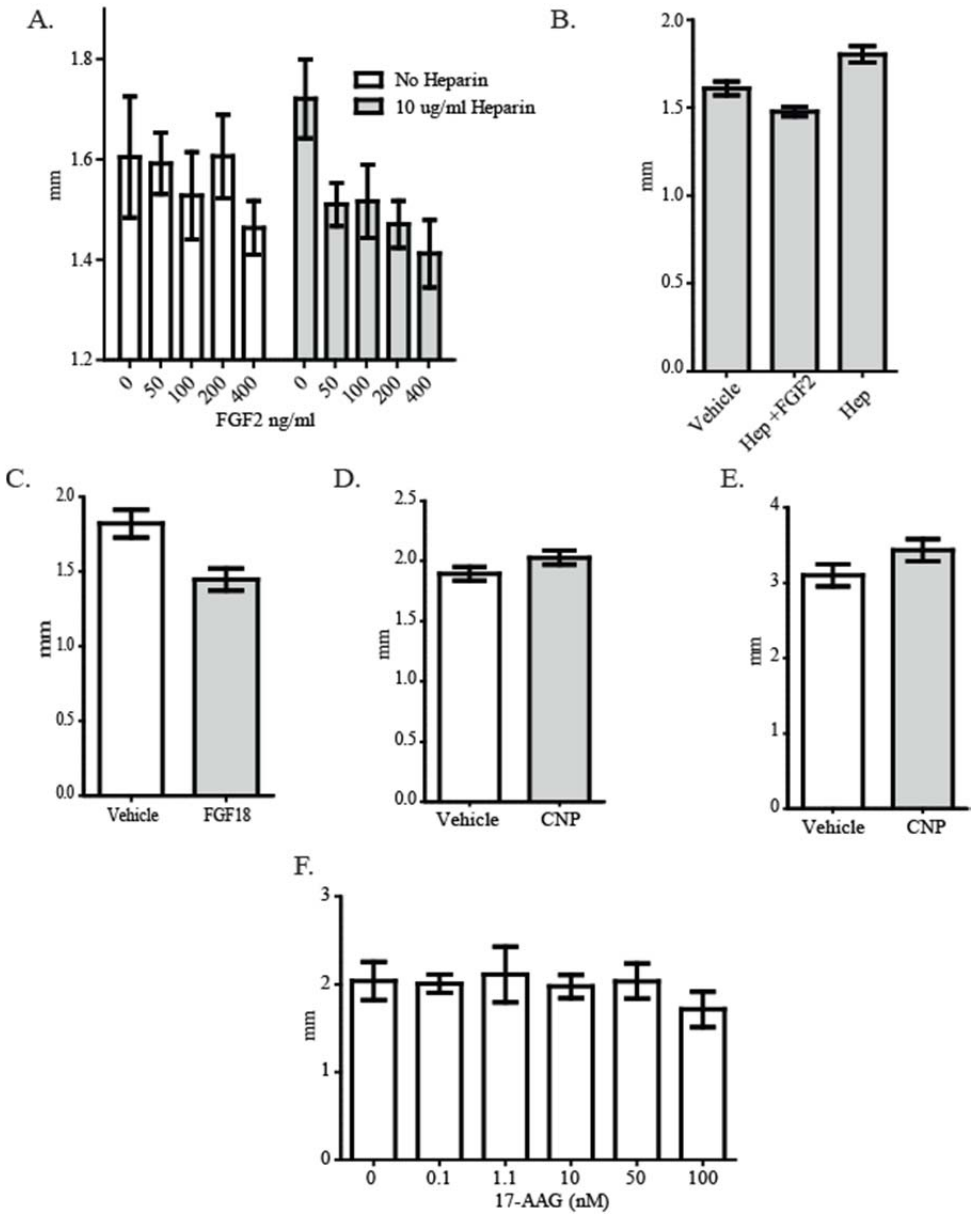

Figure A.2 *Modulation of metatarsal and tibia growth* A. FGF2 dose curve plus or minus heparin B. Metatarsal length versus treatment with 50 ng/ml FGF2, 10 μg/ml heparin or heparin alone C. Effect of metatarsal growth rate in the presence or absence of 10 ng/ml FGF18 1 μg/ml heparin D. Effect of 100 nM CNP on metatarsal growth E. Effect of 100 nM CNP on tibia growth F. Dose curve 17-AAG from 0-100 nM.

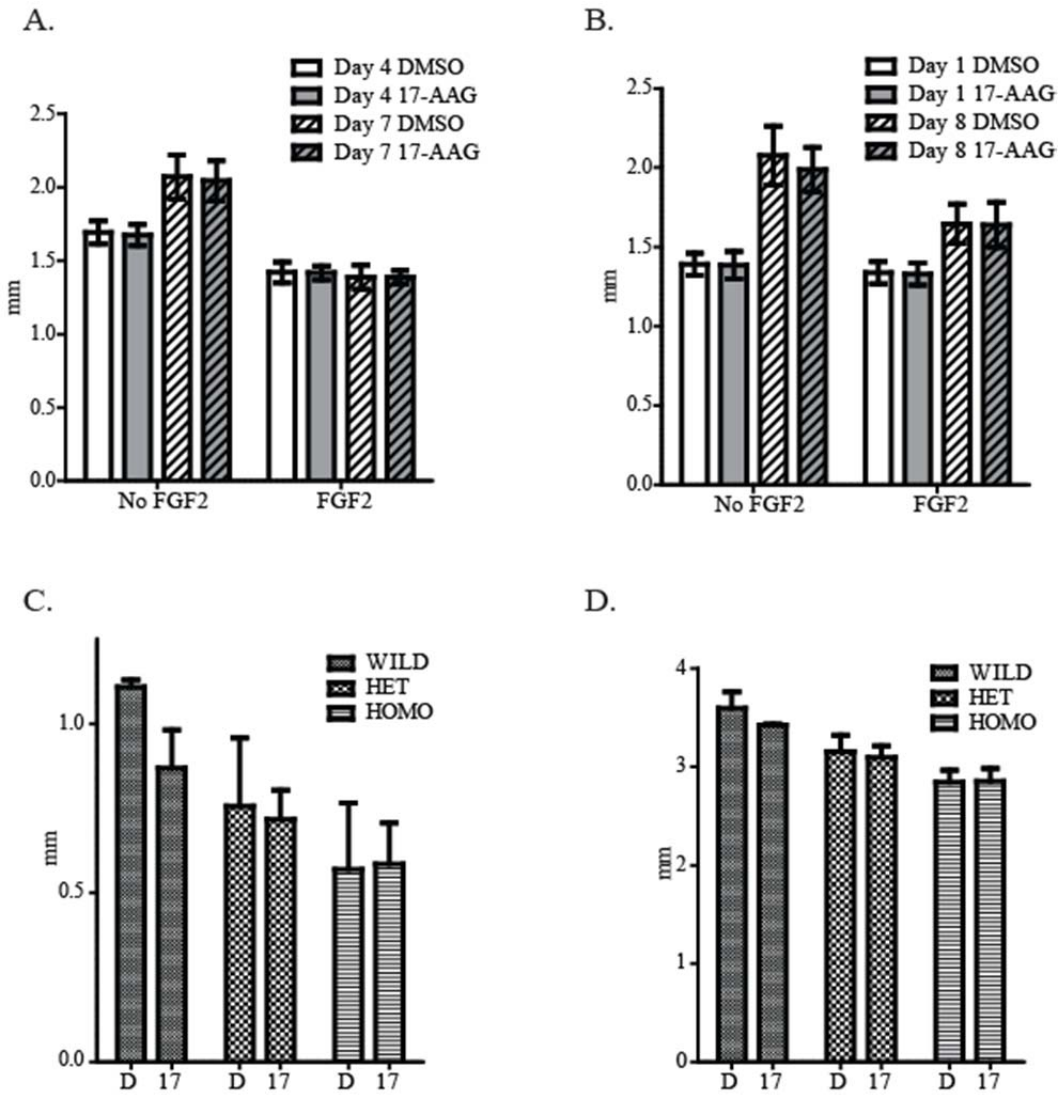

Figure A.3 *Effect of 17-AAG on metatarsal growth* A. FGF2 (200 ng/ml, 10 μg/ml heparin) induced growth retardation. B. Pre-treatment with 100 nM 17-AAG for 24 hours before addition of 200 ng/ml FGF2, 1 μg/ml heparin. C. Absolute growth of metatarsals from the CA-FGFR3 mice in the presence or absence of 5 nM 17-AAG at 72 hours. D. Growth of tibias from CA-FGFR3 mice in the presence or absence of 5 nM 17-AAG.

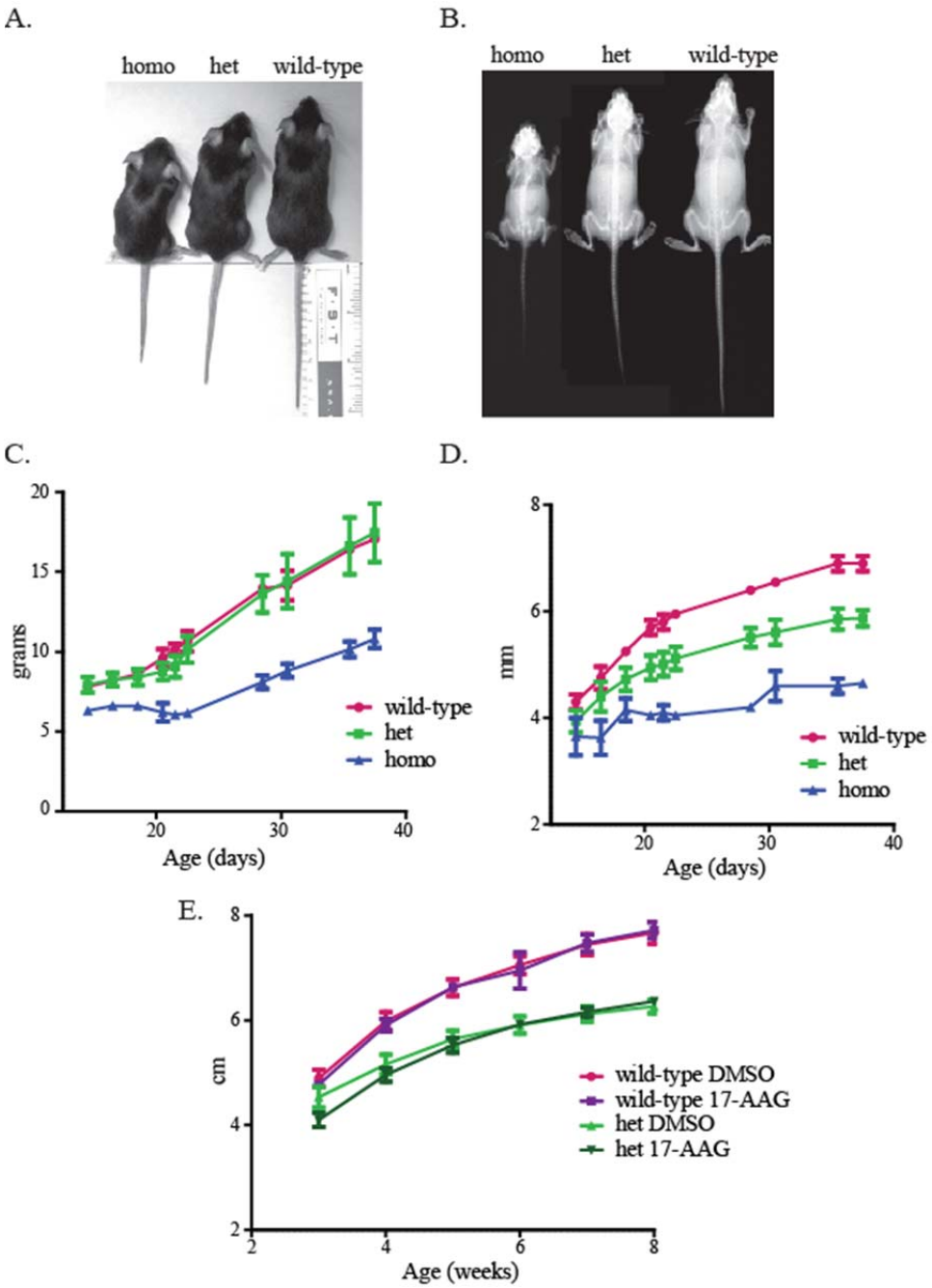

Figure A.4 *Characterization of CA-FGFR3 genotype versus phenotype: homozygous (homo), heterozygous (het), wild-type.* A. CA-FGFR3 genotype versus tail length. B. X-ray image of phenotype versus genotype. C. Plot of genotype versus weight. D. Plot of genotype versus tail length (mm). E. Plot of tail length versus genotype and treatment group.

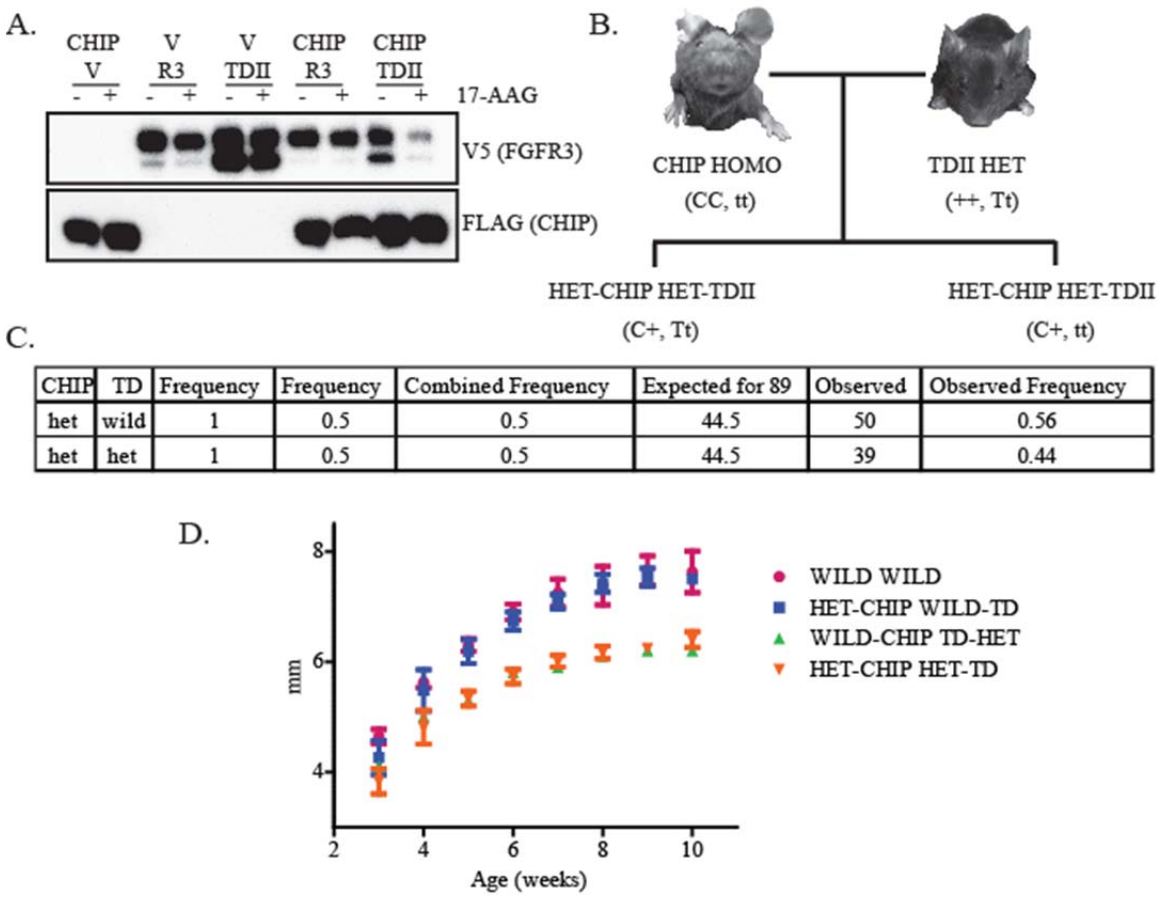

C.

CHIP	TD	Frequency	Frequency	Combined Frequency	Expected for 89	Observed	Observed Frequency
het	wild	1	0.5	0.5	44.5	50	0.56
het	het	1	0.5	0.5	44.5	39	0.44

Figure A.5 *Genetic cross of Actin-CHIP and CA-FGFR3* A. Western blot of transiently transfected CHIP, empty vector (V), FGFR3-V5, or CA-FGFR3-V5 (TDII) in the presence or absence (DMSO) of 0.5 µM 17-AAG. B. Depiction of the genetic cross between actin-CHIP homozygous and CA-FGFR3 (TDII) heterozygous mice. actin-CHIP transgene (C), wild-type (+), TDII knock-in (T), wild-type FGFR3 (t). C. Genotype frequencies of homozygous actin-CHIP crossed with heterozygous CA-FGFR3 D. Growth curve of tail length from the actin-CHIP, CA-FGFR3 (TDII) genetic cross.

REFERENCES

1. Laederich, M.B., and Horton, W.A. 2010. Achondroplasia: pathogenesis and implications for future treatment. *Current opinion in pediatrics* 22:516-523.
2. Ornitz, D.M. 2005. FGF signaling in the developing endochondral skeleton. *Cytokine & growth factor reviews* 16:205-213.
3. Haugsten, E.M., Wiedlocha, A., Olsnes, S., and Wesche, J. 2010. Roles of fibroblast growth factor receptors in carcinogenesis. *Molecular cancer research : MCR* 8:1439-1452.
4. Horton, W.A., Hall, J.G., and Hecht, J.T. 2007. Achondroplasia. *Lancet* 370:162-172.
5. Kliegman, R., and Nelson, W.E. 2011. *Nelson textbook of pediatrics*. Philadelphia, PA: Elsevier/Saunders. p. pp.
6. Brinkmann, G., Schlitt, H., Zorowka, P., and Spranger, J. 1993. Cognitive skills in achondroplasia. *American journal of medical genetics* 47:800-804.
7. Waller, D.K., Correa, A., Vo, T.M., Wang, Y., Hobbs, C., Langlois, P.H., Pearson, K., Romitti, P.A., Shaw, G.M., and Hecht, J.T. 2008. The population-based prevalence of achondroplasia and thanatophoric dysplasia in selected regions of the US. *American journal of medical genetics. Part A* 146A:2385-2389.
8. Wynn, J., King, T.M., Gambello, M.J., Waller, D.K., and Hecht, J.T. 2007. Mortality in achondroplasia study: a 42-year follow-up. *American journal of medical genetics. Part A* 143A:2502-2511.

9. Xu, W., Li, Y., Wang, X., Chen, B., Wang, Y., Liu, S., Xu, J., Zhao, W., and Wu, J. 2010. FGFR4 transmembrane domain polymorphism and cancer risk: a meta-analysis including 8555 subjects. *European journal of cancer* 46:3332-3338.

10. Velinov, M., Slaugenhaupt, S.A., Stoilov, I., Scott, C.I., Jr., Gusella, J.F., and Tsipouras, P. 1994. The gene for achondroplasia maps to the telomeric region of chromosome 4p. *Nature genetics* 6:314-317.

11. Shiang, R., Thompson, L.M., Zhu, Y.Z., Church, D.M., Fielder, T.J., Bocian, M., Winokur, S.T., and Wasmuth, J.J. 1994. Mutations in the transmembrane domain of FGFR3 cause the most common genetic form of dwarfism, achondroplasia. *Cell* 78:335-342.

12. Bellus, G.A., Hefferon, T.W., Ortiz de Luna, R.I., Hecht, J.T., Horton, W.A., Machado, M., Kaitila, I., McIntosh, I., and Francomano, C.A. 1995. Achondroplasia is defined by recurrent G380R mutations of FGFR3. *American journal of human genetics* 56:368-373.

13. Rousseau, F., Bonaventure, J., Legeai-Mallet, L., Pelet, A., Rozet, J.M., Maroteaux, P., Le Merrer, M., and Munnich, A. 1994. Mutations in the gene encoding fibroblast growth factor receptor-3 in achondroplasia. *Nature* 371:252-254.

14. Tavormina, P.L., Shiang, R., Thompson, L.M., Zhu, Y.Z., Wilkin, D.J., Lachman, R.S., Wilcox, W.R., Rimoin, D.L., Cohn, D.H., and Wasmuth, J.J. 1995. Thanatophoric dysplasia (types I and II) caused by distinct mutations in fibroblast growth factor receptor 3. *Nature genetics* 9:321-328.

15. Bellus, G.A., McIntosh, I., Smith, E.A., Aylsworth, A.S., Kaitila, I., Horton, W.A., Greenhaw, G.A., Hecht, J.T., and Francomano, C.A. 1995. A recurrent mutation in the tyrosine kinase domain of fibroblast growth factor receptor 3 causes hypochondroplasia. *Nature genetics* 10:357-359.

16. Colvin, J.S., Bohne, B.A., Harding, G.W., McEwen, D.G., and Ornitz, D.M. 1996. Skeletal overgrowth and deafness in mice lacking fibroblast growth factor receptor 3. *Nature genetics* 12:390-397.

17. Deng, C., Wynshaw-Boris, A., Zhou, F., Kuo, A., and Leder, P. 1996. Fibroblast growth factor receptor 3 is a negative regulator of bone growth. *Cell* 84:911-921.

18. Naski, M.C., Colvin, J.S., Coffin, J.D., and Ornitz, D.M. 1998. Repression of hedgehog signaling and BMP4 expression in growth plate cartilage by fibroblast growth factor receptor 3. *Development* 125:4977-4988.

19. Eswarakumar, V.P., Lax, I., and Schlessinger, J. 2005. Cellular signaling by fibroblast growth factor receptors. *Cytokine & growth factor reviews* 16:139-149.

20. Chen, H., Ma, J., Li, W., Eliseenkova, A.V., Xu, C., Neubert, T.A., Miller, W.T., and Mohammadi, M. 2007. A molecular brake in the kinase hinge region regulates the activity of receptor tyrosine kinases. *Molecular cell* 27:717-730.

21. Itoh, N., and Ornitz, D.M. 2008. Functional evolutionary history of the mouse Fgf gene family. *Developmental dynamics : an official publication of the American Association of Anatomists* 237:18-27.

22. Ornitz, D.M., Xu, J., Colvin, J.S., McEwen, D.G., MacArthur, C.A., Coulier, F., Gao, G., and Goldfarb, M. 1996. Receptor specificity of the fibroblast growth factor family. *The Journal of biological chemistry* 271:15292-15297.

23. Liu, Z., Xu, J., Colvin, J.S., and Ornitz, D.M. 2002. Coordination of chondrogenesis and osteogenesis by fibroblast growth factor 18. *Genes & development* 16:859-869.

24. Ohbayashi, N., Shibayama, M., Kurotaki, Y., Imanishi, M., Fujimori, T., Itoh, N., and Takada, S. 2002. FGF18 is required for normal cell proliferation and differentiation during osteogenesis and chondrogenesis. *Genes & development* 16:870-879.

25. Plotnikov, A.N., Schlessinger, J., Hubbard, S.R., and Mohammadi, M. 1999. Structural basis for FGF receptor dimerization and activation. *Cell* 98:641-650.

26. Hart, K.C., Robertson, S.C., and Donoghue, D.J. 2001. Identification of tyrosine residues in constitutively activated fibroblast growth factor receptor 3 involved in mitogenesis, Stat activation, and phosphatidylinositol 3-kinase activation. *Molecular biology of the cell* 12:931-942.

27. Mohammadi, M., Olsen, S.K., and Ibrahimi, O.A. 2005. Structural basis for fibroblast growth factor receptor activation. *Cytokine & growth factor reviews* 16:107-137.

28. Horton, W.A., and Degnin, C.R. 2009. FGFs in endochondral skeletal development. *Trends in endocrinology and metabolism: TEM* 20:341-348.

29. Su, W.C., Kitagawa, M., Xue, N., Xie, B., Garofalo, S., Cho, J., Deng, C., Horton, W.A., and Fu, X.Y. 1997. Activation of Stat1 by mutant fibroblast growth-factor receptor in thanatophoric dysplasia type II dwarfism. *Nature* 386:288-292.

30. Legeai-Mallet, L., Benoist-Lasselin, C., Delezoide, A.L., Munnich, A., and Bonaventure, J. 1998. Fibroblast growth factor receptor 3 mutations promote apoptosis but do not alter chondrocyte proliferation in thanatophoric dysplasia. *The Journal of biological chemistry* 273:13007-13014.

31. Sahni, M., Ambrosetti, D.C., Mansukhani, A., Gertner, R., Levy, D., and Basilico, C. 1999. FGF signaling inhibits chondrocyte proliferation and regulates bone development through the STAT-1 pathway. *Genes & development* 13:1361-1366.

32. Hart, K.C., Robertson, S.C., Kanemitsu, M.Y., Meyer, A.N., Tynan, J.A., and Donoghue, D.J. 2000. Transformation and Stat activation by derivatives of FGFR1, FGFR3, and FGFR4. *Oncogene* 19:3309-3320.

33. Choi, D.Y., Toledo-Aral, J.J., Lin, H.Y., Ischenko, I., Medina, L., Safo, P., Mandel, G., Levinson, S.R., Halegoua, S., and Hayman, M.J. 2001. Fibroblast growth factor receptor 3 induces gene expression primarily through Ras-independent signal transduction pathways. *The Journal of biological chemistry* 276:5116-5122.

34. Murakami, S., Balmes, G., McKinney, S., Zhang, Z., Givol, D., and de Crombrugghe, B. 2004. Constitutive activation of MEK1 in chondrocytes causes Stat1-independent achondroplasia-like dwarfism and rescues the Fgfr3-deficient mouse phenotype. *Genes & development* 18:290-305.

35. Zhang, R., Murakami, S., Coustry, F., Wang, Y., and de Crombrugghe, B. 2006. Constitutive activation of MKK6 in chondrocytes of transgenic mice inhibits proliferation and delays endochondral bone formation. *Proceedings of the National Academy of Sciences of the United States of America* 103:365-370.

36. Minina, E., Kreschel, C., Naski, M.C., Ornitz, D.M., and Vortkamp, A. 2002. Interaction of FGF, Ihh/Pthlh, and BMP signaling integrates chondrocyte proliferation and hypertrophic differentiation. *Developmental cell* 3:439-449.

37. Minina, E., Wenzel, H.M., Kreschel, C., Karp, S., Gaffield, W., McMahon, A.P., and Vortkamp, A. 2001. BMP and Ihh/PTHrP signaling interact to coordinate chondrocyte proliferation and differentiation. *Development* 128:4523-4534.

38. Dailey, L., Laplantine, E., Priore, R., and Basilico, C. 2003. A network of transcriptional and signaling events is activated by FGF to induce chondrocyte growth arrest and differentiation. *The Journal of cell biology* 161:1053-1066.

39. Horton, W.A. 2006. *Skeletal Development*. Weinheim: Wiley-VCH.

40. Webster, M.K., and Donoghue, D.J. 1996. Constitutive activation of fibroblast growth factor receptor 3 by the transmembrane domain point mutation found in achondroplasia. *The EMBO journal* 15:520-527.

41. You, M., Li, E., and Hristova, K. 2006. The achondroplasia mutation does not alter the dimerization energetics of the fibroblast growth factor receptor 3 transmembrane domain. *Biochemistry* 45:5551-5556.

42. Monsonego-Ornan, E., Adar, R., Feferman, T., Segev, O., and Yayon, A. 2000. The transmembrane mutation G380R in fibroblast growth factor receptor 3

uncouples ligand-mediated receptor activation from down-regulation. *Molecular and cellular biology* 20:516-522.

43. Cho, J.Y., Guo, C., Torello, M., Lunstrum, G.P., Iwata, T., Deng, C., and Horton, W.A. 2004. Defective lysosomal targeting of activated fibroblast growth factor receptor 3 in achondroplasia. *Proceedings of the National Academy of Sciences of the United States of America* 101:609-614.

44. Guo, C., Degnin, C.R., Laederich, M.B., Lunstrum, G.P., Holden, P., Bihlmaier, J., Krakow, D., Cho, Y.J., and Horton, W.A. 2008. Sprouty 2 disturbs FGFR3 degradation in thanatophoric dysplasia type II: a severe form of human achondroplasia. *Cellular signalling* 20:1471-1477.

45. Ben-Zvi, T., Yayon, A., Gertler, A., and Monsonego-Ornan, E. 2006. Suppressors of cytokine signaling (SOCS) 1 and SOCS3 interact with and modulate fibroblast growth factor receptor signaling. *Journal of cell science* 119:380-387.

46. Horton, W.A. 2003. Skeletal development: insights from targeting the mouse genome. *Lancet* 362:560-569.

47. Kronenberg, H.M. 2003. Developmental regulation of the growth plate. *Nature* 423:332-336.

48. Dailey, L., Ambrosetti, D., Mansukhani, A., and Basilico, C. 2005. Mechanisms underlying differential responses to FGF signaling. *Cytokine & growth factor reviews* 16:233-247.

49. Murakami, S., Kan, M., McKeehan, W.L., and de Crombrugghe, B. 2000. Up-regulation of the chondrogenic Sox9 gene by fibroblast growth factors is mediated

by the mitogen-activated protein kinase pathway. *Proceedings of the National Academy of Sciences of the United States of America* 97:1113-1118.

50. Kratz, C.P., Zampino, G., Kriek, M., Kant, S.G., Leoni, C., Pantaleoni, F., Oudesluys-Murphy, A.M., Di Rocco, C., Kloska, S.P., Tartaglia, M., et al. 2009. Craniosynostosis in patients with Noonan syndrome caused by germline KRAS mutations. *American journal of medical genetics. Part A* 149A:1036-1040.

51. Tidyman, W.E., and Rauen, K.A. 2009. The RASopathies: developmental syndromes of Ras/MAPK pathway dysregulation. *Current opinion in genetics & development* 19:230-236.

52. Yasoda, A., Komatsu, Y., Chusho, H., Miyazawa, T., Ozasa, A., Miura, M., Kurihara, T., Rogi, T., Tanaka, S., Suda, M., et al. 2004. Overexpression of CNP in chondrocytes rescues achondroplasia through a MAPK-dependent pathway. *Nature medicine* 10:80-86.

53. Chusho, H., Tamura, N., Ogawa, Y., Yasoda, A., Suda, M., Miyazawa, T., Nakamura, K., Nakao, K., Kurihara, T., Komatsu, Y., et al. 2001. Dwarfism and early death in mice lacking C-type natriuretic peptide. *Proceedings of the National Academy of Sciences of the United States of America* 98:4016-4021.

54. Potter, L.R., Abbey-Hosch, S., and Dickey, D.M. 2006. Natriuretic peptides, their receptors, and cyclic guanosine monophosphate-dependent signaling functions. *Endocrine reviews* 27:47-72.

55. Miyazawa, T., Ogawa, Y., Chusho, H., Yasoda, A., Tamura, N., Komatsu, Y., Pfeifer, A., Hofmann, F., and Nakao, K. 2002. Cyclic GMP-dependent protein

kinase II plays a critical role in C-type natriuretic peptide-mediated endochondral ossification. *Endocrinology* 143:3604-3610.

56. Krejci, P., Masri, B., Fontaine, V., Mekikian, P.B., Weis, M., Prats, H., and Wilcox, W.R. 2005. Interaction of fibroblast growth factor and C-natriuretic peptide signaling in regulation of chondrocyte proliferation and extracellular matrix homeostasis. *Journal of cell science* 118:5089-5100.

57. Yasoda, A., Ogawa, Y., Suda, M., Tamura, N., Mori, K., Sakuma, Y., Chusho, H., Shiota, K., Tanaka, K., and Nakao, K. 1998. Natriuretic peptide regulation of endochondral ossification. Evidence for possible roles of the C-type natriuretic peptide/guanylyl cyclase-B pathway. *The Journal of biological chemistry* 273:11695-11700.

58. Bartels, C.F., Bukulmez, H., Padayatti, P., Rhee, D.K., van Ravenswaaij-Arts, C., Pauli, R.M., Mundlos, S., Chitayat, D., Shih, L.Y., Al-Gazali, L.I., et al. 2004. Mutations in the transmembrane natriuretic peptide receptor NPR-B impair skeletal growth and cause acromesomelic dysplasia, type Maroteaux. *American journal of human genetics* 75:27-34.

59. Hartmann, J.T., Haap, M., Kopp, H.G., and Lipp, H.P. 2009. Tyrosine kinase inhibitors - a review on pharmacology, metabolism and side effects. *Current drug metabolism* 10:470-481.

60. Aviezer, D., Golembo, M., and Yayon, A. 2003. Fibroblast growth factor receptor-3 as a therapeutic target for Achondroplasia--genetic short limbed dwarfism. *Current drug targets* 4:353-365.

61. Hall, P.S., and Cameron, D.A. 2009. Current perspective - trastuzumab. *European journal of cancer* 45:12-18.

62. Rauchenberger, R., Borges, E., Thomassen-Wolf, E., Rom, E., Adar, R., Yaniv, Y., Malka, M., Chumakov, I., Kotzer, S., Resnitzky, D., et al. 2003. Human combinatorial Fab library yielding specific and functional antibodies against the human fibroblast growth factor receptor 3. *The Journal of biological chemistry* 278:38194-38205.

63. Cappellen, D., De Oliveira, C., Ricol, D., de Medina, S., Bourdin, J., Sastre-Garau, X., Chopin, D., Thiery, J.P., and Radvanyi, F. 1999. Frequent activating mutations of FGFR3 in human bladder and cervix carcinomas. *Nature genetics* 23:18-20.

64. Martinez-Torrecuadrada, J., Cifuentes, G., Lopez-Serra, P., Saenz, P., Martinez, A., and Casal, J.I. 2005. Targeting the extracellular domain of fibroblast growth factor receptor 3 with human single-chain Fv antibodies inhibits bladder carcinoma cell line proliferation. *Clinical cancer research : an official journal of the American Association for Cancer Research* 11:6280-6290.

65. Qing, J., Du, X., Chen, Y., Chan, P., Li, H., Wu, P., Marsters, S., Stawicki, S., Tien, J., Totpal, K., et al. 2009. Antibody-based targeting of FGFR3 in bladder carcinoma and t(4;14)-positive multiple myeloma in mice. *The Journal of clinical investigation* 119:1216-1229.

66. Hadari, Y., and Schlessinger, J. 2009. FGFR3-targeted mAb therapy for bladder cancer and multiple myeloma. *The Journal of clinical investigation* 119:1077-1079.

67. Kake, T., Kitamura, H., Adachi, Y., Yoshioka, T., Watanabe, T., Matsushita, H., Fujii, T., Kondo, E., Tachibe, T., Kawase, Y., et al. 2009. Chronically elevated plasma C-type natriuretic peptide level stimulates skeletal growth in transgenic mice. *American journal of physiology. Endocrinology and metabolism* 297:E1339-1348.

68. Hunt, P.J., Richards, A.M., Espiner, E.A., Nicholls, M.G., and Yandle, T.G. 1994. Bioactivity and metabolism of C-type natriuretic peptide in normal man. *The Journal of clinical endocrinology and metabolism* 78:1428-1435.

69. Yasoda, A., Kitamura, H., Fujii, T., Kondo, E., Murao, N., Miura, M., Kanamoto, N., Komatsu, Y., Arai, H., and Nakao, K. 2009. Systemic administration of C-type natriuretic peptide as a novel therapeutic strategy for skeletal dysplasias. *Endocrinology* 150:3138-3144.

70. Shukla, V., Coumoul, X., Wang, R.H., Kim, H.S., and Deng, C.X. 2007. RNA interference and inhibition of MEK-ERK signaling prevent abnormal skeletal phenotypes in a mouse model of craniosynostosis. *Nature genetics* 39:1145-1150.

71. Yoon, S., and Seger, R. 2006. The extracellular signal-regulated kinase: multiple substrates regulate diverse cellular functions. *Growth factors* 24:21-44.

72. Vabulas, R.M., Raychaudhuri, S., Hayer-Hartl, M., and Hartl, F.U. 2010. Protein folding in the cytoplasm and the heat shock response. *Cold Spring Harbor perspectives in biology* 2:a004390.

73. Hartl, F.U., Bracher, A., and Hayer-Hartl, M. 2011. Molecular chaperones in protein folding and proteostasis. *Nature* 475:324-332.

74. Broadley, S.A., and Hartl, F.U. 2009. The role of molecular chaperones in human misfolding diseases. *FEBS letters* 583:2647-2653.

75. Lee, P., Shabbir, A., Cardozo, C., and Caplan, A.J. 2004. Sti1 and Cdc37 can stabilize Hsp90 in chaperone complexes with a protein kinase. *Molecular biology of the cell* 15:1785-1792.

76. Wegele, H., Wandinger, S.K., Schmid, A.B., Reinstein, J., and Buchner, J. 2006. Substrate transfer from the chaperone Hsp70 to Hsp90. *Journal of molecular biology* 356:802-811.

77. Arlander, S.J., Felts, S.J., Wagner, J.M., Stensgard, B., Toft, D.O., and Karnitz, L.M. 2006. Chaperoning checkpoint kinase 1 (Chk1), an Hsp90 client, with purified chaperones. *The Journal of biological chemistry* 281:2989-2998.

78. Felts, S.J., Karnitz, L.M., and Toft, D.O. 2007. Functioning of the Hsp90 machine in chaperoning checkpoint kinase I (Chk1) and the progesterone receptor (PR). *Cell stress & chaperones* 12:353-363.

79. Richter, K., and Buchner, J. 2011. Closing in on the hsp90 chaperone-client relationship. *Structure* 19:445-446.

80. An, W.G., Schulte, T.W., and Neckers, L.M. 2000. The heat shock protein 90 antagonist geldanamycin alters chaperone association with p210bcr-abl and v-src proteins before their degradation by the proteasome. *Cell growth & differentiation : the molecular biology journal of the American Association for Cancer Research* 11:355-360.

81. Caplan, A.J., Mandal, A.K., and Theodoraki, M.A. 2007. Molecular chaperones and protein kinase quality control. *Trends in cell biology* 17:87-92.

82. Morishima, Y., Murphy, P.J., Li, D.P., Sanchez, E.R., and Pratt, W.B. 2000. Stepwise assembly of a glucocorticoid receptor.hsp90 heterocomplex resolves two sequential ATP-dependent events involving first hsp70 and then hsp90 in opening of the steroid binding pocket. *The Journal of biological chemistry* 275:18054-18060.

83. Balch, W.E., Morimoto, R.I., Dillin, A., and Kelly, J.W. 2008. Adapting proteostasis for disease intervention. *Science* 319:916-919.

84. Koulov, A.V., Lapointe, P., Lu, B., Razvi, A., Coppinger, J., Dong, M.Q., Matteson, J., Laister, R., Arrowsmith, C., Yates, J.R., 3rd, et al. 2010. Biological and structural basis for Aha1 regulation of Hsp90 ATPase activity in maintaining proteostasis in the human disease cystic fibrosis. *Molecular biology of the cell* 21:871-884.

85. Loo, T.W., and Clarke, D.M. 2011. Repair of CFTR folding defects with correctors that function as pharmacological chaperones. *Methods in molecular biology* 741:23-37.

86. Powers, M.V., and Workman, P. 2006. Targeting of multiple signalling pathways by heat shock protein 90 molecular chaperone inhibitors. *Endocrine-related cancer* 13 Suppl 1:S125-135.

87. Tam, L.C., Kiang, A.S., Campbell, M., Keaney, J., Farrar, G.J., Humphries, M.M., Kenna, P.F., and Humphries, P. 2010. Prevention of autosomal dominant retinitis pigmentosa by systemic drug therapy targeting heat shock protein 90 (Hsp90). *Human molecular genetics* 19:4421-4436.

88. Waza, M., Adachi, H., Katsuno, M., Minamiyama, M., Tanaka, F., Doyu, M., and Sobue, G. 2006. Modulation of Hsp90 function in neurodegenerative disorders: a molecular-targeted therapy against disease-causing protein. *Journal of molecular medicine* 84:635-646.

89. Taipale, M., Jarosz, D.F., and Lindquist, S. 2010. HSP90 at the hub of protein homeostasis: emerging mechanistic insights. *Nat Rev Mol Cell Biol* 11:515-528.

90. Ali, M.M., Roe, S.M., Vaughan, C.K., Meyer, P., Panaretou, B., Piper, P.W., Prodromou, C., and Pearl, L.H. 2006. Crystal structure of an Hsp90-nucleotide-p23/Sba1 closed chaperone complex. *Nature* 440:1013-1017.

91. Prodromou, C., and Pearl, L.H. 2003. Structure and functional relationships of Hsp90. *Current cancer drug targets* 3:301-323.

92. Hessling, M., Richter, K., and Buchner, J. 2009. Dissection of the ATP-induced conformational cycle of the molecular chaperone Hsp90. *Nature structural & molecular biology* 16:287-293.

93. Street, T.O., Lavery, L.A., and Agard, D.A. 2011. Substrate binding drives large-scale conformational changes in the Hsp90 molecular chaperone. *Molecular cell* 42:96-105.

94. Martinez-Ruiz, A., Villanueva, L., Gonzalez de Orduna, C., Lopez-Ferrer, D., Higueras, M.A., Tarin, C., Rodriguez-Crespo, I., Vazquez, J., and Lamas, S. 2005. S-nitrosylation of Hsp90 promotes the inhibition of its ATPase and endothelial nitric oxide synthase regulatory activities. *Proceedings of the National Academy of Sciences of the United States of America* 102:8525-8530.

95. Mimnaugh, E.G., Worland, P.J., Whitesell, L., and Neckers, L.M. 1995. Possible role for serine/threonine phosphorylation in the regulation of the heteroprotein complex between the hsp90 stress protein and the pp60v-src tyrosine kinase. *The Journal of biological chemistry* 270:28654-28659.

96. Scroggins, B.T., Robzyk, K., Wang, D., Marcu, M.G., Tsutsumi, S., Beebe, K., Cotter, R.J., Felts, S., Toft, D., Karnitz, L., et al. 2007. An acetylation site in the middle domain of Hsp90 regulates chaperone function. *Molecular cell* 25:151-159.

97. Trepel, J., Mollapour, M., Giaccone, G., and Neckers, L. 2010. Targeting the dynamic HSP90 complex in cancer. *Nature reviews. Cancer* 10:537-549.

98. Picard, D. 2011. Hsp90 Interactors.

99. Zhao, R., Davey, M., Hsu, Y.C., Kaplanek, P., Tong, A., Parsons, A.B., Krogan, N., Cagney, G., Mai, D., Greenblatt, J., et al. 2005. Navigating the chaperone

network: an integrative map of physical and genetic interactions mediated by the hsp90 chaperone. *Cell* 120:715-727.

100. da Rocha Dias, S., Friedlos, F., Light, Y., Springer, C., Workman, P., and Marais, R. 2005. Activated B-RAF is an Hsp90 client protein that is targeted by the anticancer drug 17-allylamino-17-demethoxygeldanamycin. *Cancer research* 65:10686-10691.

101. Li, D., Marchenko, N.D., Schulz, R., Fischer, V., Velasco-Hernandez, T., Talos, F., and Moll, U.M. 2011. Functional Inactivation of Endogenous MDM2 and CHIP by HSP90 Causes Aberrant Stabilization of Mutant p53 in Human Cancer Cells. *Molecular cancer research : MCR* 9:577-588.

102. Shimamura, T., Lowell, A.M., Engelman, J.A., and Shapiro, G.I. 2005. Epidermal growth factor receptors harboring kinase domain mutations associate with the heat shock protein 90 chaperone and are destabilized following exposure to geldanamycins. *Cancer research* 65:6401-6408.

103. Lindquist, S. 2009. Protein folding sculpting evolutionary change. *Cold Spring Harbor symposia on quantitative biology* 74:103-108.

104. Karnitz, L.M., and Felts, S.J. 2007. Cdc37 regulation of the kinome: when to hold 'em and when to fold 'em. *Science's STKE : signal transduction knowledge environment* 2007:pe22.

105. MacLean, M., and Picard, D. 2003. Cdc37 goes beyond Hsp90 and kinases. *Cell stress & chaperones* 8:114-119.

106. Lee, P., Rao, J., Fliss, A., Yang, E., Garrett, S., and Caplan, A.J. 2002. The Cdc37 protein kinase-binding domain is sufficient for protein kinase activity and cell viability. *The Journal of cell biology* 159:1051-1059.

107. Prince, T., and Matts, R.L. 2004. Definition of protein kinase sequence motifs that trigger high affinity binding of Hsp90 and Cdc37. *The Journal of biological chemistry* 279:39975-39981.

108. Scroggins, B.T., Prince, T., Shao, J., Uma, S., Huang, W., Guo, Y., Yun, B.G., Hedman, K., Matts, R.L., and Hartson, S.D. 2003. High affinity binding of Hsp90 is triggered by multiple discrete segments of its kinase clients. *Biochemistry* 42:12550-12561.

109. Zhao, Q., Boschelli, F., Caplan, A.J., and Arndt, K.T. 2004. Identification of a conserved sequence motif that promotes Cdc37 and cyclin D1 binding to Cdk4. *The Journal of biological chemistry* 279:12560-12564.

110. Vaughan, C.K., Gohlke, U., Sobott, F., Good, V.M., Ali, M.M., Prodromou, C., Robinson, C.V., Saibil, H.R., and Pearl, L.H. 2006. Structure of an Hsp90-Cdc37-Cdk4 complex. *Molecular cell* 23:697-707.

111. Terasawa, K., Yoshimatsu, K., Iemura, S., Natsume, T., Tanaka, K., and Minami, Y. 2006. Cdc37 interacts with the glycine-rich loop of Hsp90 client kinases. *Molecular and cellular biology* 26:3378-3389.

112. Siligardi, G., Panaretou, B., Meyer, P., Singh, S., Woolfson, D.N., Piper, P.W., Pearl, L.H., and Prodromou, C. 2002. Regulation of Hsp90 ATPase activity by the

co-chaperone Cdc37p/p50cdc37. *The Journal of biological chemistry* 277:20151-20159.

113. Bandhakavi, S., McCann, R.O., Hanna, D.E., and Glover, C.V. 2003. A positive feedback loop between protein kinase CKII and Cdc37 promotes the activity of multiple protein kinases. *The Journal of biological chemistry* 278:2829-2836.

114. Miyata, Y., and Nishida, E. 2004. CK2 controls multiple protein kinases by phosphorylating a kinase-targeting molecular chaperone, Cdc37. *Molecular and cellular biology* 24:4065-4074.

115. Shao, J., Prince, T., Hartson, S.D., and Matts, R.L. 2003. Phosphorylation of serine 13 is required for the proper function of the Hsp90 co-chaperone, Cdc37. *The Journal of biological chemistry* 278:38117-38120.

116. Vaughan, C.K., Mollapour, M., Smith, J.R., Truman, A., Hu, B., Good, V.M., Panaretou, B., Neckers, L., Clarke, P.A., Workman, P., et al. 2008. Hsp90-dependent activation of protein kinases is regulated by chaperone-targeted dephosphorylation of Cdc37. *Molecular cell* 31:886-895.

117. Miyata, Y. 2009. Protein kinase CK2 in health and disease: CK2: the kinase controlling the Hsp90 chaperone machinery. *Cellular and molecular life sciences : CMLS* 66:1840-1849.

118. Ballinger, C.A., Connell, P., Wu, Y., Hu, Z., Thompson, L.J., Yin, L.Y., and Patterson, C. 1999. Identification of CHIP, a novel tetratricopeptide repeat-containing protein that interacts with heat shock proteins and negatively regulates chaperone functions. *Molecular and cellular biology* 19:4535-4545.

119. Murata, S., Minami, Y., Minami, M., Chiba, T., and Tanaka, K. 2001. CHIP is a chaperone-dependent E3 ligase that ubiquitylates unfolded protein. *EMBO reports* 2:1133-1138.

120. Morishima, Y., Wang, A.M., Yu, Z., Pratt, W.B., Osawa, Y., and Lieberman, A.P. 2008. CHIP deletion reveals functional redundancy of E3 ligases in promoting degradation of both signaling proteins and expanded glutamine proteins. *Human molecular genetics* 17:3942-3952.

121. Shin, Y., Klucken, J., Patterson, C., Hyman, B.T., and McLean, P.J. 2005. The co-chaperone carboxyl terminus of Hsp70-interacting protein (CHIP) mediates alpha-synuclein degradation decisions between proteasomal and lysosomal pathways. *The Journal of biological chemistry* 280:23727-23734.

122. Okiyoneda, T., Barriere, H., Bagdany, M., Rabeh, W.M., Du, K., Hohfeld, J., Young, J.C., and Lukacs, G.L. 2010. Peripheral protein quality control removes unfolded CFTR from the plasma membrane. *Science* 329:805-810.

123. Yang, S., Qu, S., Perez-Tores, M., Sawai, A., Rosen, N., Solit, D.B., and Arteaga, C.L. 2006. Association with HSP90 inhibits Cbl-mediated down-regulation of mutant epidermal growth factor receptors. *Cancer research* 66:6990-6997.

124. Pratt, W.B., Morishima, Y., Peng, H.M., and Osawa, Y. 2010. Proposal for a role of the Hsp90/Hsp70-based chaperone machinery in making triage decisions when proteins undergo oxidative and toxic damage. *Experimental biology and medicine* 235:278-289.

125. Adachi, H., Waza, M., Tokui, K., Katsuno, M., Minamiyama, M., Tanaka, F., Doyu, M., and Sobue, G. 2007. CHIP overexpression reduces mutant androgen receptor protein and ameliorates phenotypes of the spinal and bulbar muscular atrophy transgenic mouse model. *The Journal of neuroscience : the official journal of the Society for Neuroscience* 27:5115-5126.

126. Waza, M., Adachi, H., Katsuno, M., Minamiyama, M., Sang, C., Tanaka, F., Inukai, A., Doyu, M., and Sobue, G. 2005. 17-AAG, an Hsp90 inhibitor, ameliorates polyglutamine-mediated motor neuron degeneration. *Nature medicine* 11:1088-1095.

127. Uehara, Y. 2003. Natural product origins of Hsp90 inhibitors. *Current cancer drug targets* 3:325-330.

128. Uehara, Y., Hori, M., Takeuchi, T., and Umezawa, H. 1985. Screening of agents which convert 'transformed morphology' of Rous sarcoma virus-infected rat kidney cells to 'normal morphology': identification of an active agent as herbimycin and its inhibition of intracellular src kinase. *Japanese journal of cancer research : Gann* 76:672-675.

129. Uehara, Y., Hori, M., Takeuchi, T., and Umezawa, H. 1986. Phenotypic change from transformed to normal induced by benzoquinonoid ansamycins accompanies inactivation of p60src in rat kidney cells infected with Rous sarcoma virus. *Molecular and cellular biology* 6:2198-2206.

130. Whitesell, L., Mimnaugh, E.G., De Costa, B., Myers, C.E., and Neckers, L.M. 1994. Inhibition of heat shock protein HSP90-pp60v-src heteroprotein complex

formation by benzoquinone ansamycins: essential role for stress proteins in oncogenic transformation. *Proceedings of the National Academy of Sciences of the United States of America* 91:8324-8328.

131. Supko, J.G., Hickman, R.L., Grever, M.R., and Malspeis, L. 1995. Preclinical pharmacologic evaluation of geldanamycin as an antitumor agent. *Cancer chemotherapy and pharmacology* 36:305-315.

132. Kamal, A., Thao, L., Sensintaffar, J., Zhang, L., Boehm, M.F., Fritz, L.C., and Burrows, F.J. 2003. A high-affinity conformation of Hsp90 confers tumour selectivity on Hsp90 inhibitors. *Nature* 425:407-410.

133. Pashtan, I., Tsutsumi, S., Wang, S., Xu, W., and Neckers, L. 2008. Targeting Hsp90 prevents escape of breast cancer cells from tyrosine kinase inhibition. *Cell cycle* 7:2936-2941.

134. Workman, P., Burrows, F., Neckers, L., and Rosen, N. 2007. Drugging the cancer chaperone HSP90: combinatorial therapeutic exploitation of oncogene addiction and tumor stress. *Annals of the New York Academy of Sciences* 1113:202-216.

135. Kim, Y.S., Alarcon, S.V., Lee, S., Lee, M.J., Giaccone, G., Neckers, L., and Trepel, J.B. 2009. Update on Hsp90 inhibitors in clinical trial. *Current topics in medicinal chemistry* 9:1479-1492.

136. Mollapour, M., Tsutsumi, S., Truman, A.W., Xu, W., Vaughan, C.K., Beebe, K., Konstantinova, A., Vourganti, S., Panaretou, B., Piper, P.W., et al. 2011. Threonine 22 phosphorylation attenuates Hsp90 interaction with cochaperones and affects its chaperone activity. *Molecular cell* 41:672-681.

137. Laederich, M.B., Degnin, C.R., Lunstrum, G.P., Holden, P., and Horton, W.A. 2011. Fibroblast Growth Factor Receptor 3 (FGFR3) Is a Strong Heat Shock Protein 90 (Hsp90) Client: IMPLICATIONS FOR THERAPEUTIC MANIPULATION. *The Journal of biological chemistry* 286:19597-19604.

138. Knights, V., and Cook, S.J. 2010. De-regulated FGF receptors as therapeutic targets in cancer. *Pharmacol Ther* 125:105-117.

139. Chesi, M., Nardini, E., Brents, L.A., Schrock, E., Ried, T., Kuehl, W.M., and Bergsagel, P.L. 1997. Frequent translocation t(4;14)(p16.3;q32.3) in multiple myeloma is associated with increased expression and activating mutations of fibroblast growth factor receptor 3. *Nat Genet* 16:260-264.

140. Borkovich, K.A., Farrelly, F.W., Finkelstein, D.B., Taulien, J., and Lindquist, S. 1989. hsp82 is an essential protein that is required in higher concentrations for growth of cells at higher temperatures. *Mol Cell Biol* 9:3919-3930.

141. Theodoraki, M.A., Kunjappu, M., Sternberg, D.W., and Caplan, A.J. 2007. Akt shows variable sensitivity to an Hsp90 inhibitor depending on cell context. *Exp Cell Res* 313:3851-3858.

142. Xu, W., Yuan, X., Xiang, Z., Mimnaugh, E., Marcu, M., and Neckers, L. 2005. Surface charge and hydrophobicity determine ErbB2 binding to the Hsp90 chaperone complex. *Nat Struct Mol Biol* 12:120-126.

143. Murata, S., Chiba, T., and Tanaka, K. 2003. CHIP: a quality-control E3 ligase collaborating with molecular chaperones. *The international journal of biochemistry & cell biology* 35:572-578.

144. Kamal, A., Boehm, M.F., and Burrows, F.J. 2004. Therapeutic and diagnostic implications of Hsp90 activation. *Trends in molecular medicine* 10:283-290.

145. Chiosis, G., Huezo, H., Rosen, N., Mimnaugh, E., Whitesell, L., and Neckers, L. 2003. 17AAG: low target binding affinity and potent cell activity--finding an explanation. *Mol Cancer Ther* 2:123-129.

146. Sweeney, C., Fambrough, D., Huard, C., Diamonti, A.J., Lander, E.S., Cantley, L.C., and Carraway, K.L., 3rd. 2001. Growth factor-specific signaling pathway stimulation and gene expression mediated by ErbB receptors. *J Biol Chem* 276:22685-22698.

147. VanSlyke, J.K., and Musil, L.S. 2000. Analysis of connexin intracellular transport and assembly. *Methods* 20:156-164.

148. Avantaggiati, M.L., Carbone, M., Graessmann, A., Nakatani, Y., Howard, B., and Levine, A.S. 1996. The SV40 large T antigen and adenovirus E1a oncoproteins interact with distinct isoforms of the transcriptional co-activator, p300. *EMBO J* 15:2236-2248.

149. Monsonego-Ornan, E., Adar, R., Rom, E., and Yayon, A. 2002. FGF receptors ubiquitylation: dependence on tyrosine kinase activity and role in downregulation. *FEBS letters* 528:83-89.

150. Lievens, P.M., Roncador, A., and Liboi, E. 2006. K644E/M FGFR3 mutants activate Erk1/2 from the endoplasmic reticulum through FRS2 alpha and PLC gamma-independent pathways. *J Mol Biol* 357:783-792.

151. Bernard-Pierrot, I., Brams, A., Dunois-Larde, C., Caillault, A., Diez de Medina, S.G., Cappellen, D., Graff, G., Thiery, J.P., Chopin, D., Ricol, D., et al. 2006. Oncogenic properties of the mutated forms of fibroblast growth factor receptor 3b. *Carcinogenesis* 27:740-747.

152. Germano, S., Barberis, D., Santoro, M.M., Penengo, L., Citri, A., Yarden, Y., and Gaudino, G. 2006. Geldanamycins trigger a novel Ron degradative pathway, hampering oncogenic signaling. *The Journal of biological chemistry* 281:21710-21719.

153. Xu, W., Mimnaugh, E., Rosser, M.F., Nicchitta, C., Marcu, M., Yarden, Y., and Neckers, L. 2001. Sensitivity of mature Erbb2 to geldanamycin is conferred by its kinase domain and is mediated by the chaperone protein Hsp90. *J Biol Chem* 276:3702-3708.

154. Schulte, T.W., Akinaga, S., Soga, S., Sullivan, W., Stensgard, B., Toft, D., and Neckers, L.M. 1998. Antibiotic radicicol binds to the N-terminal domain of Hsp90 and shares important biologic activities with geldanamycin. *Cell Stress Chaperones* 3:100-108.

155. Schulte, T.W., and Neckers, L.M. 1998. The benzoquinone ansamycin 17-allylamino-17-demethoxygeldanamycin binds to HSP90 and shares important biologic activities with geldanamycin. *Cancer Chemother Pharmacol* 42:273-279.

156. Jeong, J.H., An, J.Y., Kwon, Y.T., Li, L.Y., and Lee, Y.J. 2008. Quercetin-induced ubiquitination and down-regulation of Her-2/neu. *J Cell Biochem* 105:585-595.

157. Zhang, T., Li, Y., Yu, Y., Zou, P., Jiang, Y., and Sun, D. 2009. Characterization of celastrol to inhibit hsp90 and cdc37 interaction. *J Biol Chem* 284:35381-35389.

158. Citri, A., Harari, D., Shohat, G., Ramakrishnan, P., Gan, J., Lavi, S., Eisenstein, M., Kimchi, A., Wallach, D., Pietrokovski, S., et al. 2006. Hsp90 recognizes a common surface on client kinases. *J Biol Chem* 281:14361-14369.

159. Gould, C.M., Kannan, N., Taylor, S.S., and Newton, A.C. 2009. The chaperones Hsp90 and Cdc37 mediate the maturation and stabilization of protein kinase C through a conserved PXXP motif in the C-terminal tail. *J Biol Chem* 284:4921-4935.

160. Hikri, E., Shpungin, S., and Nir, U. 2009. Hsp90 and a tyrosine embedded in the Hsp90 recognition loop are required for the Fer tyrosine kinase activity. *Cell Signal* 21:588-596.

161. Margineantu, D.H., Emerson, C.B., Diaz, D., and Hockenbery, D.M. 2007. Hsp90 inhibition decreases mitochondrial protein turnover. *PLoS One* 2:e1066.

162. Sun, X., Barlow, E.A., Ma, S., Hagemeier, S.R., Duellman, S.J., Burgess, R.R., Tellam, J., Khanna, R., and Kenney, S.C. 2010. Hsp90 inhibitors block outgrowth of EBV-infected malignant cells in vitro and in vivo through an EBNA1-dependent mechanism. *Proc Natl Acad Sci U S A* 107:3146-3151.

163. Joazeiro, C.A., Wing, S.S., Huang, H., Leverson, J.D., Hunter, T., and Liu, Y.C. 1999. The tyrosine kinase negative regulator c-Cbl as a RING-type, E2-dependent ubiquitin-protein ligase. *Science* 286:309-312.

164. Zhou, P., Fernandes, N., Dodge, I.L., Reddi, A.L., Rao, N., Safran, H., DiPetrillo, T.A., Wazer, D.E., Band, V., and Band, H. 2003. ErbB2 degradation mediated by the co-chaperone protein CHIP. *J Biol Chem* 278:13829-13837.

165. Xu, W., Marcu, M., Yuan, X., Mimnaugh, E., Patterson, C., and Neckers, L. 2002. Chaperone-dependent E3 ubiquitin ligase CHIP mediates a degradative pathway for c-ErbB2/Neu. *Proc Natl Acad Sci U S A* 99:12847-12852.

166. Krejci, P., Bryja, V., Pachernik, J., Hampl, A., Pogue, R., Mekikian, P., and Wilcox, W.R. 2004. FGF2 inhibits proliferation and alters the cartilage-like phenotype of RCS cells. *Exp Cell Res* 297:152-164.

167. Mollapour, M., Tsutsumi, S., Donnelly, A.C., Beebe, K., Tokita, M.J., Lee, M.J., Lee, S., Morra, G., Bourboulia, D., Scroggins, B.T., et al. 2010. Swe1Wee1-dependent tyrosine phosphorylation of Hsp90 regulates distinct facets of chaperone function. *Molecular cell* 37:333-343.

168. Citri, A., Gan, J., Mosesson, Y., Vereb, G., Szollosi, J., and Yarden, Y. 2004. Hsp90 restrains ErbB-2/HER2 signalling by limiting heterodimer formation. *EMBO Rep* 5:1165-1170.

169. Li, R., Soosairajah, J., Harari, D., Citri, A., Price, J., Ng, H.L., Morton, C.J., Parker, M.W., Yarden, Y., and Bernard, O. 2006. Hsp90 increases LIM kinase activity by promoting its homo-dimerization. *FASEB J* 20:1218-1220.

170. Bae, J.H., Boggon, T.J., Tome, F., Mandiyan, V., Lax, I., and Schlessinger, J. 2010. Asymmetric receptor contact is required for tyrosine autophosphorylation

of fibroblast growth factor receptor in living cells. *Proc Natl Acad Sci U S A* 107:2866-2871.

171. Vecchione, A., Cooper, H.J., Trim, K.J., Akbarzadeh, S., Heath, J.K., and Wheldon, L.M. 2007. Protein partners in the life history of activated fibroblast growth factor receptors. *Proteomics* 7:4565-4578.

172. Terry, J., Lubieniecka, J.M., Kwan, W., Liu, S., and Nielsen, T.O. 2005. Hsp90 inhibitor 17-allylamino-17-demethoxygeldanamycin prevents synovial sarcoma proliferation via apoptosis in in vitro models. *Clin Cancer Res* 11:5631-5638.

173. Nakashima, T., Ishii, T., Tagaya, H., Seike, T., Nakagawa, H., Kanda, Y., Akinaga, S., Soga, S., and Shiotsu, Y. 2010. New molecular and biological mechanism of antitumor activities of KW-2478, a novel nonansamycin heat shock protein 90 inhibitor, in multiple myeloma cells. *Clin Cancer Res* 16:2792-2802.

174. Prince, T., and Matts, R.L. 2005. Exposure of protein kinase motifs that trigger binding of Hsp90 and Cdc37. *Biochemical and biophysical research communications* 338:1447-1454.

175. Dawson, M.A., Opat, S.S., Taouk, Y., Donovan, M., Zammit, M., Monaghan, K., Horvath, N., Roberts, A.W., Prince, H.M., Hertzberg, M., et al. 2009. Clinical and immunohistochemical features associated with a response to bortezomib in patients with multiple myeloma. *Clinical cancer research : an official journal of the American Association for Cancer Research* 15:714-722.

176. Keats, J.J., Reiman, T., Belch, A.R., and Pilarski, L.M. 2006. Ten years and counting: so what do we know about t(4;14)(p16;q32) multiple myeloma. *Leukemia & lymphoma* 47:2289-2300.

177. van Rhijn, B.W., Zuiverloon, T.C., Vis, A.N., Radvanyi, F., van Leenders, G.J., Ooms, B.C., Kirkels, W.J., Lockwood, G.A., Boeve, E.R., Jobsis, A.C., et al. 2010. Molecular grade (FGFR3/MIB-1) and EORTC risk scores are predictive in primary non-muscle-invasive bladder cancer. *European urology* 58:433-441.

178. Zuiverloon, T.C., van der Aa, M.N., van der Kwast, T.H., Steyerberg, E.W., Lingsma, H.F., Bangma, C.H., and Zwarthoff, E.C. 2010. Fibroblast growth factor receptor 3 mutation analysis on voided urine for surveillance of patients with low-grade non-muscle-invasive bladder cancer. *Clinical cancer research : an official journal of the American Association for Cancer Research* 16:3011-3018.

179. Richardson, P.G., Chanan-Khan, A.A., Lonial, S., Krishnan, A.Y., Carroll, M.P., Alsina, M., Albitar, M., Berman, D., Messina, M., and Anderson, K.C. 2011. Tanespimycin and bortezomib combination treatment in patients with relapsed or relapsed and refractory multiple myeloma: results of a phase 1/2 study. *British journal of haematology* 153:729-740.

180. Richardson, P.G., Mitsiades, C.S., Laubach, J.P., Lonial, S., Chanan-Khan, A.A., and Anderson, K.C. 2011. Inhibition of heat shock protein 90 (HSP90) as a therapeutic strategy for the treatment of myeloma and other cancers. *British journal of haematology* 152:367-379.

181. Karkoulis, P.K., Stravopodis, D.J., Margaritis, L.H., and Voutsinas, G.E. 2010. 17-Allylamino-17-demethoxygeldanamycin induces downregulation of critical Hsp90 protein clients and results in cell cycle arrest and apoptosis of human urinary bladder cancer cells. *BMC cancer* 10:481.

182. Cheng, L., Zhang, S., MacLennan, G.T., Williamson, S.R., Lopez-Beltran, A., and Montironi, R. 2011. Bladder cancer: translating molecular genetic insights into clinical practice. *Human pathology* 42:455-481.

183. Azab, A.K., Azab, F., Quang, P., Maiso, P., Morgan, B., Sacco, A., Ngo, H.T., Liu, Y., Zhang, Y., Roccaro, A.M., et al. 2011. FGFR3 is overexpressed Waldenstrom macroglobulinemia and its inhibition by Dovitinib induces apoptosis, and overcomes stroma-induced proliferation. *Clinical cancer research : an official journal of the American Association for Cancer Research*.

184. de Brito, L.R., Batey, M.A., Zhao, Y., Squires, M.S., Maitland, H., Leung, H.Y., Hall, A.G., Jackson, G., Newell, D.R., and Irving, J.A. 2011. Comparative pre-clinical evaluation of receptor tyrosine kinase inhibitors for the treatment of multiple myeloma. *Leukemia research*.

185. Lamont, F.R., Tomlinson, D.C., Cooper, P.A., Shnyder, S.D., Chester, J.D., and Knowles, M.A. 2011. Small molecule FGF receptor inhibitors block FGFR-dependent urothelial carcinoma growth in vitro and in vivo. *British journal of cancer* 104:75-82.

186. Uzawa, K., Ishigami, T., Fushimi, K., Kawata, T., Shinozuka, K., Kasamatsu, A., Sakamoto, Y., Ogawara, K., Shiiba, M., Bukawa, H., et al. 2011. Targeting

fibroblast growth factor receptor 3 enhances radiosensitivity in human squamous cancer cells. *Oncogene*.

187. Kovacs, J.J., Murphy, P.J., Gaillard, S., Zhao, X., Wu, J.T., Nicchitta, C.V., Yoshida, M., Toft, D.O., Pratt, W.B., and Yao, T.P. 2005. HDAC6 regulates Hsp90 acetylation and chaperone-dependent activation of glucocorticoid receptor. *Molecular cell* 18:601-607.

188. Yang, Y., Rao, R., Shen, J., Tang, Y., Fiskus, W., Nechtman, J., Atadja, P., and Bhalla, K. 2008. Role of acetylation and extracellular location of heat shock protein 90alpha in tumor cell invasion. *Cancer research* 68:4833-4842.

189. Yu, X., Guo, Z.S., Marcu, M.G., Neckers, L., Nguyen, D.M., Chen, G.A., and Schrump, D.S. 2002. Modulation of p53, ErbB1, ErbB2, and Raf-1 expression in lung cancer cells by depsipeptide FR901228. *Journal of the National Cancer Institute* 94:504-513.

190. Lane, A.A., and Chabner, B.A. 2009. Histone deacetylase inhibitors in cancer therapy. *Journal of clinical oncology : official journal of the American Society of Clinical Oncology* 27:5459-5468.

191. Aoyagi, S., and Archer, T.K. 2005. Modulating molecular chaperone Hsp90 functions through reversible acetylation. *Trends in cell biology* 15:565-567.

192. Herr, I., and Buchler, M.W. 2010. Dietary constituents of broccoli and other cruciferous vegetables: implications for prevention and therapy of cancer. *Cancer treatment reviews* 36:377-383.

193. Michaud, D.S., Spiegelman, D., Clinton, S.K., Rimm, E.B., Willett, W.C., and Giovannucci, E.L. 1999. Fruit and vegetable intake and incidence of bladder cancer in a male prospective cohort. *Journal of the National Cancer Institute* 91:605-613.

194. Tang, L., Zirpoli, G.R., Guru, K., Moysich, K.B., Zhang, Y., Ambrosone, C.B., and McCann, S.E. 2008. Consumption of raw cruciferous vegetables is inversely associated with bladder cancer risk. *Cancer epidemiology, biomarkers & prevention : a publication of the American Association for Cancer Research, cosponsored by the American Society of Preventive Oncology* 17:938-944.

195. Tang, L., Zirpoli, G.R., Guru, K., Moysich, K.B., Zhang, Y., Ambrosone, C.B., and McCann, S.E. 2010. Intake of cruciferous vegetables modifies bladder cancer survival. *Cancer epidemiology, biomarkers & prevention : a publication of the American Association for Cancer Research, cosponsored by the American Society of Preventive Oncology* 19:1806-1811.

196. Gibbs, A., Schwartzman, J., Deng, V., and Alumkal, J. 2009. Sulforaphane destabilizes the androgen receptor in prostate cancer cells by inactivating histone deacetylase 6. *Proceedings of the National Academy of Sciences of the United States of America* 106:16663-16668.

197. Ho, E., Clarke, J.D., and Dashwood, R.H. 2009. Dietary sulforaphane, a histone deacetylase inhibitor for cancer prevention. *The Journal of nutrition* 139:2393-2396.

198. Kim, S.H., and Singh, S.V. 2009. D,L-Sulforaphane causes transcriptional repression of androgen receptor in human prostate cancer cells. *Molecular cancer therapeutics* 8:1946-1954.

199. He, L., Horton, W., and Hristova, K. 2010. Physical basis behind achondroplasia, the most common form of human dwarfism. *The Journal of biological chemistry* 285:30103-30114.

200. Hertel, N.T., Eklof, O., Ivarsson, S., Aronson, S., Westphal, O., Sipila, I., Kaitila, I., Bland, J., Veimo, D., Muller, J., et al. 2005. Growth hormone treatment in 35 prepubertal children with achondroplasia: a five-year dose-response trial. *Acta paediatrica* 94:1402-1410.

201. Correll, J. 1991. Surgical correction of short stature in skeletal dysplasias. *Acta paediatrica Scandinavica. Supplement* 377:143-148.

202. Brodie, S.G., and Deng, C.X. 2003. Mouse models orthologous to FGFR3-related skeletal dysplasias. *Pediatric pathology & molecular medicine* 22:87-103.

203. Li, C., Chen, L., Iwata, T., Kitagawa, M., Fu, X.Y., and Deng, C.X. 1999. A Lys644Glu substitution in fibroblast growth factor receptor 3 (FGFR3) causes dwarfism in mice by activation of STATs and ink4 cell cycle inhibitors. *Human molecular genetics* 8:35-44.

204. Naski, M.C., Wang, Q., Xu, J., and Ornitz, D.M. 1996. Graded activation of fibroblast growth factor receptor 3 by mutations causing achondroplasia and thanatophoric dysplasia. *Nature genetics* 13:233-237.

205. Neckers, L. 2007. Heat shock protein 90: the cancer chaperone. *Journal of biosciences* 32:517-530.

206. Mukherjee, A., Dong, S.S., Clemens, T., Alvarez, J., and Serra, R. 2005. Co-ordination of TGF-beta and FGF signaling pathways in bone organ cultures. *Mechanisms of development* 122:557-571.

207. Pfaffl, M.W. 2001. A new mathematical model for relative quantification in real-time RT-PCR. *Nucleic acids research* 29:e45.

208. Egorin, M.J., Zuhowski, E.G., Rosen, D.M., Sentz, D.L., Covey, J.M., and Eiseman, J.L. 2001. Plasma pharmacokinetics and tissue distribution of 17-(allylamino)-17-demethoxygeldanamycin (NSC 330507) in CD2F1 mice1. *Cancer chemotherapy and pharmacology* 47:291-302.

209. Kamal, A., and Burrows, F.J. 2004. Hsp90 inhibitors as selective anticancer drugs. *Discovery medicine* 4:277-280.

210. Gaspar, N., Sharp, S.Y., Pacey, S., Jones, C., Walton, M., Vassal, G., Eccles, S., Pearson, A., and Workman, P. 2009. Acquired resistance to 17-allylamino-17-demethoxygeldanamycin (17-AAG, tanespimycin) in glioblastoma cells. *Cancer research* 69:1966-1975.

211. Guo, W., Reigan, P., Siegel, D., Zirrolli, J., Gustafson, D., and Ross, D. 2005. Formation of 17-allylamino-demethoxygeldanamycin (17-AAG) hydroquinone by NAD(P)H:quinone oxidoreductase 1: role of 17-AAG hydroquinone in heat shock protein 90 inhibition. *Cancer research* 65:10006-10015.